

Michael Weißl, BSc.

In-situ synthesis of metal-sulfide coated fibers in the course of the Viscose process

MASTERARBEIT

zur Erlangung des akademischen Grades

Diplom-Ingenieur

Masterstudium Technische Chemie

eingereicht an der

Technischen Universität Graz

Betreuer

Mag. Dr. Stefan Spirk

Institut für Chemische Technologie von Materialien

Eidesstattliche Erklärung

Affidavit

Ich erkläre an Eides statt, dass ich die vorliegende Arbeit selbstständig verfasst, andere als die angegebenen Quellen/Hilfsmittel nicht benutzt, und die den benutzten Quellen wörtlich und inhaltlich entnommenen Stellen als solche kenntlich gemacht habe. Das in TUGRAZonline hochgeladene Textdokument ist mit der vorliegenden Masterarbeit identisch.

I declare that I have authored this thesis independently, that I have not used other than the declared sources / resources, and that I have explicitly marked all material which has been quoted either literally or by content from the used sources. The text document uploaded to TUGRAZonline is identical to the present master`s thesis.

Datum / Date

Unterschrift / Signature

Danksagung

Das Verfassen einer Diplomarbeit und die damit verbundene Erlangung eines akademischen Titels ist ein ganz besonderer Moment im Leben eines Studenten. Stellt dieses Ereignis doch das Ende eines aufregenden, manchmal auch sehr fordernden, vor allem aber mit vielen hervorragenden Erfahrungen versehenen, Lebensabschnittes dar.

Ich wurde auf dem von mir gewählten Weg des Studiums der technischen Chemie von zahllosen großartigen Menschen begleitet und durfte in meiner Studienzeit mindestens ebenso viele kennenlernen.

Nun möchte ich diese Gelegenheit nutzen und einmal Danke sagen, Danke für alles was ich erleben durfte und Danke für alles was mir ermöglicht wurde.

Ein besonderer Dank gilt dem Betreuer meiner Diplomarbeit Stefan Spirk, welcher mir immer mit Rat und Tat zur Seite stand, wenn ich einmal nicht weiterwusste.

Auch bei Brigitte Bittschnau (XRD), Manuel Kaschowitz (SEM), Walter Gössler (ICPMS), Armin Zankel vom FELMI (SEM) und Clemens Kittinger von der Med-Uni Graz (Antibakterielle Tests) möchte ich mich herzlich für die Unterstützung bedanken.

Bei den Kollegen meiner Arbeitsgruppe, sowie bei allen anderen Kollegen am ICTM möchte ich mich für die gute Zusammenarbeit, das angenehme Arbeitsklima, die vielen hilfreichen Ratschläge, sowie für die zahlreichen Erlebnisse innerhalb sowie außerhalb des universitären Schaffens bedanken. Liebe AG Spirk, ich danke euch herzlich für das freundschaftliche Verhältnis und eure Unterstützung.

Liebe Eltern, ihr seid es, die es mir ermöglicht haben eine so fantastische Zeit zu erleben. Mit, und nur durch eure ständige Unterstützung habt ihr das Ganze erst ermöglicht. Ihr hattet immer ein offenes Ohr für meine Sorgen und seid mir immer motivierend zur Seite gestanden. Dafür kann ich euch gar nicht genug danken.

Abstract

Since Svan started with the production of the first regenerated cellulose fibers in 1884, a large variety of man-made cellulose fibers, produced through diverse processes, has captured the fiber market. One of the most important processes in this large variety is the so called viscose process, in which synthetic cellulose fibers are produced through dissolving alkali cellulose in carbon disulfide, followed by further regeneration using sulfuric acid.

Although the viscose process is one of the oldest processes in the synthetic fiber production, there are still some unresolved problems and a variety of opportunities for process and product development.

The major aim of this master's thesis is the in situ synthesis of metal sulfide particles on cellulose fibers and films in the course of the viscose process and finally the characterization of the resulting materials using a broad range of analytical methods. This work describes the successful lab scale viscose production as well as the development of an automatized lab scale fiber production unit.

The successful synthesis and the product characterization of films and fibers coated with copper, tin, silver, nickel and cobalt sulfides is documented in detail.

In a further experiment, a first possible application for the synthesized products, the antibacterial effect of copper coated cellulose films, is demonstrated.

In consideration, a large amount of results and even more experience could be generated through this master thesis. The results of this thesis provide a good starting point for further investigations and product development in this research area.

Kurzfassung

Seit Svan 1884 mit der Produktion der ersten künstlichen Zellulosefasern begonnen hat, hat sich eine große Bandbreite an verschiedenen Fasern, die über unterschiedlichste Verfahren hergestellt werden, entwickelt. Einer der wichtigsten Prozesse für die Produktion von künstlichen Zellulosefasern ist der sogenannte Viskoseprozess, in welchem synthetische Fasern durch Lösen von Alkalizellulose in Kohlenstoffdisulfid und nachfolgender Regeneration in Schwefelsäurebädern hergestellt werden.

Obwohl der Viskoseprozess zu den ältesten Prozessen in der Herstellung von Kunstfasern gehört, gibt es immer noch einige ungelöste Probleme und eine Vielzahl an Möglichkeiten um sowohl den Prozess als auch die erhaltenen Produkte weiterzuentwickeln.

Das Hauptaugenmerk dieser Masterarbeit liegt in der in-situ Synthese von Metallsulfiden auf Zellulosefasern und Zellulosefilmen im Zuge des Viskoseverfahrens, sowie in der Charakterisierung der hergestellten Produkte durch eine Vielzahl an unterschiedlichen Untersuchungsmethoden. In der Arbeit wird die erfolgreiche Herstellung von Viskose, sowie die Entwicklung einer automatisierten Faserspinnanlage im Labormaßstab beschrieben.

Die erfolgreiche Herstellung und Charakterisierung von mit Metallsulfiden bedeckten Fasern und Filmen wird im Detail erörtert.

In einer finalen Untersuchung wird eine erste mögliche Anwendung für die hergestellten Produkte, der antibakterielle Effekt von mit Kupfersulfiden umgebenen Zellulosefilmen, aufgezeigt.

Alles in allem, konnte durch diese Masterarbeit eine große Menge an interessanten Ergebnissen und noch viel mehr Wissen generiert werden. Die Ergebnisse dieser Arbeit bieten eine gute Grundlage, für weiter Untersuchungen und Produktentwicklung in diesem Forschungsgebiet.

Table of content

Eidesstattliche Erklärung.....	ii
Affidavit	ii
1. Theoretical background.....	1
1.1 The Viscose Process.....	3
1.1.1 Production of pulp for synthetic fiber synthesis	4
1.1.2 Viscose production	6
1.1.3. Viscose regeneration.....	8
1.1.4 Post-treatment of fibers and cutting process	9
1.2. Fiber modification	10
1.2.1 Influence of fiber parameters on the fiber properties.....	10
1.2.2 Surface treatments.....	11
1.2.3 Flame retardant fibers.....	12
1.2.4 Dyeing of regenerated cellulose fibers.....	14
1.2.5 Inorganic nanostructured materials for antimicrobial and further modifications.....	14
1.3 About metal sulfides, their properties and technical applications	16
1.3.1 Silver sulfide	17
1.3.2 Copper sulfide	17
1.3.3 Tin sulfide	18
1.3.4 Nickel sulfide	18
1.3.5 Zinc sulfide.....	18
1.3.6. Iron sulfide.....	19
1.3.7 Metal sulfide alloys.....	19
2. Research objectives.....	21
3. Experimental	22
3.1 Synthesis of alkali cellulose	22
3.1.1 Storage stability of alkali cellulose	22
3.2 Xanthation of alkali cellulose.....	23
3.2.1 Aging experiments with self-made viscose solution	24
3.2.2 Determination of the capillary viscometer constant k.....	24
3.3 Development of a lab scale fiber spinning process.....	25
3.3.1 Influence of the aging process and sulfuric acid concentration.....	25
3.3.2 Effect of spinning needle.....	26

3.4 Development of an automated fiber spinning process.....	26
3.4.1 Operation of the lab scale fiber plant	27
3.5 Synthesis of metal sulfide containing viscose fibers	28
3.5.1 Synthesis and structure investigation of metal sulfide containing fibers	28
3.5.2 Metal uptake in fibers in dependence of metal concentration in spinning solution	30
3.5.3 Correlation between viscose age and metal uptake	30
3.5.4 Particle size in correlation to viscose age, regeneration time and acid concentration	30
3.5.5 Effect of tempering on nickel sulfide particles.....	31
3.6 Experiments with tungsten oxide and tungsten sulfide in the Viscose	31
3.6.1 Incorporation of tungsten(VI)oxide into the viscose solution.....	31
3.6.2 Incorporation of tungsten(IV)sulfide into the viscose solution.....	32
3.7 Synthesis and investigation of cellulose and metal containing films	32
3.7.1 Cellulose film synthesis and storage stability.....	32
3.7.2 Metal containing cellulose films.....	33
3.7.3 Preparation of CuS containing films for microbiological tests	34
3.8 Antibacterial testing of cellulose films according to EN ISO 20743	34
3.9 Sample preparation and parameters for the different analytical methods.....	35
3.10 Used chemicals and materials	36
4. Results and discussion.....	37
4.1 Alkali cellulose	37
4.1.1 Storage stability of alkali cellulose	38
4.2 Xanthation	41
4.2.1 Investigation of the xanthate aging.....	42
4.3 Evaluation of suitable fiber spinning conditions	45
4.3.1 Structure analysis of the resulting fibers.....	47
4.4 Automation of the viscose spinning process.....	49
4.5 Metal sulfide containing viscose fibers	50
4.5.1 Results for the fiber spinning experiments in copper(II)chloride spinning bath.....	50
4.5.2 Results for the fiber spinning experiments in a tin(II)chloride spinning bath.....	55
4.5.3 Results for the fiber spinning experiments in a nickel(II)chloride spinning bath.....	57
4.5.4 Results for the fiber spinning experiments in a cobalt(II)chloride spinning bath	60
4.5.5 Results for the fiber spinning experiments in an iron(III)chloride spinning bath	61
4.5.6 Results for the fiber spinning experiments in a zinc(II)chloride spinning bath.....	63
4.5.7 Results for the fiber spinning experiments in a silver(I)nitrate spinning bath.....	64
4.5.8 Determination of the amount of metals fixed through fiber synthesis	66

4.5.9 Cross section analysis to investigate the fiber / metal sulfide interfaces	68
4.5.10 Final investigation to check if the presence of metal effects the regeneration step.....	70
4.6 Correlation between viscose age and metal uptake	71
4.7 Investigation of the particle size in correlation to process parameters.....	72
4.8 Incorporation of tungsten oxide and tungsten sulfide into the viscose	74
4.8.1 Results for the incorporation of WO_3 into the viscose.....	74
4.8.2 Results for the incorporation of WS_2 into the viscose solution	76
4.9 Cellulose films and the uptake of metal sulfides onto the film matrix	77
4.9.1 Storage experiments with cellulose films.....	77
4.9.2 Metal uptake in cellulose films during the regeneration step	79
4.10 Metal sulfide containing films in antibacterial studies	80
4.11 Conclusion	82
5 Appendix.....	83
5.1 List of figures	83
5.2 List of tables.....	85
5.3 List of references	86

1. Theoretical background

Basically fibers can be divided into two main groups, naturally occurring fibers and man-made fibers. Naturally occurring ones can further be classified as fibers with a protein matrix and fibers consisting of cellulose.

For the man-made fibers the variation of the basic materials is more manifold. There exist three sub groups which give a first overview about the materials the fibers are built up from. These three possible materials are either natural polymers, synthetic polymers or inorganic substances.

In the case of man-made fibers from natural polymers an equal subdivision as for naturally occurring fibers can be undertaken. Table 1 gives an overview of the different fibers available for textile and technical applications. (1)

Table 1 Overview of different fiber types used in textile and technical application (1)

Fibers					
Natural fibers		Man-made fibers			
		Natural polymers		Synthetic polymers	Inorganic substances
From protein	From cellulose	From cellulose	From protein	Polyester	Carbon
Wool	Cotton	Viscose	Casein	Polyamide	Glass
Silk	Linen	Lyocell	Collagen	Polypropylene	Ceramics
Angora	Manila	Cupro	Ardein	Polyurethane	Metals
etc.	etc.	etc.	etc.	etc.	etc.

In the years before 1900, the most common sources for the production of textiles were natural based fibers, like cotton, jute or flax. In the 19th century some important discoveries and developments were achieved in the chemical industry, which will later be declared as the basic discoveries for the production of man-made fibers. (2) (3)

The first important step was the extraction of cellulose from wood and the simultaneous characterization of the glucose as the basic molecule in the cellulose 1837 by Anselme Payen. (4) In 1848 Schönbein discovered the solubility of nitrocellulose in ether and alcohol and only a few years later, in 1857, Schweizer discovered the solubility of cellulose in cuprammonium solutions. (5) (6) Both scientists described their resulting solutions as very viscous, but neither Schönbein nor Schweizer realized the importance of their discoveries and so further 30 years passed by till Svan used the process developed by Schönbein to

produce carbon fibers for electric bulbs from nitrocellulose. Svan dissolved nitrocellulose as described by Schönbein and regenerated it later via injecting the viscous solution into a regeneration bath. 1884 Svan realized that the resulting fibers have a wonderful shining and that they may be useful in textile industry. (7)

Already 1885 the first plant for the production of artificial silk opened in France, the daily output was between 50 and 100 kg per day if nothing went wrong. Parallel to the production of nitro silk also the process upscale for the production of cuprammonium rayon takes place and finally in 1899 the “Vereinigte Glanzstoff Werke” started their production in Eiberfeld. (3)

Parallel to the beginning cuprammonium rayon production, a further important development in artificial silk production was done by the three scientists Cross, Bewan and Beadle. They discovered the reaction of alkali cellulose and carbon disulfide to cellulose xanthate and the solubility of cellulose xanthate in a diluted sodium hydroxide solution.

Later they called their product viscose and early after their discoveries a third artificial silk, the so called viscose silk was available on the markets. (3) (8)

Rapidly the viscose silk conquered the markets and replaced artificial silks made from nitro cellulose and cuprammonia. In Figure 1 the world wide fiber production from 1900 up to 2008 is illustrated, the increasing importance of man-made fibers from different sources is clearly visible. (3)

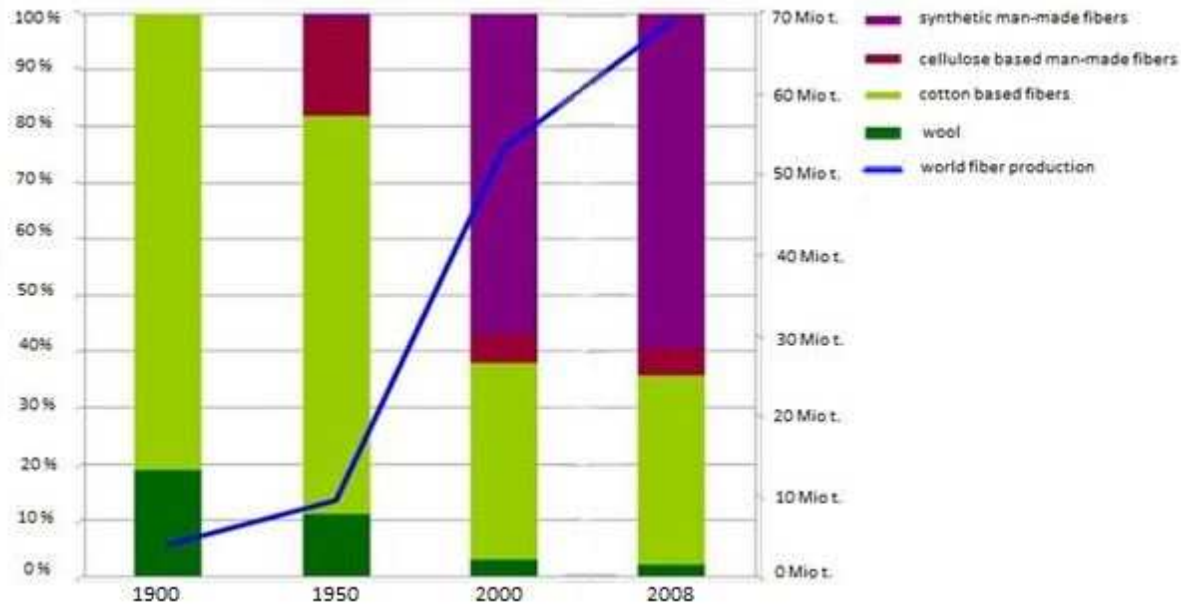


Figure 1 Worldwide fiber production from 1900 up to 2008 (2)

1.1 The Viscose Process

Due to the importance of the viscose process in the practical part of the master thesis, this process is explained in the following pages in detail. Figure 2 gives an overview of the main steps and process flows involved in the viscose fiber process and should facilitate to follow the explanations of the single process steps below.

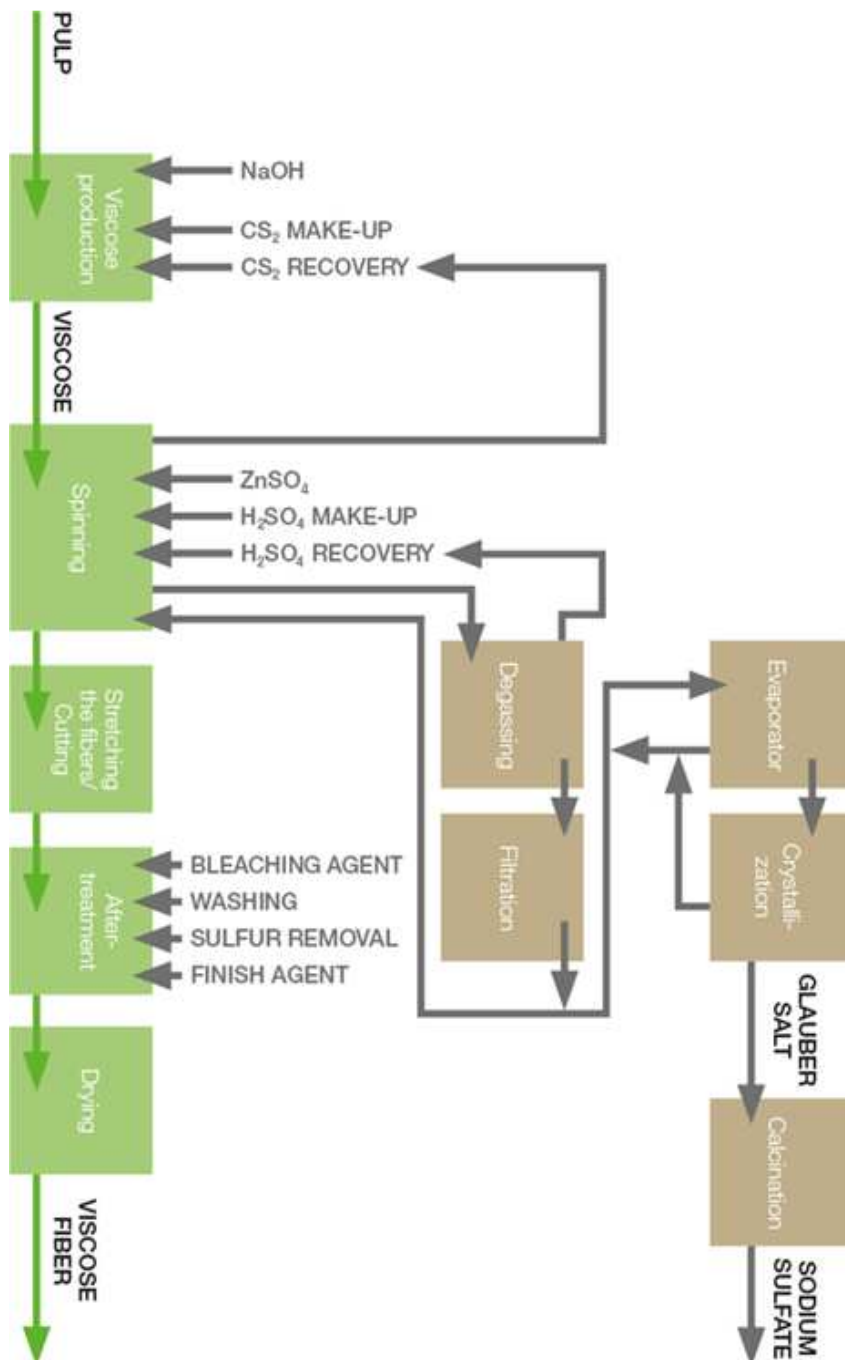


Figure 2 Flow scheme for the viscose process with all the process streams involved (1)

Cellulose occurs as 1–4 linked β -D-glucose long chained polymer, with hydroxyl groups on C2, C3 and C6, which cause lots of varying intramolecular and intermolecular interactions between the single glucose units. The manifold inter- and intramolecular interactions leads to the formation of different polymorphs. The most important forms of cellulose involved in the viscose process are cellulose I and cellulose II.

In cellulose I two intramolecular interactions (O2H-O6 bonding and O3H-O5 bonding) and one intermolecular bonding (O6H-O3) connect the cellulose macromolecules.

In cellulose II three intramolecular bonding's (O2H-O6 bonding, O3H-O5 bonding and O2H-O2 bonding) and two intermolecular interactions (O6H-O2 and O6H-O3) are present. (9) The different inter- and intramolecular bindings of cellulose I and cellulose II are illustrated in Figure 3.

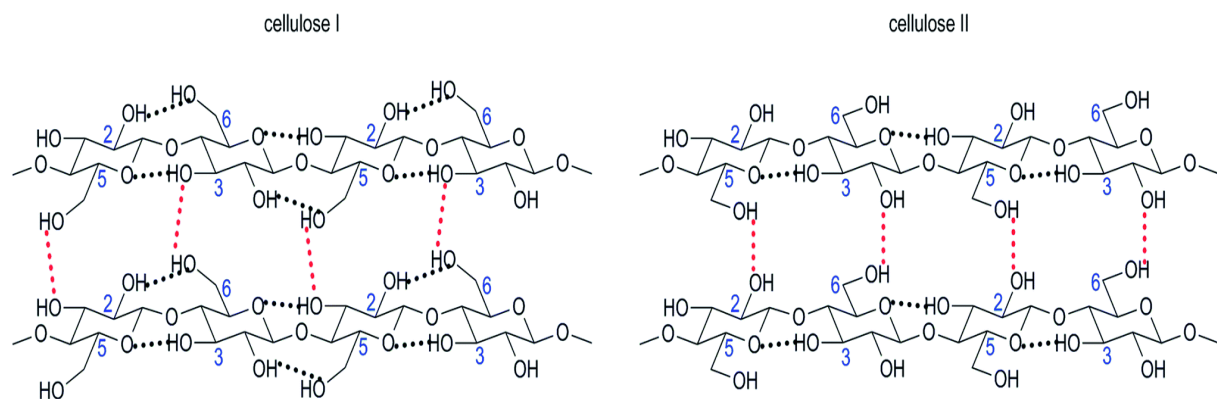


Figure 3 Overview of different intermolecular and intramolecular bindings in cellulose I and cellulose II (10)

1.1.1 Production of pulp for synthetic fiber synthesis

As pulp, the lignocellulosic material obtained through chemical or mechanical treatment of wood, crops and recycled paper is designated. In the past, many different processes for the generation of pulp stemming from diverse materials have been developed, but not all of these processes generate pulps suitable for the viscose fiber production. One of the processes providing a pulp suitable for fiber production is the so called magnesium-bisulfite process developed by the Lenzing company.

A pulp useful for fiber synthesis, should consist out of 90% α -cellulose. Alpha-cellulose is also called normal cellulose and represents the part of the cellulose which doesn't dissolve in 17.5 wt% sodium hydroxide solution, besides α -cellulose also β - and γ -cellulose occur in wood. In other words α -cellulose is the technically useable macromolecular form of

cellulose. (11) Due to the fact that the beech wood used for the process contains only 38% to 40% α -cellulose and about 60% other materials (25% lignin, 20% pentosane, 14% further hemicelluloses and 1 to 3% other ingredients) a complex separation and purification process is necessary.

The most difficult step in the process is the separation of α -cellulose from the two other major organic fractions, because of the similar chemical behavior of these compounds. In the magnesium bisulfite process hydrogen bisulfite, sulfur dioxide and magnesium oxide are the reactive compounds responsible for the pulp extraction. The hydrogen bisulfite [HSO_3^-] reacts under increased pressure and temperature with the lignin and the hemicelluloses to salt like structures, which become soluble after further reaction with sulfur dioxide. The degradative reaction can be described as hydrolysis where the glycosidic linkages are cleaved. The success of the cooking process depends strongly onto the mixing ratio between SO_2 and MgO and on other process parameters.

A reaction between the process chemicals and the desired α -cellulose is more or less prohibited due to the dense, mostly crystalline structure of the α -cellulose and the therefore around 30 times slower hydrolysis reactions of the process chemicals with the cellulose.

A complete separation between cellulose and lignin is, despite the slower degradation of the cellulose in comparison to the lignin, counterproductive because after the lignin concentration decreases down to a certain level, the degradation of the α -cellulose increases.

The cellulose chains in pulp used for synthetic fiber production can be shorter compared to the chains in pulp used for the paper production and hence the pulp process applied in fiber production yields a nearly completely opened wood. The resulting pulp remains only about 1.5% lignin, which is further removed in the following bleaching and cleaning steps. (12)

1.1.2 Viscose production

a) Alkali cellulose

The production of alkali cellulose is an important step in the mercerization process, the viscose production and the synthesis of various cellulose ethers. While the alkali treatment of cellulose during the mercerization is used to change the intermolecular bonds between the single cellulose chains, in the viscose production and also in the etherification reactions of cellulose, the alkali treatment is executed to create alkali cellulose from cellulose in a high percentage, besides breaking the supramolecular structure of the cellulose. The synthesis of sodium alkoxides is important for the following xanthation reaction in the viscose process.

In many studies, the properties of NaOH solutions in varying concentrations, as cellulose swelling agent or as cellulose solvent were investigated. At sodium hydroxide concentrations of more than 30 wt% and temperatures of 40 °C sodium hydroxide solutions dissolve cellulose, at least to large parts. It was further determined that concentrations of at least 18 wt% sodium hydroxide are needed to reach the maximum sodium exchange. At this point around 2 hydroxyl groups of the anhydrous glucose unit (AGU) are deprotonated. Between 18 wt% and 25 wt% the uptake of sodium hydroxide into the cellulose matrix can be described as sluggish. Below concentrations of 9 wt% sodium hydroxide, the deprotonation of the AGU only appears at the primary alcohols because they are much easier available for the deprotonation. Above 9 wt% sodium hydroxide also the secondary alcohols become deprotonated. (13) (14) (15)

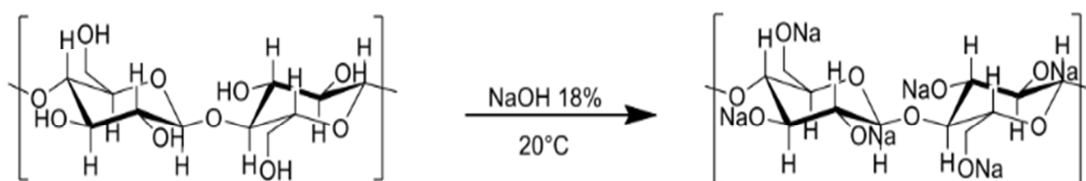


Figure 4 Illustration of the alkali cellulose synthesis, with corresponding reaction conditions and exorbitant NaOH charge

A further interesting fact is that the crystallinity is strongly decreasing with increasing sodium concentration whereas the disorder number k , which is an index for the order in the crystalline area, stays nearly constant. As a consequence it can be argued that the degree of crystallinity is already rapidly decreasing before the lattice change from cellulose I to cellulose II takes place. (13)

The alkali cellulose itself is pressed after immersion in the base solution and aged for some days. During the aging process the cellulose chains are further contracted to a degree of polymerization of around 300, which seems to be a suitable chain length for the xanthation process. (16)

b) Xanthation

Viscose process properties and also the parameters of the resulting fibers are heavily influenced by the ongoing reactions of carbon disulfide with alkali celluloses during the xanthation process. The substitution of sodium alkoxides with carbon disulfide for the formation of the so called cellulose sodium xanthate takes place at C2, C3 or C6. It was demonstrated that substitution is preferred at the primary hydroxyls at C6 because of their higher accessibility. This statement is valid for a degree of substitution (DS) between 0.3 and 0.7, the typical DS range used in technical processes. With increasing DS the number of C2/C3 substitutions increases too, which is probably caused by the saturation of the primary alcohols. The resulting cellulose xanthate is afterwards dissolved in a diluted sodium hydroxide solution to obtain the final spinning solution, called viscose. (17)

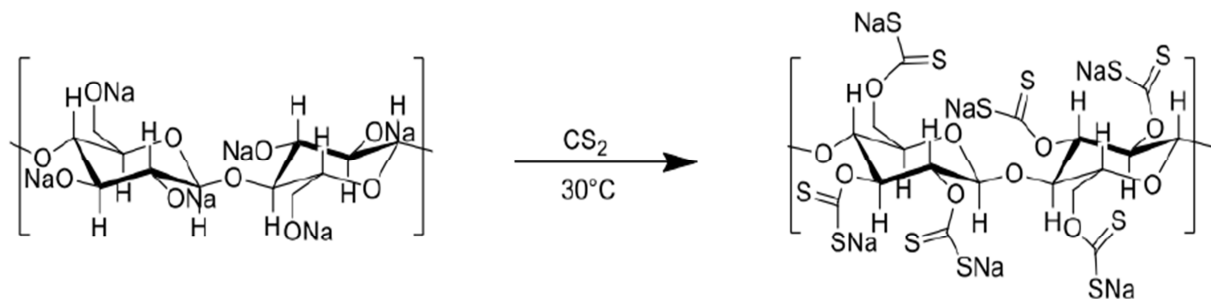


Figure 5 Illustration of the xanthation reaction with exorbitant substitution shown in the figure

The solution obtained directly after dissolving the cellulose xanthate is hardly spinnable. An aging process of several hours up to a few days depending on the regeneration process used and the fiber parameters desired is required to obtain a suitable spinning solution. During the aging process two major reactions take place, namely depletion of thiocarbonates from the cellulose xanthate and reactions between the depleted thiocarbonates and the sodium hydroxide are observed. The depletion speed of thiocarbonates is heavily influenced by the reaction temperature, e.g. an increase of 10°C leads to an 2.4 times faster depletion.

Freezing viscose at low temperatures leads almost to a complete stop of the aging process and allows a storage up to several weeks. (14)

1.1.3. Viscose regeneration

After aging, the viscose is regenerated into an acidic spinning bath to cleave the xanthates and to generate cellulose hydrate. The depletion of the xanthates is caused by the acid itself, but if the spinning bath contains diluted acid only, the resulting cellulose II materials are not really useable. In this case, coagulation and degradation of the cellulose xanthates proceed fast, resulting in fibers with a rather porous and rough structure. Therefore, complex spinning baths have been developed, to slow down coagulation and regeneration reactions while simultaneously preventing the fibers from harmful effects caused by the acid.

In the past decades, many different salts were tried as spinning bath supplements and their effects are described extensively in literature. The most important information gained from these investigations is that the exact composition of the spinning bath has to be adjusted on the viscose age and the desired fiber parameters. A spinning bath for 'normal' fiber spinning processes without any special features contains around 72% water, 10% sulfuric acid, 12% sodium sulfate, 5% magnesium sulfate and 0.5% zinc sulfate.

Due to the complex composition of the spinning bath, many different main and side reactions are initiated through the injection of the viscose into the bath. The most important reaction is the breakdown of the cellulose xanthate to cellulose II and CS₂. The thiocarbonates released in the viscose during the aging process react with the sulfuric acid and form CS₂ and H₂S.

Carbonic acid [H₂CO₃] is also formed during the regeneration process due to a reaction of sodium hydroxide and CS₂.

The mostly gaseous side products released during the spinning process cause two major problems. On the one hand the sulfur containing, gaseous compounds are toxic and on the other hand the released compounds are responsible for the bad smell around the production sites too. (18) (14)

The regeneration of the cellulose chain fragments dissolved in the viscose, starts already during their flow through the spinneret, because the single chains are adjusted in the flow direction and a first near range order develops. The first parts of the viscose which get in

contact with the spinning bath are the outer layers of the developing fiber strain. Hence a thin cellulose skin is developed around the inner viscose solution, which has to be penetrated by the spinning bath to initiate the coagulation of the inner cellulose xanthate. The degree of orientation decreases in the direction from the outer side of the cellulose fiber to the inner side. This can be explained by the fact that the inner parts of the viscose flow are more restricted than the outer parts of the flow and therefore the executed pulling force is higher in the outer layers, which causes a higher orientation of the cellulose strains in the outer parts of the fiber. (14)

1.1.4 Post-treatment of fibers and cutting process

The generated viscose fibers include many contaminations like acid residues, sulfur and various salts and therefore have to be purified and further treated in a row of post spinning baths

a) De-sulfurization bath

The de-sulfurization of the fibers is the first step in the post treatment. The sulfur fixed in the outer fiber matrix is removed easily through washing the fibers in hot water. The sulfur fixed in the inner cellulose matrix is removed in the same bath with the help of additional sodium sulfide in a concentration range of 1 up to 3 g/L, to convert the sulfur into thiocarbonates and polysulfides. (14)

b) Bleaching bath

As bleaching compounds, sodium hypo-chlorite and hydrogen peroxide are used. The chloride concentration in the bath is somewhere between 0.7 g and 1.5 g active chloride per liter, but depends strongly on the color of the unbleached fibers and on the desired degree of whiteness. (14)

c) Brightening bath

This bath is also called "Avivage bath" and represents the final step in the post fiber treatment. The function of the avivage bath is to balance the differences between normal and synthetic fibers and hence to ensure a trouble free processing of viscose fibers to textiles and non-wovens. Natural and synthetic cellulose fibers for example differ in friction and warping properties, because synthetic cellulose fibers do not contain any natural waxes,

due to the production process. The avivage is coated in thin layers onto the fiber surface, to modify the fiber surface and to compensate for the missing effects of natural fibers. As basic materials herbal, mineral, animal fats, oils or various waxes are used in many variations. The typical avivage concentrations vary between 2 and 5 g per liter. (14) (19)

Fiber cutting and drying

The cutting of the endless fiber filament is either done before or after the post treatment process. The most important thing in the cutting process is a continuous and repeatable fiber length.

The drying of the viscose fibers is usually performed after the cutting step and starts with a centrifugation or squeezing step followed by a finite drying step in dryers at 40 to 80°C. Higher temperatures would cause a decrease in the degree of polymerization. (14)

1.2. Fiber modification

The modification of synthetic cellulose fibers has attended great interest due to its large influence on various fiber properties. Modification of cellulose fibers can be achieved in many different ways. One of the most important modification techniques is the incorporation of functional additives into the fiber matrix. Some modifications based on this principle, have already reached great success in technical and industrial applications. The most important examples are flame retardant fibers, synthetic and natural polymer fiber composites, like chitin incorporated viscose, and dye variant rayon's. (20) (21)

1.2.1 Influence of fiber parameters on the fiber properties

Although regenerated cellulose fibers are already suitable for many different processes due to their manifold properties like hydrophilicity, absorbency, skin friendliness, mechanical and thermal stability, in some cases they have to be further modified to increase the range of applications. Fiber modification is performed via many different physical and chemical ways, one of the rather simple ways is the adjusting of fiber parameters to improve performance. (22)

Fiber length

The length of the fiber correlates directly with the bending stiffness and the embedding in fiber composites and hence a change in the length has a large influence in the processing and product qualities. (22)

Fiber fineness

Fineness is calculated by dividing the fiber mass through the fiber length and represents the cross section area of a fiber at given density. Usual viscose fibers possess a diameter of 6 to 30 μm which corresponds to 0.5 up to 30 decitex. (1 decitex equates to 1 g/10000 m) (22)

Cross section

A mature parameter to influence fiber properties is the cross section area. Varying cross sections change the fiber stiffness or the fluid absorbency due to the formation of capillaries for example. (22)

1.2.2 Surface treatments

Despite all the excellent properties of cellulose and regenerated cellulose fibers discussed above there are still some problems, as the poor resistance to moisture absorption, which limits the use of cellulose. To bypass these problems, many different surface manipulation technologies are available, a few of them are discussed below. (23)

Mercerization

Alkali treatment of fibers causes a breakdown of the fiber bundle to smaller pieces and hence a reduction of the fiber diameter, a better fiber matrix adhesion, an increase in mechanical properties and an increase of possible reactive sites is caused. (24)

Acetylation

Acetylation is the reaction of cellulose hydroxyl groups with acetic anhydride substitutes. The technique is originally applied to wood cellulose, to stabilize the cell walls against moisture uptake and biological degradation. (25)

Etherification

New properties of cellulose can be realized by etherification. An important role in this process is the previously described mercerization, which transfers the OH groups into more reactive intermediates. Epoxides, allyl bromides or benzyl chlorides are only a few substances used for the modification of cellulose and lead to cellulose derivatives with high shear stability or to extrudable cellulose compounds for example. (26)

Graft copolymerization

The basis of this process is the formation of an active site on a preexisting polymer backbone and the following reaction of these active groups with an appropriate monomer to a graft copolymer. Grafting of vinyl and allyl cellulose derivatives with maleic acid ester are frequently applied examples. (27)

1.2.3 Flame retardant fibers

The main developments in the evolution of flame retardants for natural as well as synthetic fibers have been achieved in the time between 1950 and 1980, in this time frame, a broad range of useable and recommended flame retardants based on many different chemical and physical principles has been developed. The last 20-30 years no real improvements in flame retardant chemistry were reached, with the one exception of increasing interest in nanostructures as flame retardants. In the following, the main concepts behind the varying flame retardants and the most common substances used, are presented. (28)

Gas theory

The flame retardant dissociates at elevated temperatures and forms inert or hardly oxidizable gases. Hence the resulting pyrolysis gases are diluted and the supply of oxygen is limited. The most important gases involved in these processes are carbon dioxide, ammonia, hydrogen chloride and sulfur dioxide. Flame retardants following this principle are composed of ammonium salts or carbonates. The advantage is the cost competitiveness of the used materials, while disadvantages comprise secondary reactions as the evolution of aggressive gases and washing instabilities. (29)

Coating theory

Inorganic phosphor-, boron- and silicon- compounds have their melting point below the flame temperature of cellulose fibers and hence the textiles are coated and therefore protected through these glassy melting's. (29)

Heat abstraction

In this technique, the majority of the heat is transferred away from the textiles through a spontaneous endotherm reaction of the flame retardant. Endothermic reactions which enable the heat transfer could be water depletion, as it is the case in the frequently used hydrous aluminum sulfate, or melting reactions or decompositions. (29)

Chemical theory

Another possibility to hinder flammability is to control the decomposition of the cellulose matrix via of dehydration or char evolution. The most prominent compounds in this class are alkalis (alkali silicates, ammonium phosphates and ammonium sulfates), acids (phosphoric acids and their salts and organic phosphor compounds) and oxidizing agents.

The acid catalyzed dehydration, shown in Figure 6, leads to a cellulose residue with a high carbon content which is much more flame resistant. (29)

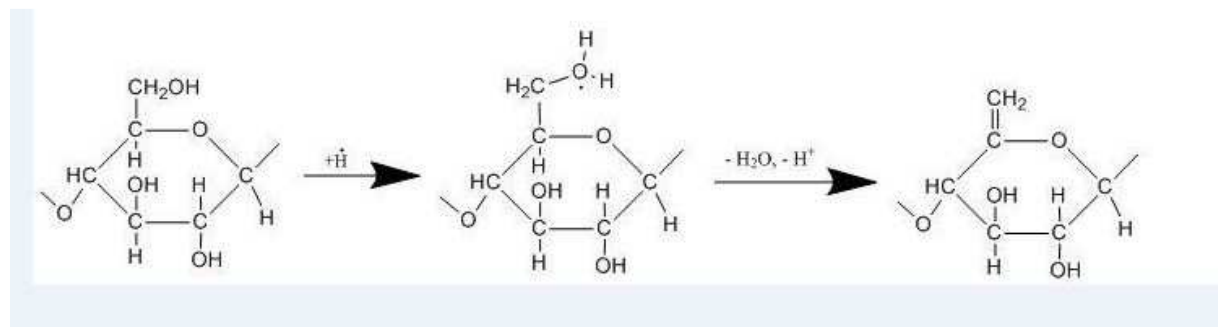


Figure 6: Acid catalyzed dehydration of cellulose (29)

Another chemical way to prevent cellulose from burning is to capture the free radicals accruing during the burning process with scavengers like chlorine or bromine radicals.

The most important factor in the production of flame retardant textiles, is the upset technology used. The two easiest technologies are up-drying and up-condensation of the flame retardants onto the textiles, but both processes bear some important disadvantages such as washing and drying instabilities.

A better method is the direct incorporation of flame retardants into the fiber matrix either through addition of the chemicals into the viscose solution before spinning (for example mixing of halogenated phosphoric ester into the viscose) or their addition to the cellulose fibers through chemical binding onto the hydroxide groups of the cellulose in the fiber post treatment process. (29)

1.2.4 Dyeing of regenerated cellulose fibers

Among all the different fiber modifications, fiber dyeing is one of the most important modifications because it allows the use of regenerated cellulose fibers in clothing, drapery and many other industrial areas which depend on colored fibers.

Cellulose fibers are commonly dyed with direct, reactive, vat and azotic dyes, consisting mostly of anionic diazo or triazo compounds. The dyeing process itself is controlled by the transport and diffusion of the anions from an aqueous bath containing an electrolyte and hence by the attraction between the dye anions and the nonionic cellulose matrix. Different types of intermolecular forces are involved in the sorption of dyes on the fibers. Because cellulose shows a strong hydrogen bonding to water, the hydrogen bonds alone cannot cause the sorption of dyes, rather a combination of relatively weak forces, including van der Waals forces are responsible for the sorption. In order to facilitate dyeing of cellulosic materials very often cationization of the cellulose is accomplished to increase the amount of adsorbed dye. (30)

1.2.5 Inorganic nanostructured materials for antimicrobial and further modifications

One suitable substrate for the growth of microorganisms are textiles, especially in the warm and humid atmosphere around the body. Therefore, the investigation of antimicrobial textiles has attracted major research interest in the last years. The use of inorganic nanostructures, which have already shown their antimicrobial properties in several investigations, is one potential alternative to classic antimicrobial agents.

Titan dioxide nanostructures

A high stability, long lasting, high safety and the broad spectrum antibiosis as well as the photocatalytic activities are only some of the unique properties of TiO₂ nanoparticles. These properties allow the input of TiO₂ in self-cleaning, environmental purification, solar cells and gas sensors beside their use as antimicrobial agents. (31) (32)

Silver nanoparticles

Silver nanoparticles as antimicrobial agents are in the focus of science since ancient times. In comparison to other organic and inorganic antimicrobial agents, silver is demanded to be safe. The antimicrobial effect of silver is proven against more than 650 pathogenic organisms. Similar numbers can be derived for silver ions and nano particles, which are also declared as non-toxic. Through the use of nano silver the antibacterial effects can even be increased due to the increasing particle number. The antibacterial effect of silver is induced by a multiple interaction of silver with pathogens, including an inhibition and damage of the enzyme system responsible for growth and viability and a rupture of bacteria membranes. The addition of sulfur enhances the antibacterial properties and the stability of silver ions according to Jeong et al. (33) (34) (35) (36)

ZnO nano structures

Besides TiO₂, zinc oxide is a further n-type semiconductor. Zinc oxide is applied in solar cells, photo diodes, displays and many other piezoelectric devises. Further, it is used in sun creams to protect human skin. Compared to silver, zinc nano particles have some advantages like lower costs, higher availability and the ability to block UV light. Also in textile applications ZnO is already used because of its manifold properties. A mature application for zinc oxide in textiles is the antibacterial effect, which is already investigated and confirmed in many studies. As a consequence of their strength and high Young's-modulus they are used as anti-sliding and wear resistant increasing phases too. (37) (38) (39)

Copper nano particles

Copper has been tested as UV protector, electric conductor and antimicrobial agent in textile applications. For the antibacterial tests, it can be said that an antibacterial activity exists, but less than in silver. The conductivity could be increased significantly through the incorporation of copper particles. (40)

Gold nano particles

With gold, the third precious metal is tested as property-enhancing nanostructure for textiles. Studies have shown that gold inhibits the growth of fungi, as well as gram positive and gram negative bacteria. (41)

Table 2 Overview of possible applications for different inorganic nano structures on cellulosic fibers (42)

<i>Inorganic material</i>	<i>Characteristics and possible applications</i>
<i>TiO₂</i>	Antibacterial, photo-catalyst, self-cleaning, UV protecting, water and air purifier, gas sensor, solar cell, co catalyst for cotton crosslinking
<i>Ag</i>	Antimicrobial, disinfectant, electrical conductive, UV protection, anti-fungal
<i>ZnO</i>	Antibacterial, UV blocking, super hydrophobic, photo catalyst
<i>Cu</i>	Antibacterial, electrical conductive, UV protection
<i>Au</i>	Antimicrobial, electrical conductive

1.3 About metal sulfides, their properties and technical applications

The combination of inorganic and organic materials also called hybrid materials provides a group of highly interesting and multifaceted adjustable class of materials with a wide range of possible applications, which relates to their versatile chemical and physical properties. One especially interesting class of hybrid materials, the so called nanocomposites, are accessible through incorporation of inorganic nanocrystals with special properties (e.g. antibacterial) into a polymer matrix. Nanocomposites allow for the combination of easy and processing methods for polymers with all the special application properties provided by inorganic materials, in this case metal sulfides. (43) Metal sulfides in combination with organic matrices are for example used in photochromic- and electroluminescent devices, and in polymer–nanoparticle hybrid solar cells so far. (44) (45) (46)

So, due to the enormous interest in hybrid materials also the possible applications for metal sulfide containing viscose fibers should be discussed and therefore in this chapter, the most interesting properties and applications of some metal sulfides which can be fixed on the viscose fibers are summarized.

1.3.1 Silver sulfide

Ag_2S is one of the most important metal sulfides, because it is a direct narrow band gap (1.1 eV) semi-conductor and it is often used in photo catalysis, for example in the photocatalytic degradation of organic pollutants, H_2 production via photo catalysis and in solar cells. (47) (48) In addition to the application of silver sulfide in photocatalytic processes, Ag_2S is also used in the form of quantum dots for fluorescence labelling of biological objects. Because aqueous solutions of Ag_2S are non-toxic, an application in biological systems seems to be another promising field for the use of silver sulfide. (49)

1.3.2 Copper sulfide

Since the photocatalytic activity of CuS in contact with CdS is recognized, increasing interest in the copper system is observed. Additionally to CuS also three other stable CuS phases (chalcocite Cu_2S , djurlite $\text{Cu}_{1.95}\text{S}$ and anilite $\text{Cu}_{1.75}\text{S}$) exist at room temperature. Copper sulfides already posses a wide range of applications, in the form of copper sulfide thin films for example they are used in photothermal conversion, photovoltaic units, electroconductive electrodes and also in microwave shielding or solar control coatings. (50) (51) (52) Another field of application is the photocatalytic degradation of organic pollutants caused by copper sulfide nanostructures. (53)

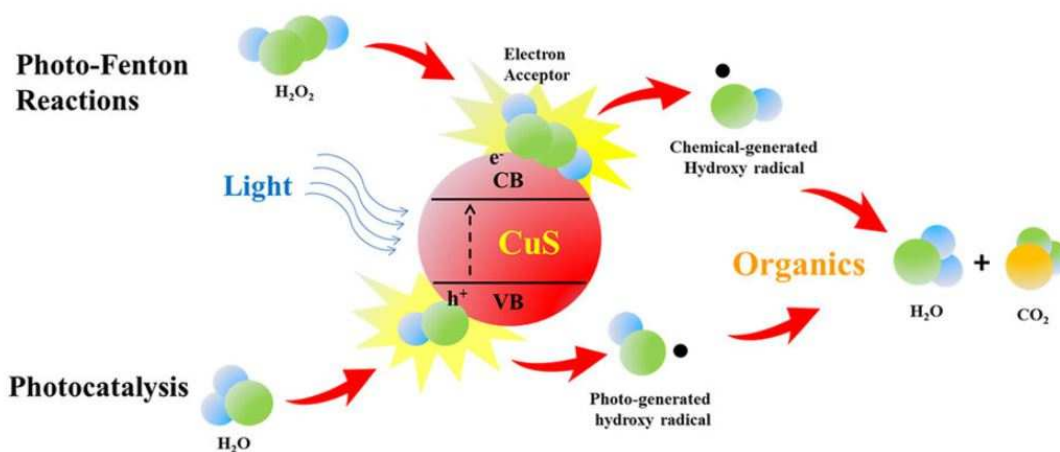


Figure 7 Nano crystalline copper sulfides as photo catalysts in the degradation of organic pollutants (53)

1.3.3 Tin sulfide

The use of tin sulfide, a semiconductor compound for groups IV to VI, is a promising alternative in solar cell applications due to the large optical absorption coefficient of 10^4 and the direct band gap of 1.2 – 1.75 eV. Furthermore SnS is relatively inexpensive and nontoxic compared to other materials used and both elements appear frequently on earth. (54) (55) (56)

Another industrial application for tin sulfides is their use as friction minimizer in a wide temperature, speed and pressure range through the development of a third body layer. Due to the raising third body layer the wearing, for example in brake discs, is reduced. (57)

1.3.4 Nickel sulfide

Due to its outstanding electro catalytic and electrochemical properties also nickel sulfide aroused attention, like many other metal sulfides did in this area too. (58) Nickel sulfide is mainly used in energy conversion and storage devices like supercapacitors, batteries, oxygen and hydrogen evolution reactions or solar cells. (59) (60) (61) (62) The downsizing to nanoscale NiS structures as nanoparticles, nanotubes or nanoframes is one of the most important things for the use of NiS in electrical storage devices, because it leads to a boost in the electrochemical activity of NiS. (63)

1.3.5 Zinc sulfide

Group II to IV semiconductors like ZnS are often discussed as important semiconductors in a wide range of technical applications like in photo catalytic processes for the decomposition of organic pollutants. Beside the other semiconducting metal sulfides, zinc sulfide is favored because of its high chemical stability, its classification as non-toxic and its environmental safety. Further arguments for the application of zinc sulfides are the high thermal stability, the high electron mobility and excellent transport properties. (64) (65) (66)

Zinc sulfide exists in two known crystalline forms, sphalerite (cubic phase) and wurtzite (hexagonal phase), both with a band gap of around 3.6 eV at room temperature (67) (68)

1.3.6. Iron sulfide

Beside the already listed classical uses for metal sulfides as high energy density batteries, solar energy materials, starting materials for the synthesis of superconductors or photo electrolysis, iron sulfides are also recognized as sufficient adsorbents for heavy metal ions in the waste water treatment and purification. (69) (70) (71)

1.3.7 Metal sulfide alloys

Because all the above discussed semiconducting metal sulfides can be mixed to alloys, combining the single properties, there is also extensive literature on the investigation, characterization and possible application of metal sulfide alloys.

One example are $\text{Ag}_2\text{S}/\text{ZnS}$ carbon nanofiber (CNF) ternary composites for H_2 production with a high photocatalytic performance. The hydrogen production from water through semiconducting photo catalysts, like varying metal sulfides, has attract increasing interest because it seems to be a possible strategy to solve problems in energy supply and environmental chemistry. (72)

ZnS appears as suitable semiconductor for H_2 production due to many arguments listed above, Ag_2S is used as co-catalyst, because of its ability to capture the generated electrons/holes and therefore enhancing the charge transfer, a phenomena with a large influence on the H_2 production. (73) (74) (75)

As organic matrix CNF is used because of its mechanical, physiochemical and electronic properties in combination with the large surface area and the chemical stability. (76)

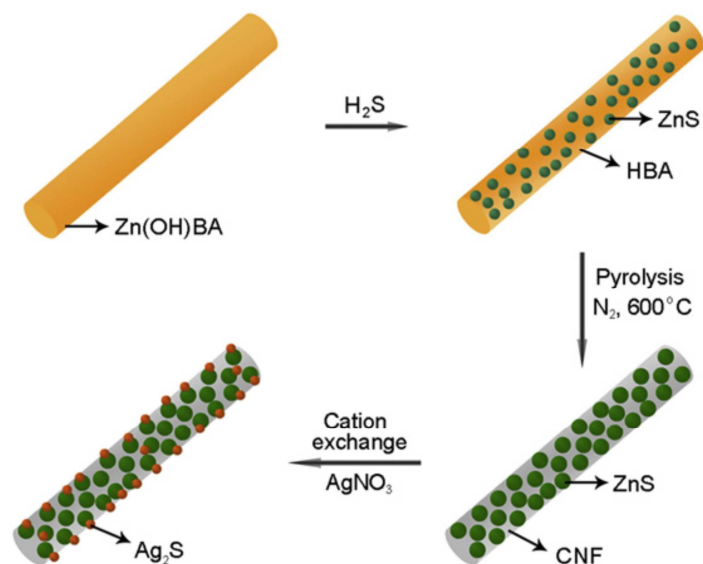


Figure 8 Production scheme for high performance hydrogen producing hybrid materials (72)

Figure 8 shows the production scheme for this high performance hydrogen producing nanocomposites. To sum the reaction way up, ZnS nanoparticles embedded in CNF are synthesized via in-situ sulfidation from ZnOH-benzoic anions to ZnS/benzoic acid. The synthesis is completed through a direct cation exchange between ZnS/CNF with the desired amount of AgNO_3 . (72)

In conclusion, there are a wide range of possible applications for metal sulfides and metal sulfide hybrid materials. Although most of the described applications are in contrast to the semiconducting properties of metal sulfides, there also exist a few other interesting possibilities for the application of metal sulfides in waste water purification and biological systems. (71) (49)

2. Research objectives

The major aim of this master thesis is to develop an in situ synthesis of metal sulfides in the course of the viscose process and the characterization of the resulting products by light microscopy, scanning electron microscopy, infrared spectroscopy, X-ray diffraction, and inductively coupled plasma mass spectrometry.

To reach these goals the following strategy is applied:

- The first important step is the development of a lab scale viscose production starting from cellulose I sources. The process development includes the mercerization of the starting material to alkali cellulose and the xanthation of the alkali cellulose to cellulose xanthate.
- The second important step is the upscale of the fiber synthesis from a staple fiber technology to an automated wet spinning process applicable in the laboratory. The generation of monofilament fibers is necessary because they behave different to staple fibers, and hence only data obtained by investigating monofilament fibers enable industrially applicable conclusions.

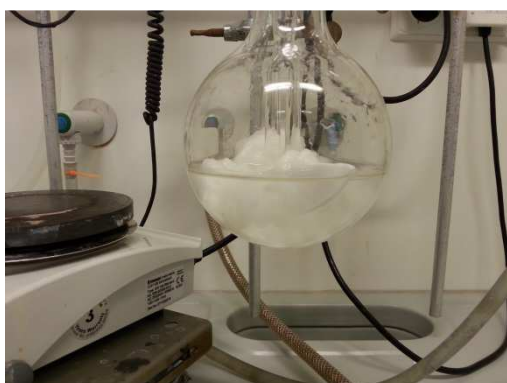
After production and characterization of the resulting products, also possible applications for the metal sulfide coated viscose products should be investigated.

3. Experimental

3.1 Synthesis of alkali cellulose

The synthesis of alkali cellulose is the first step on the way to the laboratory scale viscose fiber production. To ensure constant conditions for the synthesis of alkali cellulose, always the same starting material, a 100% pure cotton fleece is used. 5 g of this fleece are cut into small pieces of approximately 2 square centimeters in size. The cut cotton source is stirred with the aid of a KPG stirrer in 150 mL of an 18% NaOH solution for 2 hours at room temperature.

After stirring, the saturated cellulose is pressed manually and dried for 24 hours at room temperature. The dried alkali cellulose is stored at 4 °C in the fridge. The fundament for the synthesis of alkali cellulose is the synthesis directive: "Preparation of alkali cellulose" from reference (15).



b) Stirring of cut cotton fleece



a) Alkali cellulose after 24h drying

Figure 9 Alkali cellulose syntheses in laboratory scale a) stirring of cotton in NaOH solution b) 24h dried alkali cellulose

3.1.1 Storage stability of alkali cellulose

To gain some information about the storage stability of the self-made alkali cellulose, three experiments are performed, one to check the effects of the storage temperature, the second to investigate the effects of light on the stored alkali cellulose and the last one to observe the effects of remaining NaOH solution in the stored cellulose.

Storage temperature

The alkali cellulose is produced as described in 3.1. The resulting alkali cellulose is split into three equal fractions and stored at -18°C, 4°C and at room temperature for 30 days, with optical and IR-spectroscopic inspection after 7, 15 and 30 days.

Effects of light

Another batch of alkali cellulose is also divided into two equal fractions and stored for 30 days, one under the influence of daylight the other fraction under exclusion of light with optical and IR-spectroscopic inspection after 7, 15 and 30 days.

Effects of remaining NaOH solution

After the cellulose is stirred for two hours in NaOH solution, the remaining liquid is usually removed by pressing. However, in this experiment the alkali cellulose is stored without pressing the alkali cellulose. The effects of remaining NaOH solution is controlled optically and via IR-spectroscopy after 7, 15 and 30 days.

3.2 Xanthation of alkali cellulose

The xanthation of the previously produced alkali cellulose is the second reaction step in the synthesis of viscose fibers. For the xanthation reaction 7 g of alkali cellulose (dried for 24 hours) are placed in a three necked flask and preheated to 30°C via a water bath. After heating up the alkali cellulose, a KPG stirrer, a reflux cooler and a dropping funnel are fixed onto the flask. 10 mL of CS₂ are added dropwise to the slowly stirring alkali cellulose. The mixture is stirred for four hours at 30°C, resulting in an orange, sticky pulp. This pulp is dissolved in 200 mL NaOH (4 wt. %) over a period of three hours-while stirring. The final product is an orange solution ('viscose'), which represents the basic product for the production of viscose fibers. The viscose solution is characterized by IR spectroscopy. The fundament for the xanthation is the synthesis directive: "Xanthogenation"; according to a literature procedure. (15)

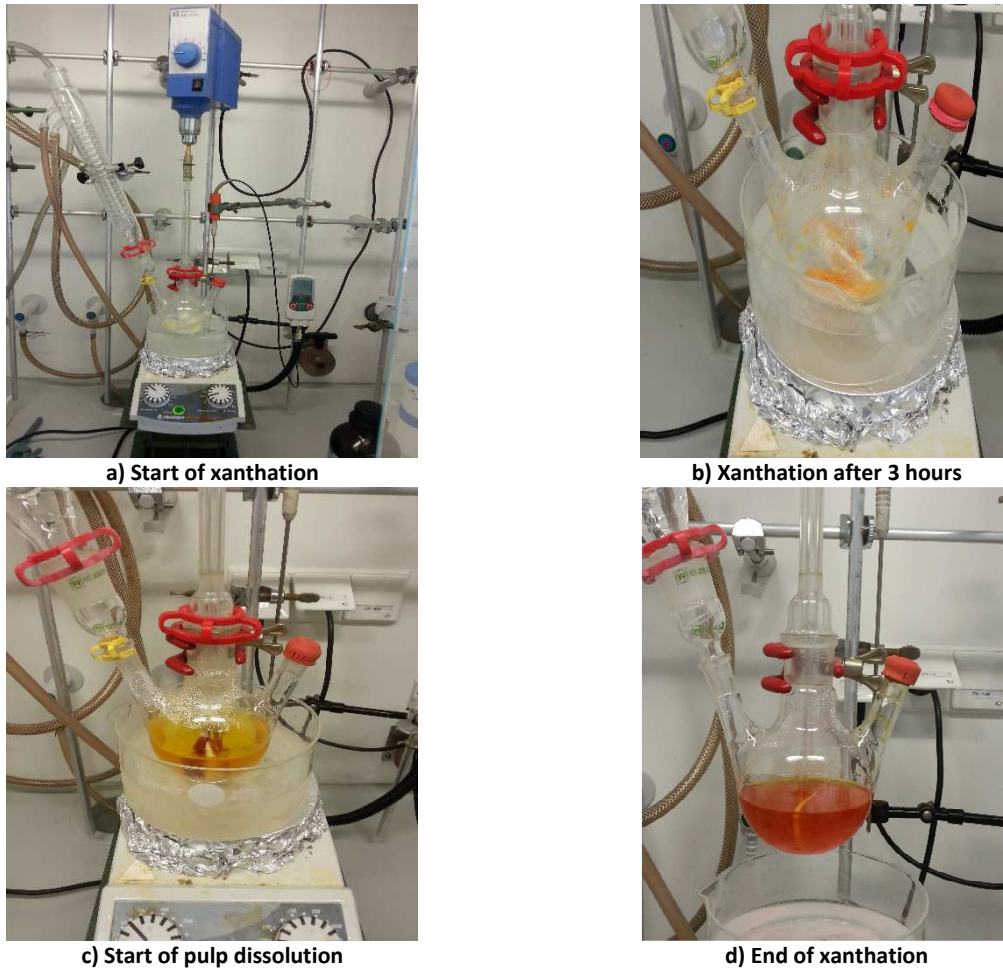


Figure 10 Different process steps in the xanthation of alkali cellulose to cellulose xanthate in the laboratory scale

3.2.1 Aging experiments with self-made viscose solution

The aging process of the viscose solution is an important parameter in the viscose fiber production. One batch is divided into two equal amounts to gain information about the aging speed of the viscose. One fraction of the viscose solution is stored under the influence of air, the other fraction is stored under nitrogen. The viscosity of the two differently stored solutions and therefore the aging process is controlled and observed with a capillary viscometer over a period of four days at room temperature and at 30°C. (14)

3.2.2 Determination of the capillary viscometer constant k

Because the constant k is directly depending to the inner surface of the capillary and the volume of the sample reservoir, the constant has to be determined before each use of the viscometer. To determine k , the retention time of *m*-cresol, a solvent with known dynamic

viscosity at certain temperature is measured. The constant k is afterwards determined via transforming the formula of dynamic viscosity.

$$\nu = k * t \quad \rightarrow \quad k = \frac{\nu}{t}$$

Where ν is the dynamic viscosity in [$\text{m}^2 \cdot \text{s}^{-1}$], k is the capillary viscometer constant in [mm^2/s^2] and t is the retention time in [s].

3.3 Development of a lab scale fiber spinning process

The regeneration of the cellulose xanthate solution back to cellulose is the final step of the viscose process. The success of the process is determined by the impact of many variables. The age of the used viscose, the concentration of the sulfuric acid and the geometry of the spinning nozzle are only a few of the parameters which are able to influence the quality and the structure of the resulting fibers. (14)

To develop a reproducible spinning method, the impact of three different process parameters: the age of the viscose solution, the concentration of the sulfuric acid and the influence of the used spinning needle are observed.

3.3.1 Influence of the aging process and sulfuric acid concentration

Parallel to the investigation of the viscose aging process, the spinnability of the viscose solution is investigated. Therefore, every day after measuring the viscosity, fiber spinning is accomplished into 10%, 15% and 25% and 50% sulfuric acid solutions. The resulting fibers are coiled around a stirring bar and regenerated for 5 minutes in the acid bath. After regeneration, the fibers are washed in de-ionized water for 5 minutes and finally, they are dried at 50°C for four hours in a drier. The fibers are characterized by optical microscopy and SEM.

3.3.2 Effect of spinning needle

Because the design and the development of a spinning nozzle is a very complex process, simple injection needles are used for the production of viscose fibers in lab scale. Three different needles with diameters of 0.45 mm, 0.7 mm and 0.8 mm are tested on their potential for the fiber spinning process.



Figure 11 Needles tested for fiber spinning

3.4 Development of an automated fiber spinning process

To be able to produce higher amounts of viscose fibers and to avoid permanent contact with the toxic substances (18) which are released during the regeneration of the cellulose xanthate, it is necessary to develop a process which can be automatically operated in large parts.

Therefore two important things have to be considered, first of all an appreciable amount of viscose solution has to be injected regularly and adjustably into the acidic spinning bath. The second thing to consider is that the generated fibers have to be collected without destroying the fiber structure. Last but not least the injection unit and the fiber collection have to be connected through a suitable spinning bath.

A syringe pump is seen as an optimal injection unit for a lab scale fiber plant, because an amount of up to 25 mL viscose solution can be injected at once and the injection speed is controllable in an easy way.



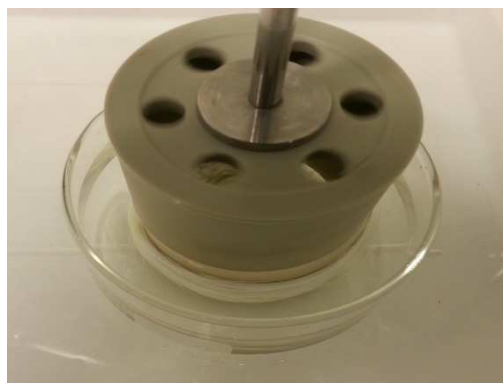
a) Roller to collect the fibers



b) Intersection from injection to spinning bath



c) Lab scale fiber plant with all parts



d) Final fiber washing

Figure 12 Developing of a automatized lab scale viscose fiber production unit with all the single parts needed

A device, suitable to wind up the generated fibers was not available and hence an own fiber roller had to be designed. As impulse for the roller a KPG stirrer with changeable stirring speed is used, the roller itself has to be made from a material which is inert to sulfuric acid solutions. So a polypropylene tube with 10 cm in diameter, a length of 15 cm and a wall thickness of 6 mm is used as roller unit. A cavity of 2 mm is shaped along the surface of the roller, to simplify the fiber uptake and to prevent the fibers from sliding down.

The link between the injection unit and the roller is the so called spinning pan, an acid inert plastic pan with a lateral rubber membrane as an inlet for the injection needle.

All the compounds together represent the lab scale fiber plant shown in Figure 12. Because the space in the flue is limited and also to simplify the manufacturing process, the post processing of the fibers with de-ionized water is integrated in the fiber plant. Hence a beaker, directly situated under the roller after spinning the fibers, is used as water bath.

3.4.1 Operation of the lab scale fiber plant

After developing an automated production unit for the fiber synthesis, the right operating conditions like injection speed, type of injection needle, amount of spinning solvent and the speed of the fiber roller have to be determined. Hence viscose solutions aged for one, two or three-days are used to evaluate the operation conditions. After regeneration and washing the fibers for 5 minutes respectively, they are dried for 4 hours at 50°C. The fibers are characterized via optical microscopy and SEM

3.5 Synthesis of metal sulfide containing viscose fibers

The synthesis of metal sulfide containing fibers and their characterization is the main aim of this master's thesis.

The resulting products are investigated and characterized by a wide range of analytical methods. Further, also the influence of changing various conditions and parameters in the fiber production on fiber properties is an object of interest in this master's thesis.

3.5.1 Synthesis and structure investigation of metal sulfide containing fibers

The first step is to explore which metal sulfides can be synthesized from which source and the metal sulfides are fixed on the fiber matrix. As possible metal cation sources copper(II)chloride, iron(III)chloride, nickel(II)chloride as nickel(II)chloride-hexahydrate, cobalt(II)chloride, zinc(II)chloride, tin(II)chloride as tin(II)chloride-dihydrate and silver(I)nitrate have been used.

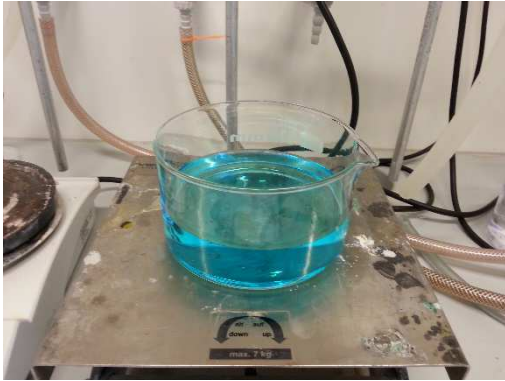
The fibers are synthesized manually with syringe and needle as injection unit and the fiber roller as collector.

In a first try, a viscose aged for three days is placed in a syringe and fiber synthesis is accomplished by 15% sulfuric acid (200 mL) to obtain reference fibers. For copper sulfide containing fibers the spinning bath is a 15% sulfuric acid solution (200 mL) containing 1 wt% copper(II)chloride (2 g). The fibers are regenerated for 5 minutes, washed for 5 minutes in de-ionized water and finally dried at 50°C for four hours. The products are characterized via optical microscopy and SEM-EDX

In further trials, the metal salt precursors have been alerted. For this purpose, viscose fibers are made from a viscose (aged for three days) by regeneration in 150 mL 15% sulfuric acid solution containing 0.5 wt% up to 1 wt% of either iron(III)chloride, nickel(II)chloride zinc(II)chloride tin(II)chloride, silver(I)nitrate or cobalt(II)chloride. After regeneration, the fibers are washed for five minutes each and dried afterwards.

The samples of the experiments are characterized with optical microscopy, SEM, SEM-EDX, XRD analysis and ICPMS analysis.

Figure 13 shows some process steps in the described fiber synthesis and the fiber treatment in execution.



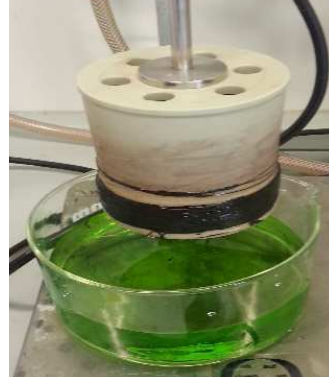
a) CuCl_2 containing spinning solution



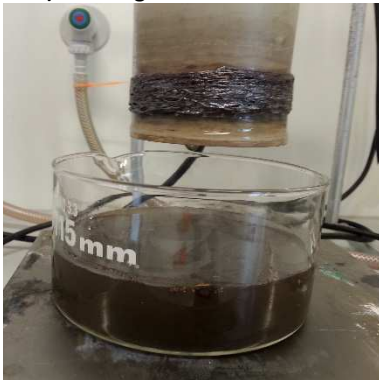
b) CuCl_2 solution after spinning



c) Washing of CuS coated fibers



d) NiS coated fibers after spinning



e) Ag_2S containing fibers after spinning



f) SnS containing fibers after drying

Figure 13 Process steps in the synthesis of metal sulfide coated viscose fibers

3.5.2 Metal uptake in fibers in dependence of metal concentration in spinning solution

The dependence between metal uptake in the fibers and metal concentration in the spinning solution is investigated through an ICPMS study of four different metal sulfide containing fibers, synthesized in two varying salt concentrations. For this test a three day old viscose solution is used to produce fibers in a 15% sulfuric acid solution including 0.25 wt% (0.63 g) or 1 wt% (2.5 g) of the following metal sources: copper(II)chloride, tin(II)chloride, nickel(II)chloride or silver(I)nitrate.

The fibers are regenerated for 5 minutes in the spinning solution, washed for another 5 minutes in de-ionized water and finally dried at 50°C for four hours.

The amount of metal sulfides fixed onto the cellulose matrix is determined via ICPMS.

3.5.3 Correlation between viscose age and metal uptake

The correlation between metal uptake in the fiber and viscose age (one day versus three days of aging) is investigated in a side experiment, by comparison of two samples produced from the same batch of viscose. Both samples are spun into a 15% sulfuric acid solution containing 1 wt% (2 g) copper(II)chloride. Regeneration time, washing and drying of the fibers is equal to the experiments described above.

3.5.4 Particle size in correlation to viscose age, regeneration time and acid concentration

Another field of interest is the influence of different parameters on the particle size of the generated metal sulfides

The influence of the acid concentration is checked through, copper sulfide fibers synthesized from a two day old viscose solution with varying acid concentrations of 15, 25 and 40%, respectively. The copper(II)chloride concentration is 0.5 wt%, the regeneration and washing time is 5 minutes each, drying for four hours at 50 °C completes the fiber production.

In a second series, viscose fibers are regenerated in a 0.5 wt% copper(II)chloride containing 15% sulfuric acid spinning solution for 5, 10 and 20 minutes. The synthesis procedure is equal to the first test series.

In a final test series, the effect of the viscose age on the particle size is investigated. Therefore fibers are spun in a 1 wt% copper source containing, 15% sulfuric acid spinning

solution on three consecutive days. The following fiber treatment is equal to the other two test series.

SEM imaging was attempted to determine the particle size on the fibers.

3.5.5 Effect of tempering on nickel sulfide particles

Nickel sulfide containing fibers are synthesized by spinning a two day old viscose solution in a 1 wt% nickel(II)chloride containing, 15% sulfuric acid spinning bath. Fiber treatment after the spinning process is executed as usual.

The fibers are characterized by XRD analysis to get information about the containing nickel sulfides. After the XRD measurement the fibers are tempered at 150°C for one hour under nitrogen flow and measured again.

A second heat treatment (1 hour) is done at 400°C under Argon flow, afterwards the fibers are characterized a third time via XRD analysis.

3.6 Experiments with tungsten oxide and tungsten sulfide in the Viscose

Additionally, it was explored whether tungsten containing compounds can be implemented in this process. The water solubility of the available tungsten sources (WO_3 , WS_2) is rather pure, therefore tungsten compounds have been directly added into the viscose solution.

3.6.1 Incorporation of tungsten(VI)oxide into the viscose solution

Concentrations of 1 wt% and 2 wt% tungsten are added into viscose solution (aged for two days), the solution is heated to 40°C and stirred for four hours before regeneration. The viscose is spun into 15% sulfuric acid bath, as product green fibers are obtained. The resulting fibers are washed with de ionized water and dried at 50°C

An XRD analysis is used to investigate if there is any remaining tungsten in the fibers and if so, in which form it occurs.

3.6.2 Incorporation of tungsten(IV)sulfide into the viscose solution

Nanocrystalline WS₂ is directly mixed into a viscose aged for one day and stirred overnight. After one day of continuous stirring the WS₂ particles are completely dispersed in the viscose. WS₂ containing viscose fibers are obtained through spinning the viscose solution into a 15% sulfuric acid solution. After washing the fibers for 20 minutes and drying them at 50°C, XRD characterization is used.

3.7 Synthesis and investigation of cellulose and metal containing films

The production of cellulose films from cellulose xanthate is another aim of interest in these investigations: Such films of regenerated cellulose also known as cellophane which is another popular product gained from cellulose xanthate. (77)

3.7.1 Cellulose film synthesis and storage stability

To produce cellulose films via regenerating a dried xanthate film, viscose solution aged for one day is transferred into a petri dish. The dish is slowly jiggled on a plate vibrator for 30 minutes to create a continuous and even film. After jiggling, the xanthate film is dried overnight at 50°C. On the following day, the dried xanthate film is regenerated in a 15% sulfuric acid solution and afterwards the film is thoroughly washed with de-ionized water.

Because the films are shrinking and therefore losing their texture if being dried again after regeneration, an alternative storage method, the conservation in 2%, 5% and 10% glycerol solution is performed. For this experiment the films are either placed directly after the washing step into the glycerol solution, after drying for four hours at room temperature or after drying for four hours at 50°C.

The films are stored in the different solutions for 1 week and afterwards dried again, to check if the weight or the structure has changed in dependence of the glycerol concentration.

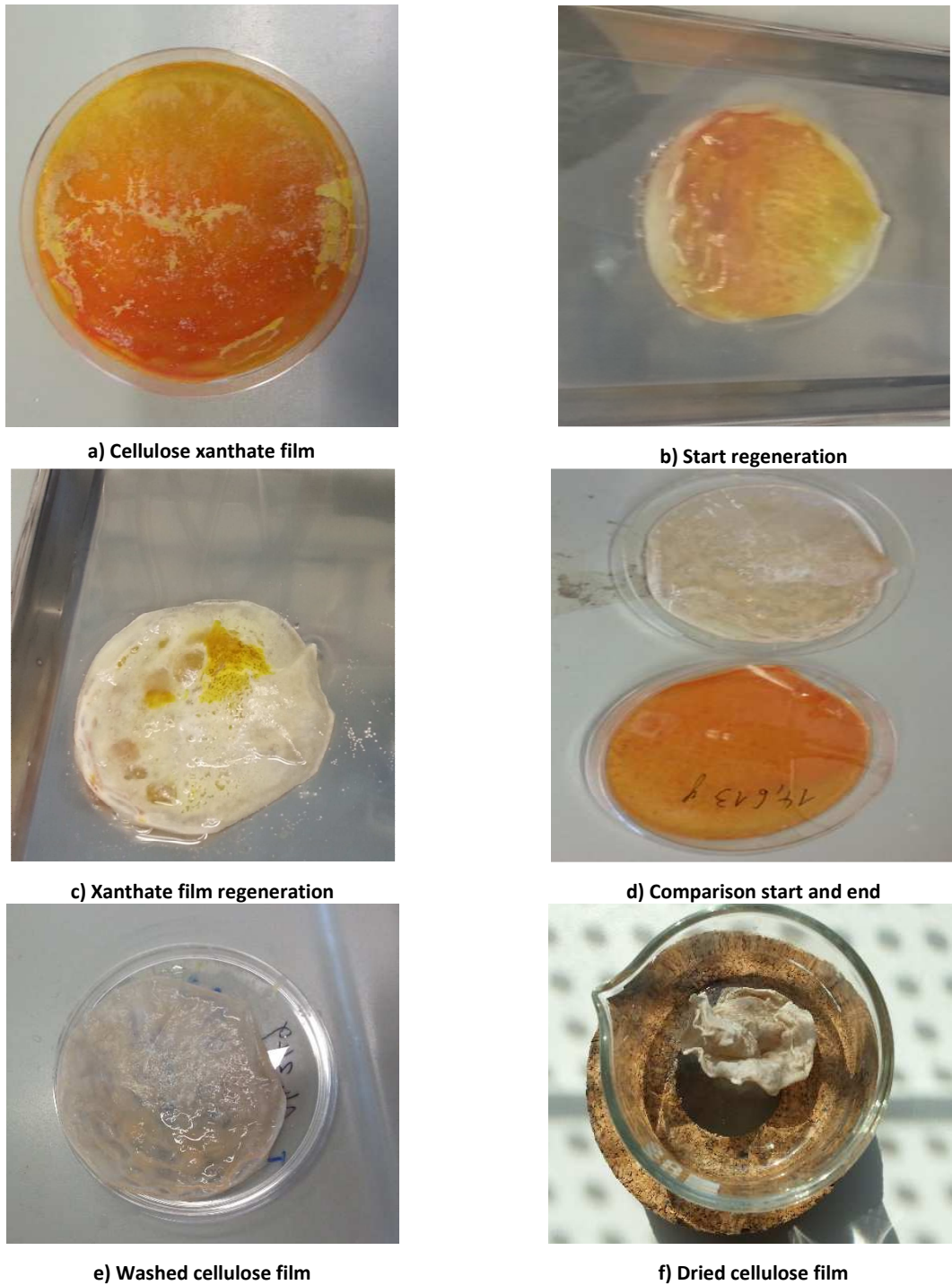


Figure 14 Illustrations of the production steps in cellulose film synthesis

3.7.2 Metal containing cellulose films

For the synthesis of metal sulfide containing cellulose films, also dried xanthate films of a viscous solution aged for one day, are regenerated in 15% sulfuric acid solution. However, the regenerating solution contains additionally also 0.5 wt% of a metal source

(copper(II)chloride, cobalt(II)chloride, iron(II)chloride, zinc(II)chloride, tin(II)chloride, nickel(II)chloride or silver(I)nitrate).

The regenerated films are dried at 50°C after washing with de-ionized water and stored as dried films.

3.7.3 Preparation of CuS containing films for microbiological tests

From a viscose solution aged for one day, 30 xanthate films are produced as described in this chapter. 10 films are regenerated in a pure 15% sulfuric acid bath and 20 films are regenerated in a 15% sulfuric acid solution containing 0.25 wt% copper(II)chloride. Washing with de-ionized water and drying at 40°C completes the process.

Since rather flat films are required for the microbiological testing, a perforated plastic slide is laid on the films during drying. In a final step, the films are sterilized by depositing them in a 70% ethanol solution for 10 minutes and drying the films again at room temperature.

3.8 Antibacterial testing of cellulose films according to EN ISO 20743

After sterilization of the cellulose films, 200µl of a solution, which contains staphylococcus aureus in a concentration of $10^4 \cdot L^{-1}$, are transferred onto the two different films (pure cellulose- and CuS- film). This process is repeated 6 times for each material. After absorption of the bacterial solution in the films, 3 films of each test material are incubated at 37°C for 24 hours.

The other three films are used to determine the zero concentration. Therefore directly after absorption of the bacteria solution in the films, 20 mL SCDLP solution are added to the films, to recover the bacteria. After shaking the solution 5 times for 5 seconds, once 100 µl and once 500 µl of the solution are transferred on agar plates to determine the remaining bacteria concentration through the plate counting method after 24 hours of incubation at 37 °C

For the samples, which have been incubated for 24 hours after the addition of the bacteria solution, the recovery and counting procedure is repeated in the same manner.

3.9 Sample preparation and parameters for the different analytical methods

Optical light microscopy

The light microscopy investigations are carried out on an Olympus BX60 fitted with an Olympus E-520 camera. Before investigating the samples, the fibers are placed on a glass layer and capped with a cover glass.

Scanning electron microscopy coupled with energy dispersive X-ray spectroscopy

Surface characterization is performed with a VEGA II from Tescan. For sample preparation the fibers are fixed on a graphene tape. Those samples which are not investigated by SEM-EDX are additionally coated with a thin gold layer. The electrons are accelerated through a voltage of 10.00 kV, as detector for the normal images a secondary electron detector is used, for the EDX characterization a back scattered electron detector is used.

Infrared spectroscopy

The infrared spectra are recorded through an Alpha spectrometer from Bruker. The scan range is from 4000 cm^{-1} to 400 cm^{-1} using 48 scans for each spectrum.

For the transmission measurements 3 mg of the sample are incorporated in 250 mg KBr and pressed to tablets. For the ATR measurements no additional sample preparation is necessary.

X-ray diffraction analysis

For the XRD analysis, a Bruker Advance D8 unit with LynxEye detector is used. The powder diffractograms are recorded in a range from 10° to 100° 2θ , with a recording time of 2 seconds per step and a step width of 0.02° . Rietveld refinements are performed with XPert High Score Plus, structural data are from ICSD.

Inductively coupled plasma mass spectrometry

Prior to the determination, a digestion of the fibers in nitric acid is carried out. The final element analysis itself is performed on an Agilent 7500ce unit.

3.10 Used chemicals and materials

Table 3 Sum up of the used chemicals

<i>Chemical</i>	<i>Company</i>	<i>Batch number</i>	<i>Chemical purity</i>
<i>Sodiumhydroxide</i>	VWR Chemicals	13/020011	p.a
<i>Sulfuric acid</i>	VWR Chemicals	16B100512	p.a
<i>Cotton fleece</i>	Fisher Scientific	143523/60	
<i>Copper(II)chloride</i>	Fluka	367987/120698	p.a
<i>Iron(III)chloride</i>	Sigma Aldrich	SZBC0710V	p.a
<i>Nickel(II)chloride-hexahydrate</i>	Roth	157740-1004	p.a
<i>Cobalt(II)chloride</i>	Sigma Aldrich	BCBG0246V	p.a
<i>Zinc(II)chloride</i>	Merck	1133120	p.a
<i>Tin(II)chloride-dihydrate</i>	Riedel de H�en	70510	p.a
<i>Silver(I)nitrate</i>	Alfa Aesar	10P025	p.a
<i>Tungsten(VI)oxide</i>	Fluka	G08021	p.a
<i>Tungsten(IV)sulfide</i>	Aldrich	MKBQ1666V	p.a
<i>Glycerol</i>	Sigma	BCBK0214V	
<i>Carbondisulfide</i>	Merck	1.002210.1000	p.a

All the chemicals listed in Table 3 are used without further purification or any other treatments.

4. Results and discussion

4.1 Alkali cellulose

The synthesis of alkali cellulose was performed using 18 wt% NaOH, whereas in all repetitions similar results were obtained. A list of all the individual performed reactions is shown in Table 4.

Table 4 List of alkali cellulose reactions

<i>Batch number</i>	<i>Cotton [g]</i>	<i>18wt% NaOH [mL]</i>	<i>24h drying [g]</i>
1	5.32	200	17.51
2	5.43	100	17.85
3	4.86	150	16.37
4	6.31	150	20.01
5	5.66	150	19.45
6	5.39	150	21.01
7	5.28	150	20.12
8	5.35	150	19.58
9	5.56	150	20.08
10	6.34	150	21.34
11	5.36	150	20.03
12	5.57	150	20.36
13	5.22	150	19.55
14	5.31	150	18.74

The resulting product can be described as white, greasy pulp with an acetous smelling. There is water in the cellulose matrix indicated by the high weight increase which cannot be caused by the substitution of hydrogen through sodium only. Further the IR spectrum of alkali cellulose, shown in Figure 15, confirmed that the synthesis is successful. In Figure 15, an ATR-IR spectrum of a cotton fleece used as starting material for the synthesis is compared to a spectrum of the synthesized alkali cellulose. The cotton fleece shows the characteristic cellulose absorption bands at 3500 – 3100 cm^{-1} due to the OH stretching vibrations, at 2800 cm^{-1} (CH stretching vibrations), at 1480 – 1400 cm^{-1} (CH_2 deformation vibrations), as well as at 1250 – 1000 cm^{-1} a series of strong overlapping bands due to CO stretching vibrations and in the fingerprint region at 800 – 600 cm^{-1} caused by CH_2 deformation vibrations. (78)

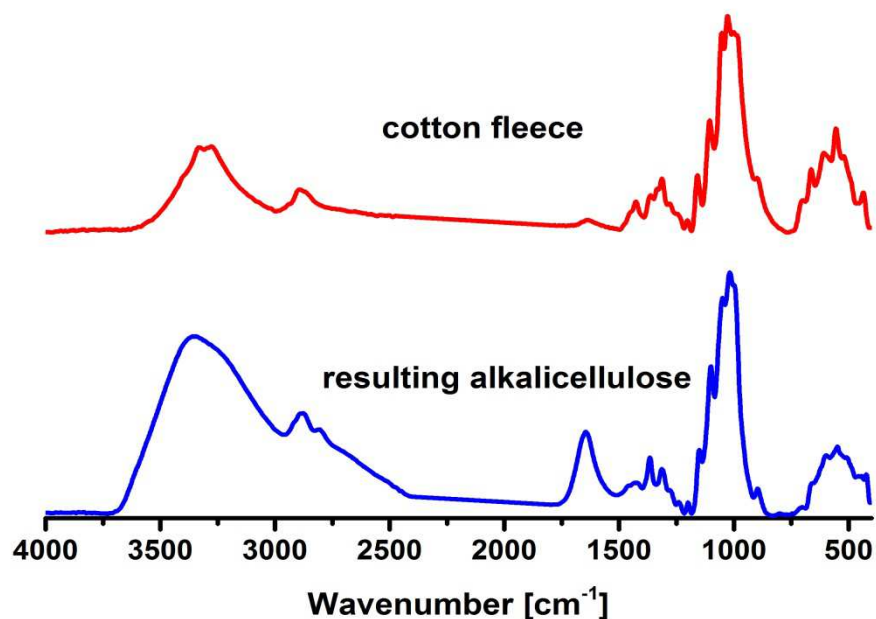


Figure 15 AT-IR spectra of cotton fleece (starting material) and alkali cellulose

The alkali cellulose spectrum differs clearly from the cotton bands. The broad band at 3600 – 3000 cm^{-1} in the alkali cellulose spectrum has a higher intensity compared to the cotton spectrum and is shifted from 3500 cm^{-1} to 3650 cm^{-1} . The increasing intensity indicates that there are more OH stretching vibrations detectable in the alkali cellulose sample, a reason for this could be some remaining water. At 1650 cm^{-1} a new band appears, this band is also caused by the water embedded in the cellulose matrix and represents OH deformation vibrations. (78)

4.1.1 Storage stability of alkali cellulose

After 24 hours drying at room temperature there is still some NaOH in the alkali cellulose as proven by IR spectroscopy. This is of particular importance since during the aging process further intermolecular bonds are broken and therefore their accessibility for CS_2 in the xanthation step increases. (79) Besides NaOH, it is of interest whether light and temperature have an influence on stored alkali cellulose which was observed over a period of 30 days.

Effects of storage temperature on alkali cellulose

A batch of alkali cellulose is divided in three equal fractions and stored at -18°C , 4°C or room temperature for duration of 30 days. After 7, 15 and 30 days the effects of different temperatures are optically inspected and an IR spectrum is also recorded after 30 days of storage. There is no any optical difference between the three storage temperatures, even after 30 days of storage. Also the ATR-IR spectra of stored celluloses are identical to the spectrum recorded at the beginning of the experiment. In Figure 16 a representative ATR-IR spectrum of dried alkali cellulose (24 hours) is compared to a sample which has been stored at 4°C over a period of 30 days. The other samples featuring different storage conditions exhibit more or less identical IR spectra.

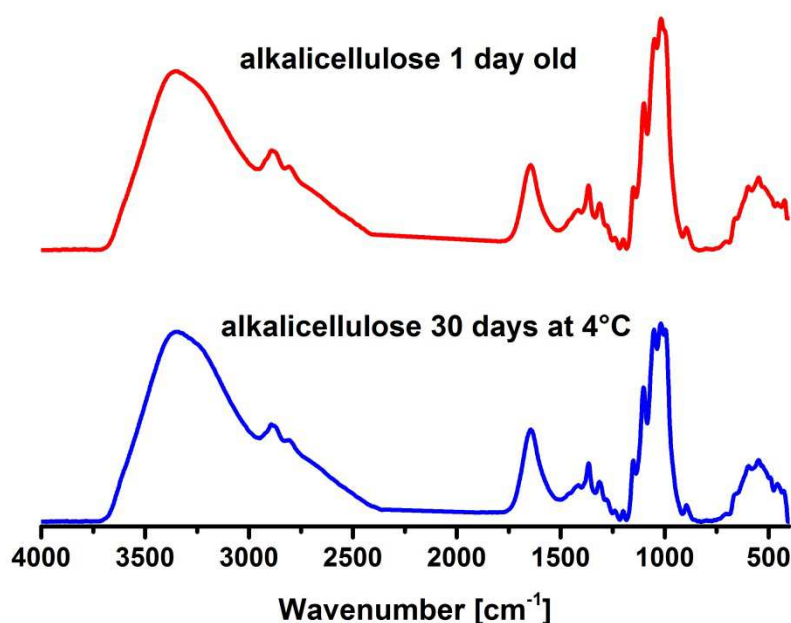


Figure 16 ATR-IR spectra of freshly prepared alkali cellulose and a sample stored at 4°C over a period of 30 days

Effects of light

To evaluate whether daylight and sunlight affect the aging process of alkali cellulose, a batch of synthesized alkali cellulose is divided into two equal fractions, one is stored under influence of light and one is stored in the dark for 30 days. After 7, 15 and 30 days an optical control is done and after 30 days also an IR spectrum is recorded. In the optical control any differences between the samples could not be found, neither spectroscopically, nor visual.

The IR spectra are identical to the spectra shown in Figure 16 and are therefore not presented in the work.

Effects of remaining NaOH solution

Further, the effect of remaining solvent in the alkali cellulose on aging is investigated. Therefore, the normally removed NaOH solution stays in the cellulose matrix. The batch is stored for 30 days at room temperature under exclusion of light.

After 7, 15 and 30 days the alkali cellulose is analyzed optically for any changes. After 15 days of storage a change in color (from white to yellowish) and an alteration in the smell was observable, and after 30 days these effects have been even more pronounced.



a) Alkali cellulose stored at different temperatures



b) Alkali cellulose stored under light exposure

Figure 17 30 day long stored alkali cellulose at different temperature or varying light exposure

Table 5 gives an overview of the different experiments on the storage stability of alkali cellulose under varying conditions. The only visible change in the cellulose matrix could be detected in alkali cellulose stored with remaining NaOH solution. The change in color is caused by further degradation of the cellulose matrix by the sodium hydroxide solution and the uptake of oxygen by the alkali cellulose. (80) The influence of light and temperature seems to have only negligible effects on the storage of alkali cellulose.

Table 5 Summary of the experiments to the alkali cellulose stability

<i>Sample</i>	<i>Storage condition</i>	<i>Obersvable effects</i>
<i>Alkali cellulose batch1</i>	dried, 30 days, -18°C	none
<i>Alkali cellulose batch1</i>	dried, 30 days, 4°C	none
<i>Alkali cellulose batch1</i>	dried, 30 days, RT	none
<i>Alkali cellulose batch2</i>	dried, 30 days, exposed	none
<i>Alkali cellulose batch2</i>	dried, 30 days, dark	none
<i>Alkali cellulose batch3</i>	wet, 30 days, dark	change in color, smell

It can be concluded that the degradation of alkali cellulose and therefore the stability is mainly governed by the remaining content of NaOH in the cellulose matrix, which is responsible for further degradation of the cellulose chains during the storage period.

4.2 Xanthation

The xanthation reaction as described in 3.2 was executed several times. A list of all different performed xanthation reactions is presented in Table 6. The result of the xanthate reaction can be described as an orange viscous solution with a sweetish smell. The density of the resulting spinning solution is about 1.5 g/mL.

Table 6 Overview of xanthation reactions

<i>Batch number</i>	<i>Alkali c.[g]</i>	<i>CS₂ [mL]</i>	<i>4wt% NaOH [mL]</i>
1	6.35	6	100
2	7.22	6	100
3	13.96	10	200
4	14.52	12	200
5	7.11	6	100
6	14.03	11	200
7	13.98	11	200
8	13.92	10	200
9	14.03	11	200
10	6.85	5	100
11	14.23	10	200
12	14.19	11	200
13	14.31	11	200

The success of this reaction is monitored by ATR-IR spectroscopy of dried cellulose xanthate films. The spectrum of the xanthate film, a spectrum of the cotton fleece used as starting material and the alkali cellulose spectrum are shown in Figure 18 to illustrate the change in the cellulose structure caused by the different reaction steps. The spectrum of the xanthate

shows a broad band at $3500 - 3000 \text{ cm}^{-1}$ (stretching vibrations of unsubstituted OH groups), in the area of $1500 - 1250 \text{ cm}^{-1}$ two intensive but overlapping bands can be detected (stretching vibrations of the CS double bond, CO stretching vibrations) and a sharp band at $900 - 800 \text{ cm}^{-1}$ (stretching vibrations of the CS single bond). In the fingerprint region the CH_2 deformation vibrations are visible. (81) (78).

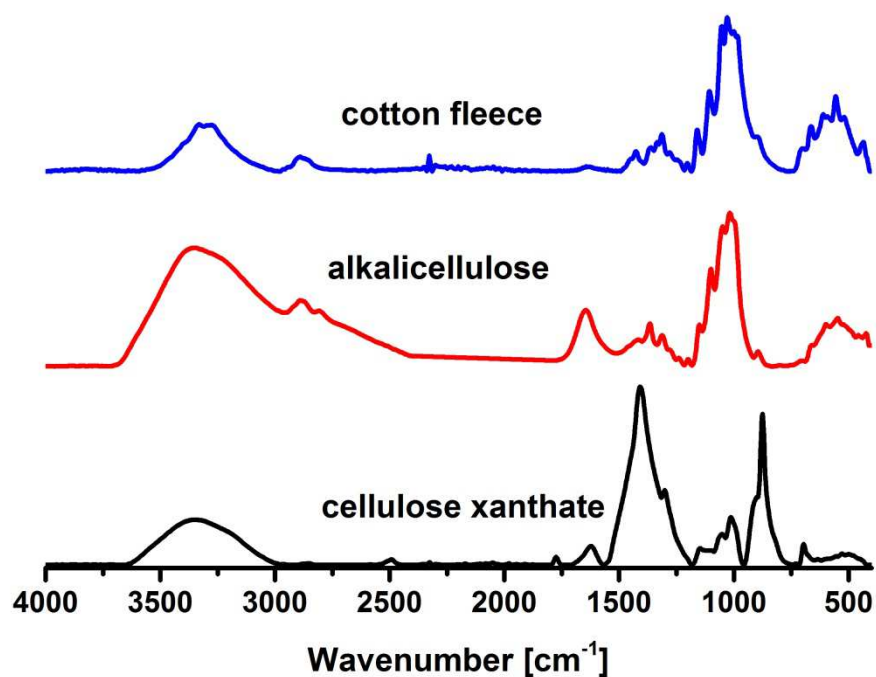


Figure 18 IR spectra of the cotton fleece, the alkali cellulose and the resulting cellulose xanthate

4.2.1 Investigation of the xanthate aging

Because it was noticed in the first xanthation reactions, that the cellulose xanthate solution is changing its viscosity within a few days after the reaction, an investigation of this process is necessary to determine a time frame where the viscose solution is spinnable. As already mentioned in the description of the viscose process, de-xanthation and redistribution of cellulose xanthates during the aging period are responsible for the observed effects. (82)



a) Cellulose xanthate spinning solution



b.) spinning solution after aging for 5 days

Figure 19 Cellulose xanthate after a storage period of 1 respectively 5 days under atmospheric influence

In Figure 19a, a spinning solution aged for one day is shown, the solution is clear and viscous and completely soluble in NaOH (4 wt%). Figure 19b represents a spinning solution aged for five days, the solution consists of two phases. The first phase can be described as aqueous phase, the second phase as tough, orange slurry. If the aging duration is prolonged to 14 days, the effects of the viscose aging process are visible even more explicit, as shown in Figure 20.



a) Viscose aged one day



b) Viscose aged 14 days

Figure 20 Influence of a 14 day lasting storage period onto a cellulose xanthate solution

For evaluation of the time frame which allows for spinning of the viscose solution, aging studies of two differently stored viscose solutions, one under oxygen and one under nitrogen are evaluated. The aging process and therefore the increasing viscosity of the solution is observed by a capillary viscometer

Prior to measurements, the Ubbelohde viscometer is calibrated using *m*-cresol, a solvent with a viscosity of 1.03 g/cm^3 referred to as in literature. (83). From this calibration tests a capillary constant k of $0.0474 \pm 0.0001 \text{ [mm}^2/\text{s}^2]$ is obtained, the single measurements are presented in Table 7.

Table 7 Single calibration measurements with *m*-cresol for the determination of *k*

<i>Throughput time [s]</i>	<i>Temperature[°C]</i>	<i>k of measuring instrument[mm²/s²]</i>
215	20	0.00479
219	20	0.00470
214	20	0.00481
220	20	0.00468
218	20	0.00472
219	20	0.00470
218	20	0.00472
217	20	0.00475

The resulting dynamic viscosity numbers for the viscose solution stored under oxygen or nitrogen atmosphere are listed in Table 8 and Table 9, respectively, whereas the measurements have been executed at room temperature and 30°C.

Table 8 Aging process of viscose solution stored under oxygen atmosphere documented through the kinematic viscosity

<i>Throughput time[s]¹</i>	<i>Days aged</i>	<i>Temperature[°C]</i>	<i>Dynamic viscosity[m²·s⁻¹]</i>
1486	1	20	70
1775	2	20	84
1906	3	20	90
2421	4	20	110
<i>Throughput time[s]</i>	<i>Days aged</i>	<i>Temperature[°C]</i>	<i>Dynamic viscosity[m²·s⁻¹]</i>
1471	1	30	70
1688	2	30	80
1850	3	30	88
2320	4	30	109

Table 9 Aging process of viscose solution stored under nitrogen atmosphere documented through the kinematic viscosity

<i>Throughput time[s]¹</i>	<i>Days aged</i>	<i>Temperature[°C]</i>	<i>Dynamic viscosity[m²·s⁻¹]</i>
1488	1	20	71
1707	2	20	81
1890	3	20	90
2281	4	20	108
<i>Throughput time[s]</i>	<i>Days aged</i>	<i>Temperature[°C]</i>	<i>Dynamic viscosity[m²·s⁻¹]</i>
1456	1	30	69
1569	2	30	74
1775	3	30	84
2196	4	30	104

¹ The throughput time is the averaged value of three measurements

Taking the results into consideration, the viscosity of the solution increases during aging whereas an increase in temperature leads to a decrease of the viscosity. The storage conditions did not really impact the viscosity and viscosities for samples storage under nitrogen and those stirred under ambient temperature are essentially the same. After a storage period of five days, the viscosity is not measureable any longer since the viscosity solidifies.

Besides the determination of the viscosity also the spinnability of the differently stored solutions was investigated. Both solutions were spinnable in the viscosity range of 69 up to 110 [m²·s⁻¹]

4.3 Evaluation of suitable fiber spinning conditions

The spinning process, which is the step where the cellulose xanthate is regenerated back to cellulose II, is influenced by many impact factors like the concentration of sulfuric acid in the spinning bath, the age of the used cellulose xanthate, the geometry of the spinning nozzle and many other parameters. (14) To evaluate practicable conditions for the spinning process, not only the spinnability in respect to the viscose age is investigated, also the influence of the sulfuric acid concentration in the spinning bath and the usability of the individual injection needles used as spinning nozzle have to be determined.

To check the effects of the sulfuric acid concentration in the spinning bath, fiber spinning with a viscose solution aged for a one, two, three or four days, has been performed in 10, 15, 25 and 50% sulfuric acid solutions. The results are summed up in Table 10.

Table 10 Effects of the sulfuric acid concentration on the viscose spinning process

Aging time [days]	Sulfuric acid concentration [%]			
	10	15	25	50
1	not spinnable	spinnable	spinnable	spinnable, cellulose dissolved
2	hardly spinnable	spinnable	spinnable	spinnable, cellulose dissolved
3	spinnable	spinnable	spinnable	spinnable, cellulose dissolved
4	spinnable	spinnable	spinnable	spinnable, cellulose dissolved

For the viscose solution, aged for one and two days, the spinning process in a 10% sulfuric acid solution can be described as difficult. It was hard to get a monofilament and if, the fibers ruptured after short time. Fiber spinning into the 15% and 25% sulfuric acid solutions worked well. Also the fiber spinning in the 50% sulfuric acid bath itself worked without any

problems but the viscose fibers were nearly dissolved after a regeneration time of 5 minutes due to hydrolysis. Therefore fiber spinning in 50% sulfuric acid solution is not practicable. In terms of economic efficiency a 15% sulfuric acid regeneration bath can be considered most practicable. Figure 22 depicts a viscose fiber obtained after 5 minutes of regeneration in 15% sulfuric acid while Figure 21 shows a fiber directly after regeneration in a 25% sulfuric acid solution.



Figure 21 Fiber in 25% sulfuric acid



Figure 22 Fiber after regeneration in 15% H₂SO₄

The injection needles are used as alternative to the very complex, time and cost intensive development of a spinneret. Needles with a diameter of 0.45mm, 0.7mm and 0.8mm and a corresponding length of 25mm, 50mm, and 100mm were available and their suitability for the fiber spinning is tested.

All the needles can be used to spin viscose fibers, due to the high length of the needles with a diameter of 0.8mm the handling is relatively complex and therefore these needles are not used for further fiber spinning experiments. Also the high fiber diameter obtained for fibers regenerated with the large needles, is an argument against their use.

4.3.1 Structure analysis of the resulting fibers

After the evaluation of the right conditions for the spinning process, the resulting fibers are characterized through light microscopy and IR spectroscopy.

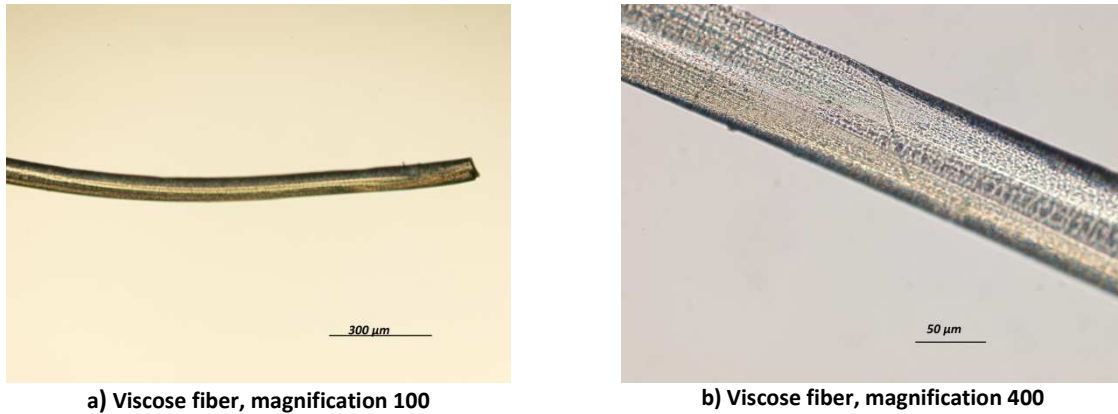


Figure 23 Images of a viscose fiber, obtained from standard spinning process in varying magnifications

In Figure 23, a obtained viscose fiber is presented, the fiber can be described as regular filament, without any irregularities in the matrix, and also the fiber surface can be described as smooth and regular.

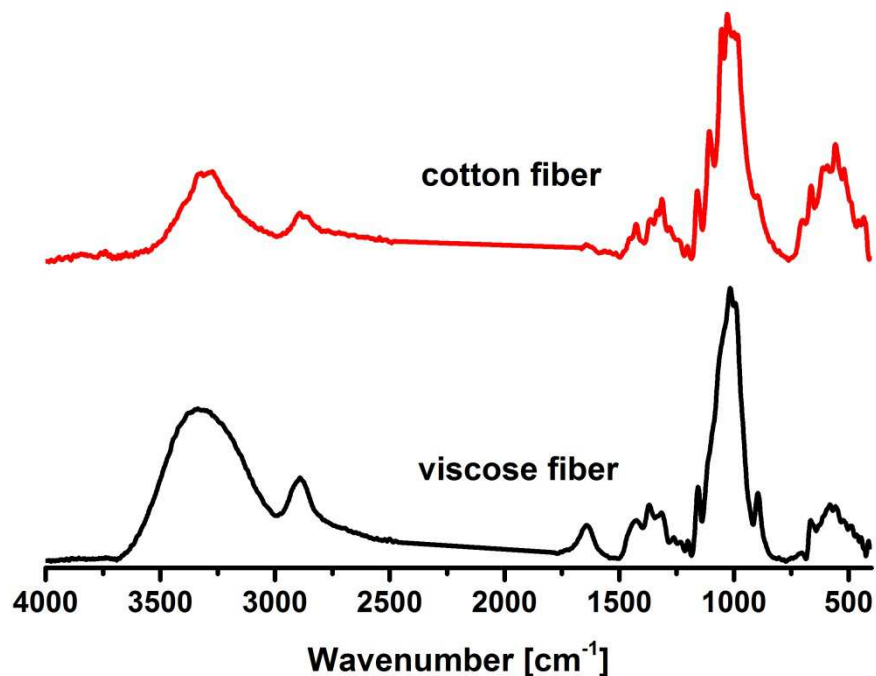


Figure 24 ATR-IR spectra of a cotton fiber and a viscose fiber

In Figure 24 the ATR-IR spectra of cotton fibers and regenerated viscose fibers are shown. In both spectra the same bands, which are all typical for cellulose fibers, with the only exception of a small band at 1650 cm^{-1} in the viscose fiber spectrum, occur. The band at 1650 cm^{-1} represents OH deformation vibrations caused by remaining water in the sample. But there is one obvious difference visible, between the two broad bands located in the region $3600 - 3000\text{ cm}^{-1}$ in the spectra. In the spectrum of the viscose fibers, this band looks like a normal constant broad IR band. The same band in the cotton fiber spectrum looks a little bit like two overlapping bands. This little difference allows to distinguish between cellulose I, the cellulose present in the cotton fibers and cellulose II, the cellulose obtained through a successful viscose process. Hence it can be said that the production of viscose fibers with all the associated reaction steps is done with success.

4.4 Automation of the viscose spinning process

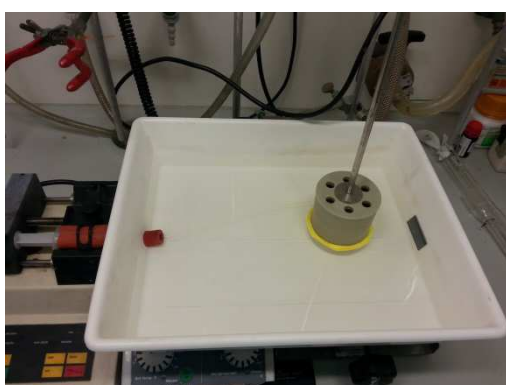
The ideal operation conditions for the developed laboratory scale fiber plant, which has been already described in section 3.4 with all its single parts in detail, have to be determined.

The first important parameter for the success of the fiber synthesis is the injection speed of the viscose solution into the spinning bath. Therefore, one, two and three day old viscose solutions are injected via a needle having a diameter of 0.45 mm. The injection speed is varied from 1.5 up to 3 mL per minute. A feed rate of 2 mL per minute seems to be ideal for all the tested viscose solutions, if the feed rate was lower the formation of a viscose drop around the needle tip could be observed. A higher feeding rate causes an enhanced back pressure and the syringe pump stops automatically.

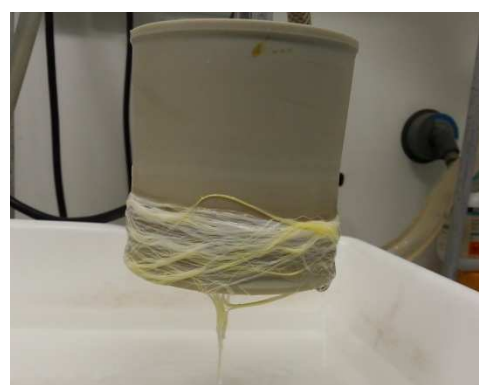
The second parameter which has to be adjusted is the rotation speed of the fiber roller. If the roller speed is too slow the fibers will tangle up in the spinning bath, if the roller is too fast the filament is going to break.

For the defined feeding rate of 2 mL per minute, the roller works with an ideal speed if it is operated at step 1 or 1.5. (around 60 rpm) After the ideal operating conditions have been found, the lab fiber plant works without any problems. The only critical point left is the presence of air bubbles in the viscose solution, which cause a break of the fiber filament.

Figure 25 shows the fiber plant in operation mode and the resulting product, viscose fibers after five minutes of regeneration in the spinning bath are presented.



a) Fiber plant in operation



b) Resulting viscose fibers unwashed

Figure 25 The fiber plant in operation and the resulting fibers after the regeneration in 15% sulfuric acid

4.5 Metal sulfide containing viscose fibers

The basic idea for the in situ synthesis of metal sulfides in the course of the viscose process is the displacement of sodium cations in the xanthate group through other metal cations present in the spinning bath and the following reaction of the inserted metal cations with released sulfur during the regeneration step to metal sulfides. Through the exchange of the sodium with the desired metal cation, the cation is directly taken into the outer side of the developing viscose fiber.

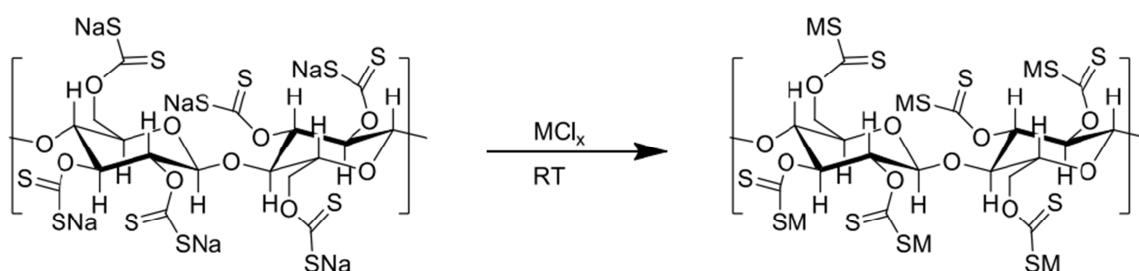


Figure 26 Scheme of sodium exchange due to the presence of metal chloride salts in the spinning bath

In Figure 26 the exchange of sodium by other metal cations dissolved in the spinning solution is visualized, the degree of substitution obtained in xanthation of alkali cellulose is not three, as shown in the figure, but somewhere between 0.3 up to 0.7. In the figure the DS equals to 3 to point out the ongoing process.

4.5.1 Results for the fiber spinning experiments in copper(II)chloride spinning bath.

To gain copper sulfide containing viscose fibers from copper(II)chloride, the metal salt is used in concentrations from 0.25 wt% up to 1.5 wt% in the spinning baths. It is obvious that the presence of an additional compound, namely a metal salt, may have an impact on the regeneration and spinning conditions. A major difference is the appearance of black particles in the spinning bath, right after injecting the cellulose xanthate. Further, the texture and the color of the fibers are completely different. Instead of white to yellowish fibers, purely black fibers have been obtained that are additionally rather brittle. In Figure 27, fibers gained by the standard viscose process and the resulting fibers in the presence of copper cations in the spinning bath are compared. Even during the washing process, the fibers remain unchanged and in the case of copper chloride there is not any leaching into the washing solution.

The black fibers are first investigated by light microscopy and compared to normal viscose fibers presented in Figure 23. If the fibers are compared (Figure 28) to standard viscose



Figure 27 Standard and in CuCl_2 regenerated fibers

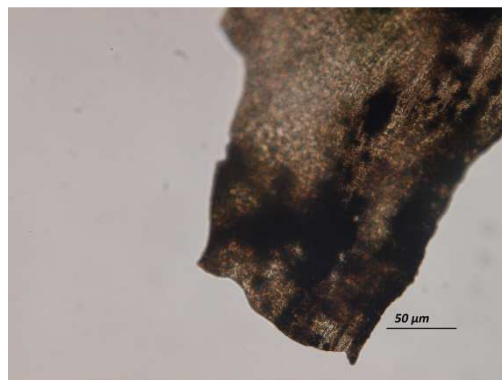
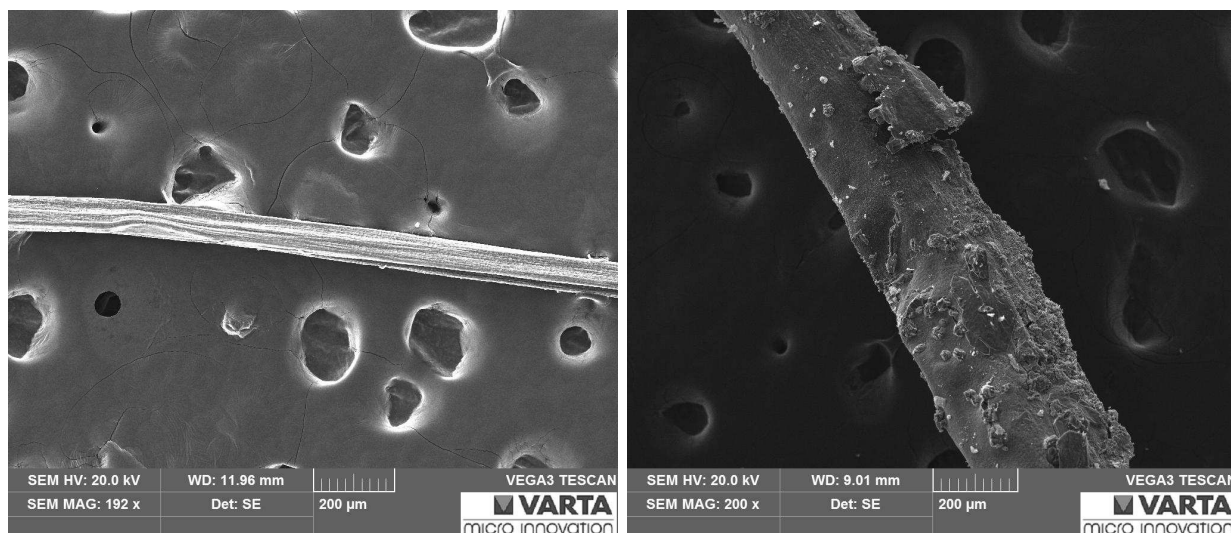


Figure 28 CuS containing fiber magnification 400

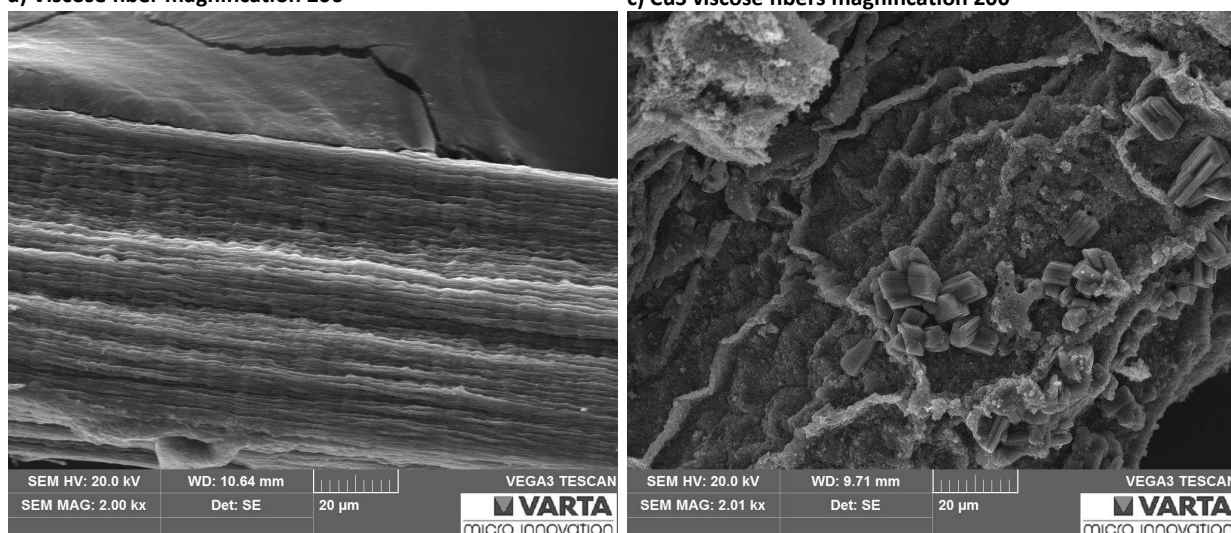
fibers using light microscopy, the copper containing fibers show a clear difference in transparency and also the fiber edges differ, in a way that the frames of normal fibers are smooth and in the dark fibers they are rather irregular.

Further, SEM images of the fibers have been acquired to explore the morphology of the attached sulfide particles. In the SEM images, the fibers show some well defined regular structures on their surface and in a higher magnification these structures can even be identified as regular crystals with a size up to about $10\mu\text{m}$. Comparing these images to SEM images of standard viscose fibers, which show a very defined structure and a surface without any irregularities also in high magnifications, the appearance of crystals on the fiber is a clear sign for the presence of CuS at least on the fiber surface. In Figure 29 SEM images of normal viscose fibers and the fibers obtained in attendance of CuCl_2 in the spinning bath are shown.



a) Viscose fiber magnification 200

c) CuS viscose fibers magnification 200



b) Viscose fiber magnification 2000

d) CuS viscose fibers magnification 2000

Figure 29 Comparison between non-treated and CuS modified viscose fibers obtained from the lab scale fiber plant

Moreover, SEM-EDX is employed for semi quantitative elemental analysis of the fibers. From the SEM-EDX measurements some important information is derived. The elemental composition of the crystals reveals a rather high copper and sulfide content on the crystals. The second thing is that the SEM-EDX point measurements of the crystals do not differ significantly to area measurements of the viscose fibers in the copper content. The specific element contents obtained for the area and crystallite measurements are summarized in Table 11.

Table 11 List of elemental contents in fiber matrix and crystallites detected through SEM-EDX

Element	Fiber matrix		crystal structure	
	Weight%	Atomic%	Weight%	Atomic%
Carbon	45.8	54.5	48.0	58.1
Oxygen	49.3	44.0	42.7	38.8
Sulfur	1.6	0.7	4.5	2.1
Copper	3.2	0.7	4.7	1.1

The third point of interest is the fact, that there is also a significant amount of copper detectable in fiber regions where no well defined crystal structures are detectable. This could be an indication for the presence of copper below the fiber surface and not only on the fiber surface. Another possibility to explain this fact is the presence of smaller crystal, which cannot be detected with this SEM setup.

Another interesting fact is the presence of a high amount of sulfur on the fiber surface as well as in crystal structures too. This could be an indication for the presence of the desired copper sulfides or as indication for sulfur purification in the fibers.

In order to assign the copper sulfide phase present on the fibers, and to determine their exact chemical and structural composition, XRD studies have been performed.

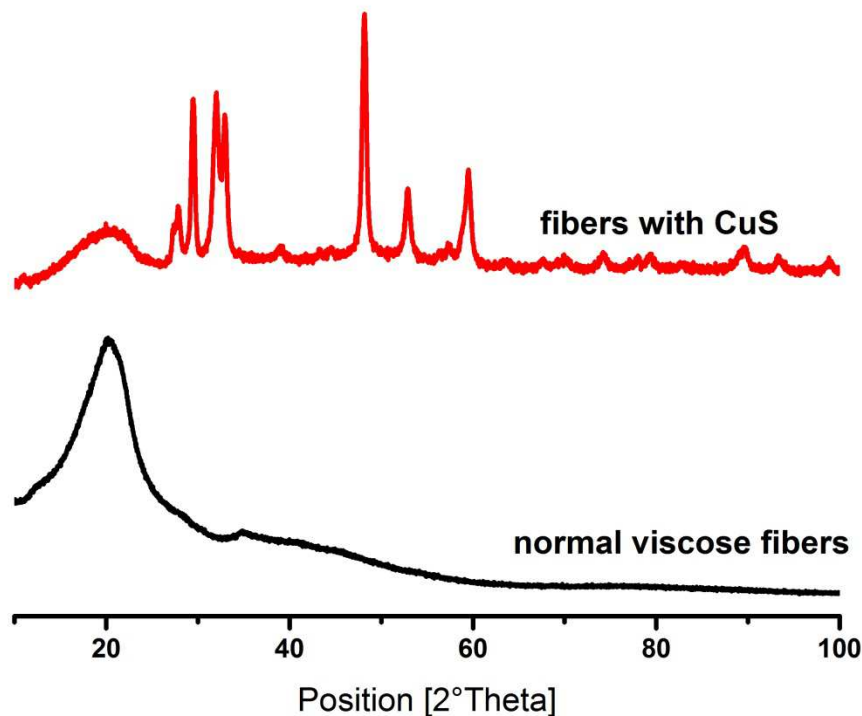


Figure 30 XRD analysis of normal and CuS containing viscose fibers

Figure 30 is an illustration of the XRD measurements of standard viscose fibers and CuS containing fibers, the standard fibers show only one broad reflection signal at the beginning. This broad reflection is the standard signal obtained in XRD measurements for polymeric materials. (9) A comparison of the cellulose II reflections with reflections of CuS coated fibers reveals large differences in the number of appearing reflections. The high number of sharp reflections indicates the presence of crystalline structures, in this case CuS structures. An exact crystal structure including the crystal lattice type, is gained by comparing the measured spectrum to spectra of other CuS structures.

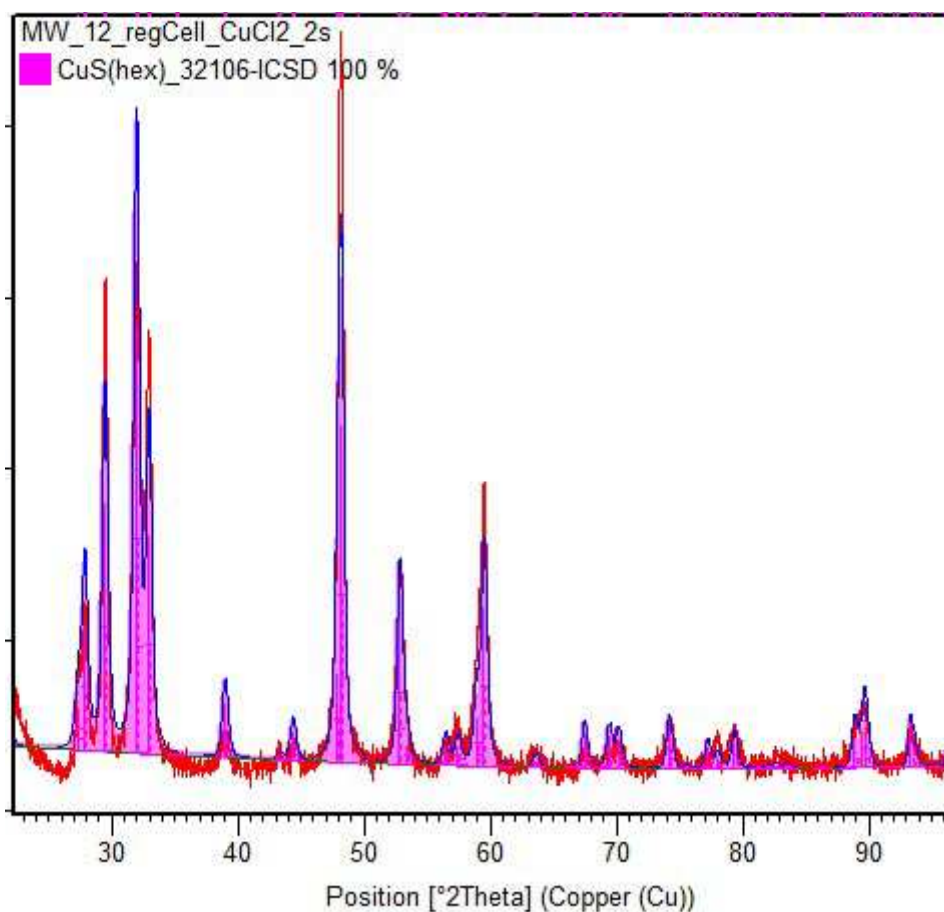


Figure 31 measured XRD spectrum of viscose fibers with CuS compared to a spectrum of hexagonal CuS

Figure 31 shows the XRD signals of the CuS viscose fibers compared with an XRD pattern of hexagonal copper sulfide. As it can be seen in the figure the two spectra have a conformity of 100 %, and therefore this is the proof for the presence of phase pure CuS crystals on the fibers. To emerge phase pure copper sulfides is rather unexpected, as copper sulfides are known to form a variety non stoichiometric and mixed phases. (84)

4.5.2 Results for the fiber spinning experiments in a tin(II)chloride spinning bath

Beside the synthesis of viscose fibers with CuS onto the matrix, the spinning of viscose into a SnCl₂ containing spinning bath has been explored too. Also in the synthesis of tin sulfide coated fibers in a concentration range of 0.25 wt% up to 1.5 wt% black particles appeared in the spinning bath, right after injecting the cellulose xanthate. Further, the texture and the color of the fibers are completely different. Instead of white to yellowish fibers, purely black fibers have been obtained that are additionally rather brittle, comparable to the copper sulfide coated fibers.



a) Viscose fibers spun into SnCl₂ spinning bath

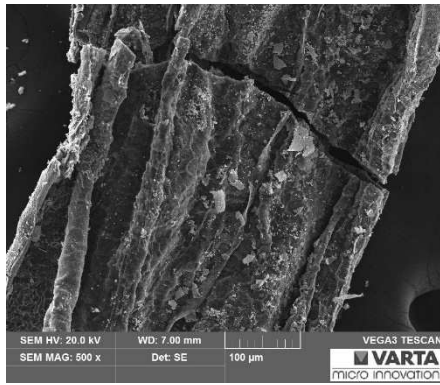


b) Obtained fibers after drying

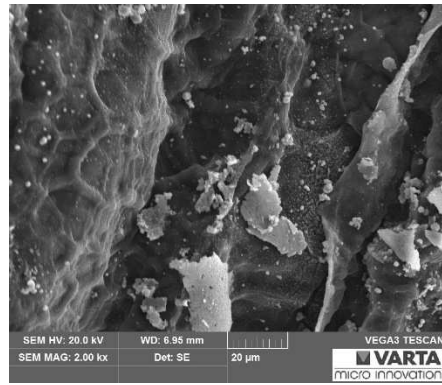
Figure 32 Viscose fibers spun into a SnCl₂ containing spinning bath directly after the spinning process and after drying

The fibers are investigated by light microscopy as well as scanning electron microscopy. The light microscopy images reveal only a difference in transparency and roughness compared to normal viscose fibers. The change in transparency is a first hint, for the presence of tin compounds on the fiber matrix.

In the SEM investigations, the fiber surface shows crystalline particles, comparable to those on CuS containing viscose fibers. However, the shape of the crystals is not regular and well defined.



a) SnS viscose fibers magnification 500



b) SnS viscose fibers magnification 2000

Figure 33 SnS particles on viscose fibers regenerated in a spinning bath with SnCl₂ inside, detected through SEM

The XRD pattern reveals sharp reflections which can be assigned to three different species, namely cubic tin sulfide (66%) another phase of tin sulfide (10%) and tin sulfate (25%) (Figure 34).

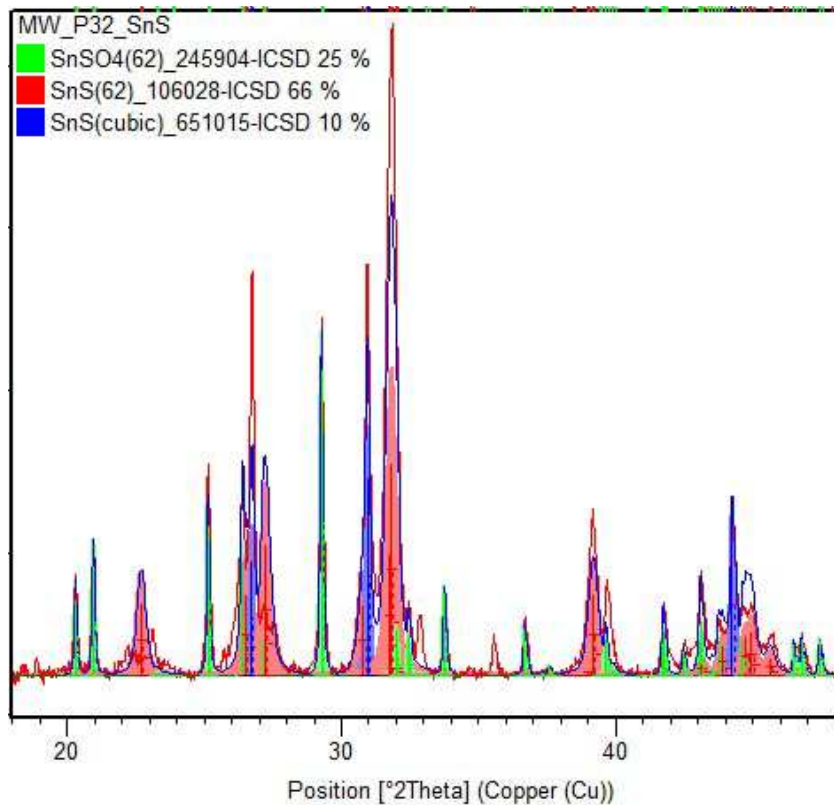


Figure 34 Spectra of tin particle containing fibers compared with other tin crystal

In consideration, the synthesis of tin sulfide in the fiber matrix or at least on the fiber matrix through spinning of viscose in a tin chloride containing spinning bath is successful, but tin particles are not obtained phase pure, as it is the result in the synthesis of copper sulfide coated viscose fibers. A possible explanation for this could be that some tin sulfate remained on the fibers during the washing process and is therefore determined in the XRD analysis.

4.5.3 Results for the fiber spinning experiments in a nickel(II)chloride spinning bath

Also in the case of nickel(II)chloride used to spin fibers into, black particles arose directly after injecting viscose into the spinning bath. The obtained fibers showed a clear difference to standard viscose fibers due to their brownish color. During the washing step of viscose fibers with copper and tin sulfide particles, the washing solution was clear and free of visible particles, but in the case of nickel coated fibers, the washing solution is turbid and full of visible particles after five minutes.



a) washing solution of fibers spun into nickel chloride



b) washing solution of fibers spun in copper chloride

Figure 35 Washing solutions after five minutes of fiber washing

In Figure 35 the mentioned difference in the washing step of copper sulfide containing fibers and fibers regenerated in a nickel chloride spinning bath is visualized. The washing solution is turbid by nickel particles which cannot be fixed on in the fiber matrix and therefore are washed away.

The obtained fibers are investigated through light and electron microscopy. In the light microscopy images, the fibers do not show a real difference to viscose fibers produced by the standard viscose process, whereas the transparency as well as the fiber structure is comparable.

In the high resolution images enabled via scanning electron microscopy, finally a difference between the standard fibers and fibers spun in nickel chloride is discovered. The fibers obtained in the presence of nickel salt, show small undefined particles on the fiber surface. But the particles cannot be detected over the whole fiber surface in a regular distribution, rather they are located in colonies.

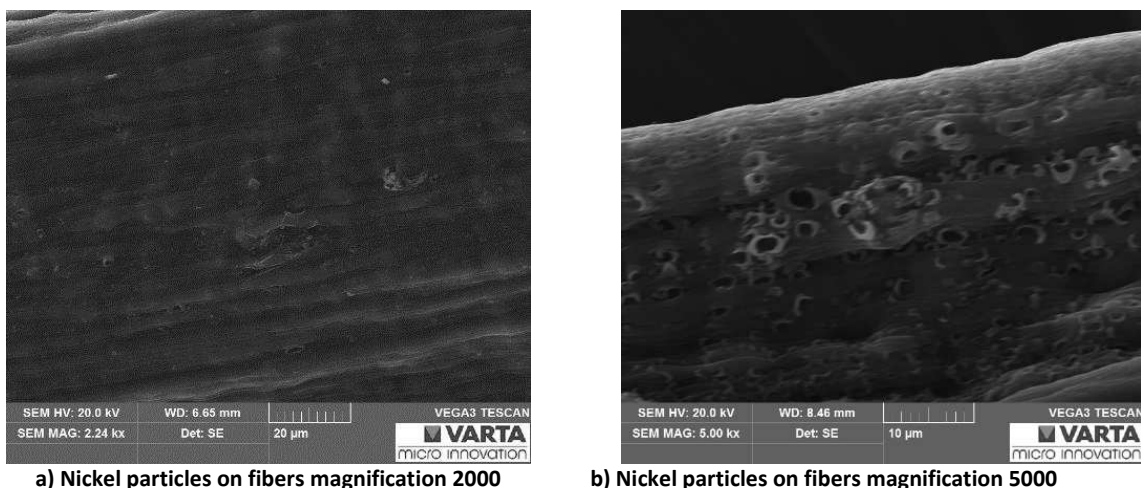


Figure 36 Viscose fibers regenerated in a nickel containing spinning bath and the particles detected on the fiber surface

After the detection of the particles in the SEM images, the fibers are pestled and investigated through XRD to characterize the chemical composition of the present nickel sulfide particles. In the first XRD analysis only the classic cellulose II reflection is detected, this could be caused by the small amount of particles present on the fiber surface or by the undefined form of the particles. Larger particles are produced by heating the fibers up to 150°C under nitrogen flow for 1 hour, to sinter the maybe present nickel sulfide crystals.

After the first sinter process, another XRD is recorded but there is still only the cellulose II reflection visible in this spectrum and therefore another sinter process is performed. This time the fibers are heated up to 400°C under argon flow with a temperature ramping of 15°C/min. The temperature is hold for 1 hour and afterwards the sample is cooled down to room temperature again.

A third XRD spectrum is recorded from the carbonized fibers and this time additional to the cellulose II reflection also reflections suitable for nickel particles are visible.

Figure 37 illustrates the measured XRD spectra of normal viscose fibers, non-tempered nickel particle carrying fibers and heat treated fibers with nickel particles on the surface. As said before, the reflections in the spectra of normal fibers and the reflections resulted for the non-tempered fibers are the same ones and represent present cellulose II. At $2\theta = 43^\circ$ an additional reflection appears in the spectrum obtained for the carbonized fibers. A reflection in this region is not typical for cellulose(II) and therefore has to be caused by another chemical compound, most likely through the nickel particles detected in the SEM.

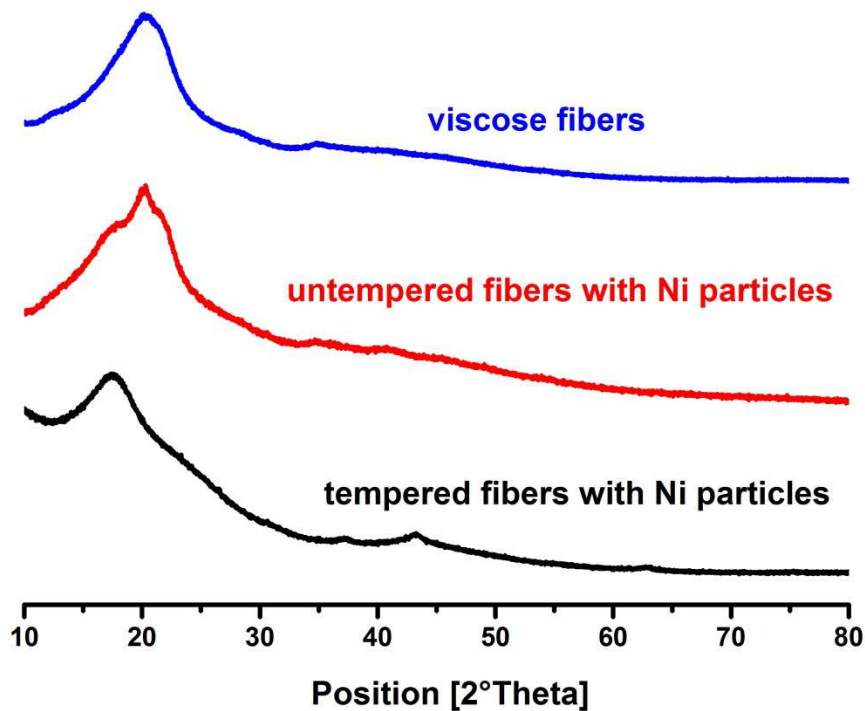


Figure 37 XRD spectra of standard viscose fibers, untampered and carbonized Ni particle carrying fibers

To identify the chemical composition of the nickel species found in the spectrum, the attending reflection is magnified and compared to spectra of further nickel crystals. The spectrum of cubic nickel oxide shows an accordance of 100% (Figure 38) to the reflections recorded in the XRD analysis of the heat treated viscose fibers.

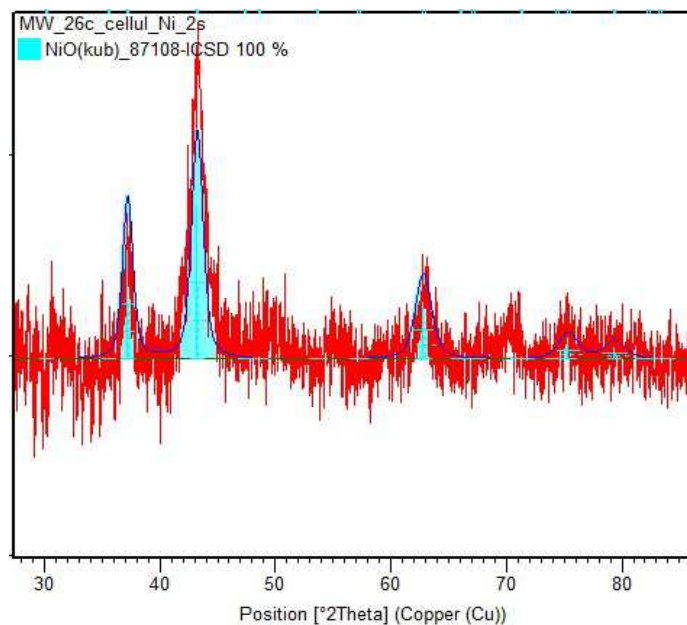


Figure 38 Accordance from XRD spectra of nickel oxide and viscose fibers with Ni particles

So the XRD analysis can be seen as proof for the presence of nickel oxide in the fibers, but nickel oxide is not the desired nickel species. One reason for this could be the oxidation of

nickel sulfide before or more likely during the heat treating at 400°C. Already minimal traces of oxygen are required to oxidize nickel sulfide to nickel oxide at a temperature of 400°C. (85)

In summary, the synthesis and adhesion of nickel particles during regeneration of viscose in a nickel chloride containing spinning bath is possible. Upon heating, the obtained nickel sulfide crystals are oxidized through a tempering process.

4.5.4 Results for the fiber spinning experiments in a cobalt(II)chloride spinning bath

Cobalt(II)chloride is investigated as well in a concentration range of 0.25 wt% up to 1.5 wt% for the in situ synthesis of metal sulfides in during the viscose process. The reactions observed during the regeneration of viscose into a cobalt containing spinning bath and during the washing process are equal to the reactions observed during the fiber regeneration in the nickel(II)chloride containing spinning bath. The regenerated fibers have a brownish color, the spinning bath turns turbid directly after injection of the viscose and the washing solution features a brown color and is full of particles after washing the fibers for 5 minutes.

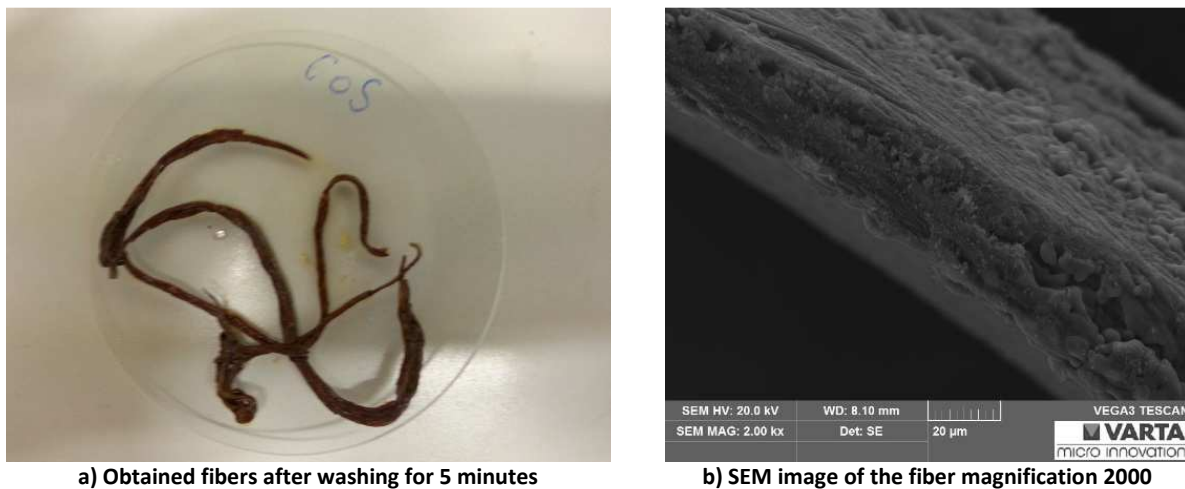


Figure 39 Illustration of the obtained fibers after spinning in a cobalt containing bath and a SEM image of the fibers

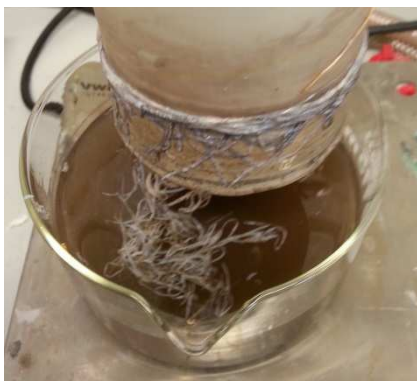
In Figure 39, the brown viscose fibers after the washing process and a SEM image of the fibers are presented. The light microscopy images reveal no difference to normal viscose fibers except the slightly different. By having a closer look to the fibers through scanning electron microscopy, the same effect as for nickel carrying fibers is observable, partly small and irregularly distributed crystals can be detected.

The characterization of these particles is also attempted by XRD analysis, but the diffractogram obtained for the non-tempered fibers does not show any reflections beside the typical broad reflection caused by cellulose II. Further tempering experiments and investigations to characterize the detected particles have not been performed.

Based on these findings it can be assumed that the success in the in situ synthesis of cobalt sulfides is comparable to the in situ synthesis of nickel sulfides.

4.5.5 Results for the fiber spinning experiments in an iron(III)chloride spinning bath

Due to the fact, that iron(III)chloride was easier available as iron(II)chloride, this salt is used in a concentration range of 0.25 wt% up to 1.5 wt% to explore the in situ synthesis of iron sulfide by regenerating viscose. In contrast to all the salts investigated before, in the case of iron present in the spinning bath, the fibers obtained are white and therefore equaly to the fibers obtained in the normal viscose process. In contrast to the equal looking fibers, the spinning bath is as cloudy as in all the other experiments undertaken before.



a) Iron salt containing spinning bath after viscose injection

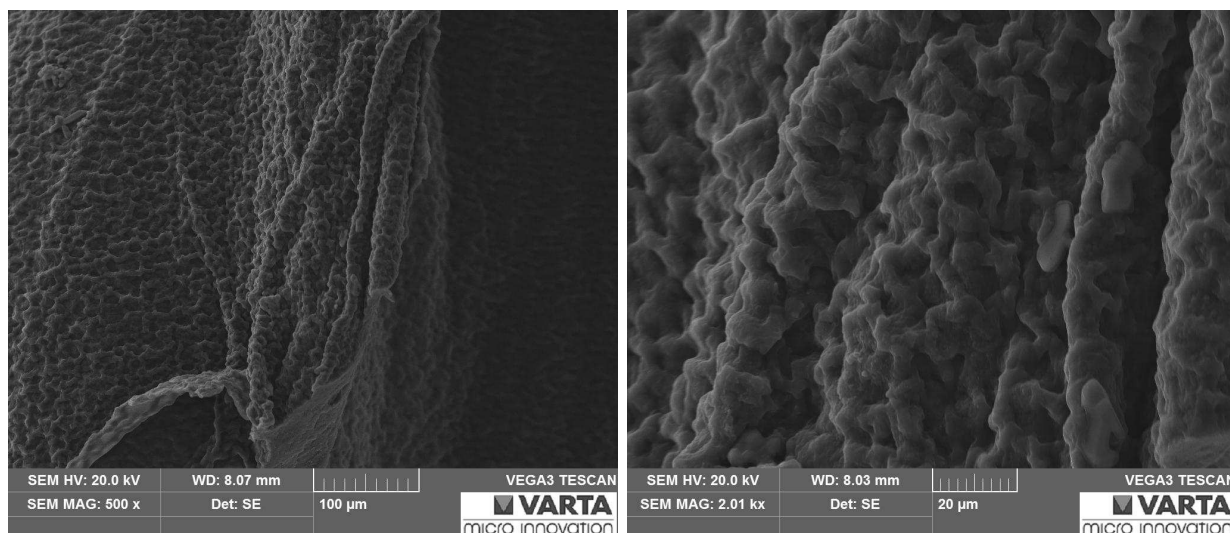


b) Obtained fibers after washing step

Figure 40 Illustration of the fibers obtained after the spinning process and after 5 minutes of washing in de ionized water

The uncolored fibers presented in Figure 40 are a first hint that something in the synthesis differs to all the in situ metal sulfide synthesis tried before.

By means of light microscopy and scanning electron microscopy the fibers are compared to normal viscose fibers. In the light microscopy images the fibers do not differ from normal fibers, neither the transmittance nor the fiber structure is changed. In the electron microscopy any noticeable particles on the fiber surface cannot be detected.



a) Fiber spun in iron containing bath, magnification 500 b) Fiber spun in iron containing bath, magnification 2000

Figure 41 SEM images of the fibers obtained through viscose spinning in an iron containing spinning bath

Although in the SEM images presented above, no particles can be seen on the fiber surface, the surface texture of the fibers presented in Figure 41, itself is very interesting. The fiber surface is not as smooth as it is in the case of normal viscose fibers instead the surface looks like a crater landscape. This could be caused through already during the regeneration phase dissolved iron particles.

Never the less a XRD diffractogram for the resulting fibers is recorded, but as expected no reflections which would indicate the presence of iron sulfides or other iron species are visible.

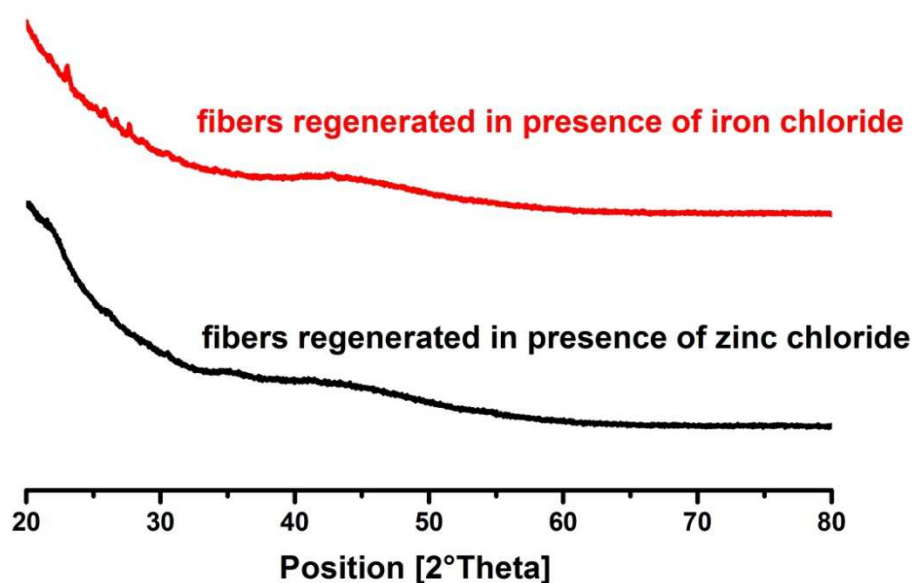
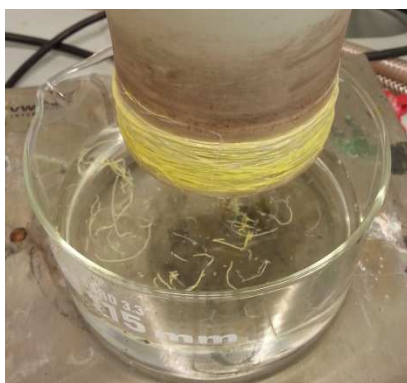


Figure 42 XRD spectra for fibers regenerated in presence of iron and zinc salts in the spinning bath

To sum up, the immobilization of iron sulfides or any other iron species into regenerated cellulose is not successful. Maybe there are still some traces of iron in the fiber matrix, but these traces cannot be detected neither by SEM imaging nor by XRD analysis.

4.5.6 Results for the fiber spinning experiments in a zinc(II)chloride spinning bath

The last chloride salt employed for the in situ synthesis of metal sulfides onto the fiber matrix by means of the viscose process is zinc(II)chloride. The concentration range in which zinc is used is equal to the reactions investigated before. During the regeneration of viscose in a zinc containing spinning bath some interesting observations are made. The zinc bath is the first bath which does not get turbid by rising particles after the injection of the viscose solution. The fibers obtained are comparable to the fibers resulted in the normal fiber spinning process.



a) Fibers obtained in presence of zinc, after regeneration



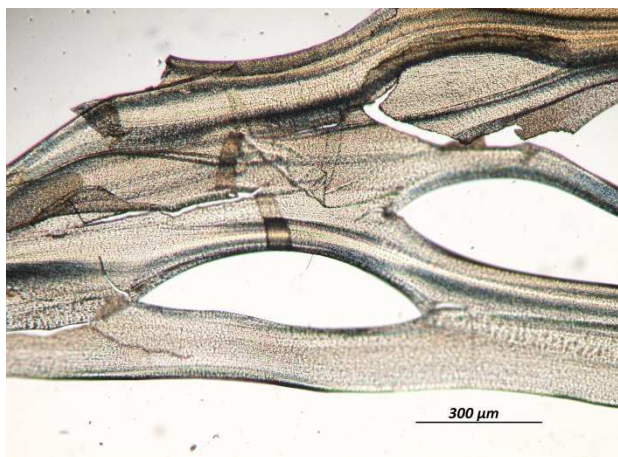
b) Fibers obtained in presence of zinc, after drying

Figure 43 Fibers obtained after injection of viscose in a zinc(II)sulfide containing spinning bath

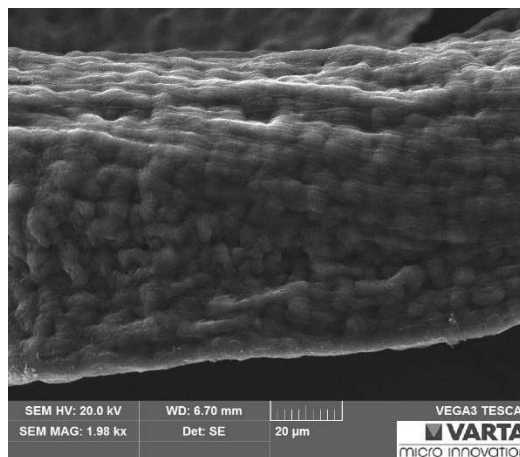
The fibers presented in Figure 43 have the same yellowish color as the fibers obtained after spinning in pure 15% sulfuric acid solution, also after the washing and drying step, the fibers look like normal viscose fibers, this is a clear hint that no zinc particles can be fixed during fiber spinning process.

To be sure that there are no zinc particles in the fibers or on the fiber surface the same investigations as used for all the other samples, are performed.

Neither in the light microscopy nor in the electron microscopy there are any particles or other differences to standard fibers determined. Two examples of the resulting images are presented in Figure 44.



a) Fibers obtained in presence of zinc, magnification 100



b) Fibers obtained in presence of zinc, magnification 500

Figure 44 A light microscopy and an SEM image of the viscose fibers obtained by spinning in presence of zinc(II)chloride

With the final XRD analysis, where also no hint for the presence of any zinc particles is found (Figure 42), it can be considered that there is no in situ synthesis of zinc species during the regeneration of viscose under the investigated conditions.

4.5.7 Results for the fiber spinning experiments in a silver(I)nitrate spinning bath

In a final fiber regeneration experiment silver(I)nitrate is used as salt for the in situ synthesis of silver sulfides during the regeneration step. The concentration range of 0.25 wt% up to 1.5 wt% is equal to the experiments undertaken before. This time similar abnormalities as in the regeneration of viscose in a copper or tin containing spinning bath are observable.



a) AgNO_3 containing spinning bath after regeneration

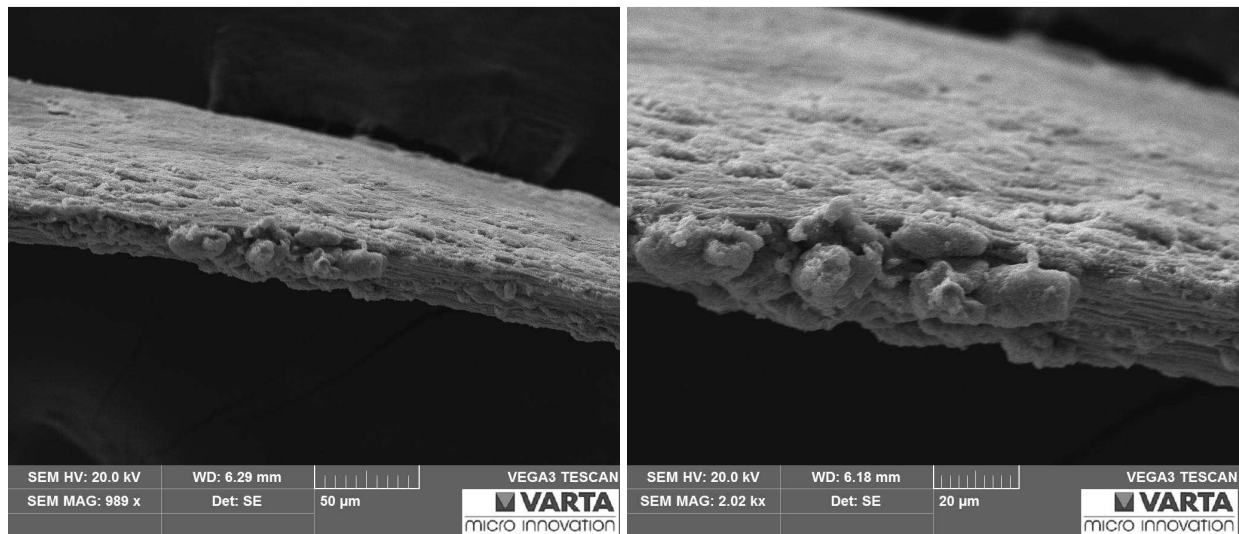


b) Obtained fibers after the drying

Figure 45 Illustration of the fibers and the spinning bath after fiber synthesis and of the dried silver containing particles

Figure 45 presents the turbid spinning bath obtained immediately after injecting the viscose, in the figure also the black fibers obtained after the drying are shown. The washing solution is clear and any visible brown particles are not detectable, after washing the fibers for five minutes.

The total opacity of the fibers, detected in the microscopy investigation is caused by a high silver load on the fibers. In the SEM images (Figure 46) a large amount of crystalline structures with a regular distribution onto the whole fiber surface are detected.



a) Fiber spun in silver containing bath, magnification 1000

b) Fiber spun in silver containing bath, magnification 2000

Figure 46 SEM images of the fibers obtained through viscose spinning in a silver(I)nitrate containing spinning bath

The diffractogram shows a lot of sharp reflections beside the broad cellulose II reflection, and therefore indicates the presence of a crystalline substance, most likely silver sulfides, in the fiber matrix or at least on the fiber surface.

An exact crystal structure including the crystal lattice type, is gained by comparing the measured diffractogram to other Ag_2S structures. Figure 47 clearly shows that monoclinic Ag_2S is present in the fiber matrix.

In consideration the immobilization of silver disulfide on viscose fibers is proved, it is further confirmed that the in situ synthesis of phase pure silver disulfide during regeneration of viscose in a silver(I)nitrate containing spinning bath works under the tried conditions.

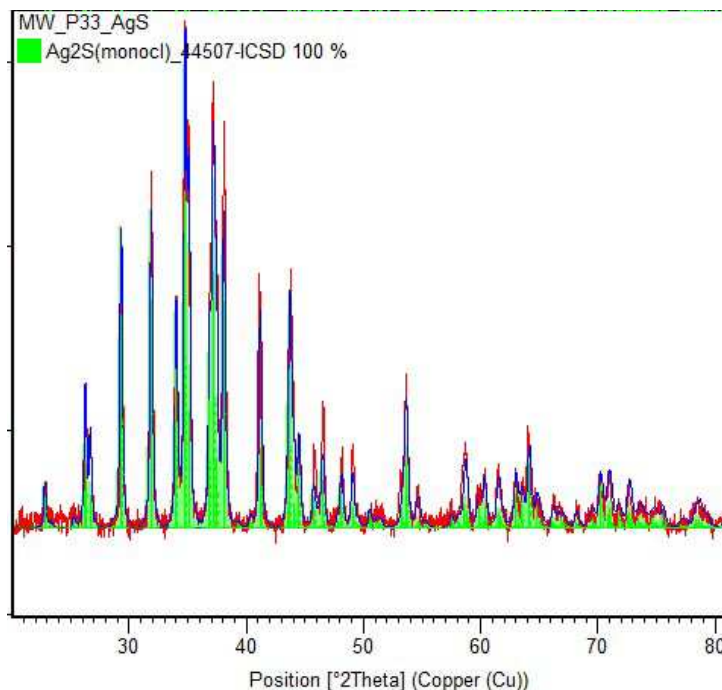


Figure 47 Spectra of silver particle containing fibers compared to silver disulfide

4.5.8 Determination of the amount of metals fixed through fiber synthesis

After it was demonstrated by light microscopy, scanning electron microscopy and XRD analysis the amount of the metal sulfides fixed onto the fibers is determined by ICPMS. To find out, in which way the concentration of the metal salt present in the spinning bath affects the amount of metal take up, fibers for the analysis are regenerated in two different metal salt concentrations (0.25 wt% and 1 wt%), respectively.

In addition, also the fibers spun in a zinc or iron salt containing bath are investigated to confirm the results obtained by microscopy and XRD analysis.

Table 12 represents an overview of the data obtained through ICPMS analysis and includes a few results which are rather unexpected and discussable.

The first thing to discuss is the high amount of metal sulfides in the case of copper, tin and silver. In presence of 1 wt% silver salt, the silver content in the fiber is by about 600 mg/g, an enormous amount, but also the reachable copper (about 250 mg/g) and tin (about 270 mg/g) contents present in the fiber are impressive. The high amounts of metal detected in these samples correlate with the SEM and XRD analysis gained before, which all show a high amount of particles on the fiber surface. In the case of the silver sulfide, it is possible that

there is some metal sulfide remaining between the single fibers after the washing step and therefore pushing the silver content.

The second interesting point is that a reduction of the salt content in the spinning bath down to 25% of the primarily used amount of this salt only causes a decrease in the metal uptake by the half. In the case of tin sulfide, a reduction of the salt content leads to a drastic reduction of the tin amount fixed on the fibers.

Table 12 Overview of the metal uptake by varying salt concentrations in the spinning bath

Sample	Cu [g/kg]		Ag [g/kg]		Sn [g/kg]	
	Average	Deviation	Average	Deviation	Average	Deviation
1wt% CuCl ₂	255	12				
0.25wt% CuCl ₂	130	6				
1wt% AgNO ₃			628	35		
0.25wt% AgNO ₃			228	14		
1wt% SnCl ₂					276	9.2
0.25wt% SnCl ₂					16	17
Sample	Ni [g/kg]		Fe [g/kg]		Zn [g/kg]	
	Average	Deviation	Average	Deviation	Average	Deviation
1wt% NiCl ₂	53	3				
0.25wt% NiCl ₂	29	1				
1wt% FeCl ₃			3.7	0.3		
1wt% ZnCl ₂					1.7	0.2

Another interesting fact is the amount of nickel found on the fibers, because in both investigated concentrations, a significant amount of metal sulfide is detectable. Although the amounts measured are much lower than those of copper, silver and tin, 53 mg/g and 29 mg/g fiber for the lower concentration are detected. Also these results are in accordance with the results of the SEM and XRD measurements, where only a small amount of nickel sulfide particles was determined.

The last thing to note is that the amount of iron and zinc detected by ICPMS also correlates with the investigations discussed before. In both cases, neither in the SEM images nor in the XRD analysis, any particles could not be detected. Also the amounts detected in the ICPMS (0.4% in the case of iron and 0.2% in the case of zinc) are rather negligible.

4.5.9 Cross section analysis to investigate the fiber / metal sulfide interfaces

Through SEM-EDX investigations of fibers fixed in horizontal direction to the electron beam, the cross sections of two metal sulfide containing fibers are investigated. One sample is a fiber regenerated in a 0.25 wt% copper salt containing spinning bath, the second sample is a fiber regenerated into a 1 wt% silver containing acid bath.

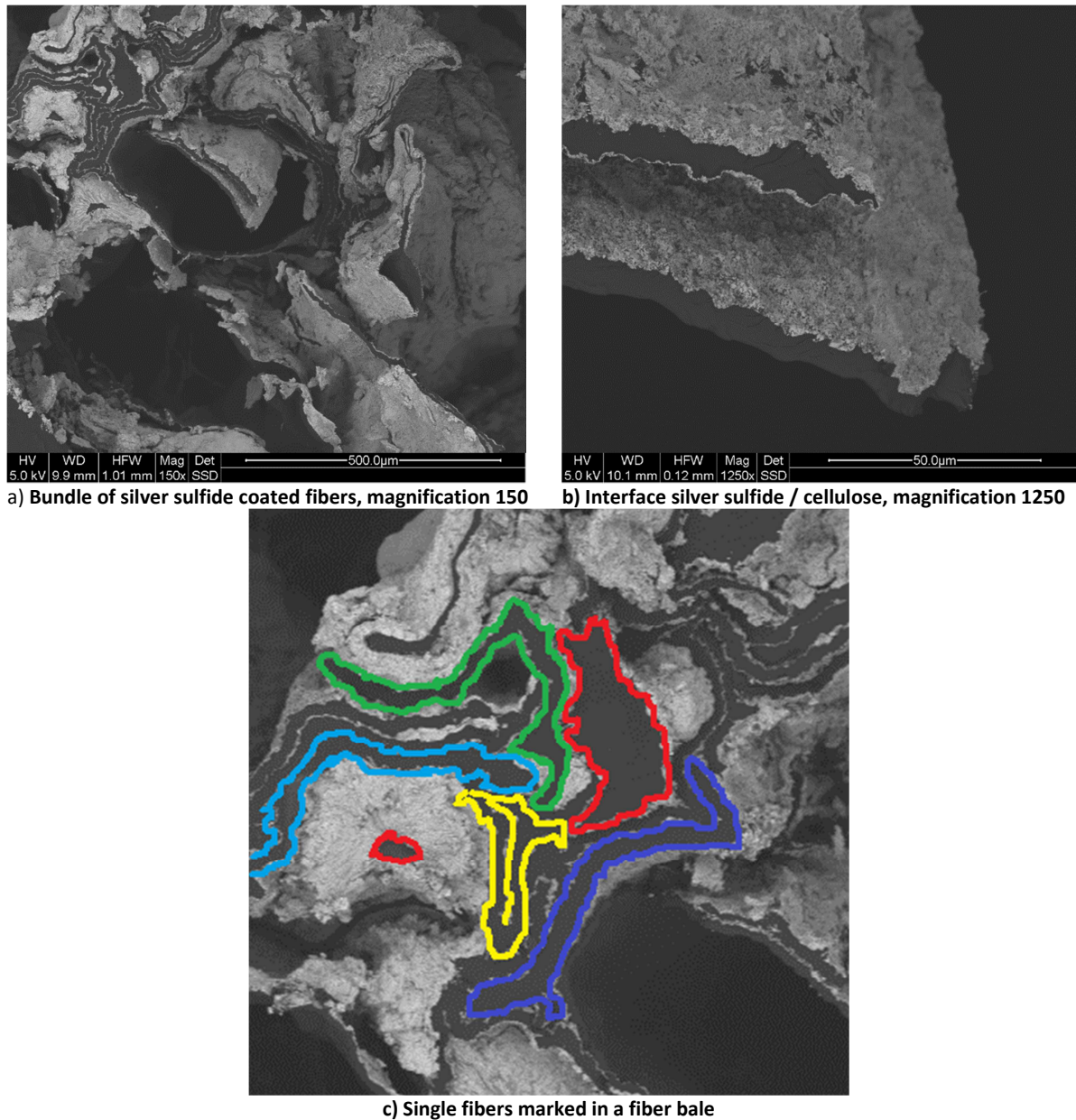


Figure 48 Cross section of cellulose fibers regenerated in a silver cation containing spinning bath in varying magnification

Figure 48 above, shows the cross section images of the fibers regenerated in the silver cation containing bath. As it can be seen in the images the silver sulfide and the fiber matrix are strictly separated in two phases and no inclusion of silver sulfide clusters into the fiber

matrix is visible. The EDX spectra recorded for both the metal and the cellulose dominated region underline this assumption, because hardly any silver was found in the cellulose region and the spectrum of the metal region is dominated by the silver reflection. More interesting is the silver cellulose interface because there exists no strict border line between the two phases instead the border can be described as blurred.

In the image, it can be seen that the fibers are squeezed and silver sulfide is embedded between the single fiber strains. The squeezing is probably caused during the collection of the fibers on the fiber roller, due to the high number of overlapping fiber filaments on the roller it is likely that excess silver sulfide cannot be washed away during the washing process in de-ionized water and therefore increases the silver content in the samples significantly.

The same statements are valid for the copper sulfide coated fibers, with the only visible distinction in the thickness of the copper sulfide layers. Due to the lower metal salt content in the bath, the thinner layers can be explained. But as determined in the ICPMS analysis the copper content in the fibers decreases much slower than the content of copper cations is reduced in the regeneration bath. Therefore, the layer thickness determined for the copper coated fibers seems to be the more realistic one.

These results clearly show that the fibers are only coated with the developing metal sulfides and no inclusion of the metal sulfides into the inner of the fiber matrix takes place. This could be explained by the fiber regeneration which proceeds from the outer to the inner layer and therefore it is unlikely that the dissolved metal cations diffuse into the inner fiber layers and substitute the sodium cations of the xanthate groups. (14)

4.5.10 Final investigation to check if the presence of metal effects the regeneration step

One last investigation is necessary, after it is shown through ICPMS and SEM cross section analysis that high amounts of metal sulfides can be fixed on the fibers. In this final analysis the effect of the metal salts present during the fiber regeneration, is investigated. In the normal viscose process the resulting product is, as already mentioned before cellulose II. Through ATR IR spectroscopy it is investigated if there is any difference between the fibers obtained in the normal spinning process and the fibers obtained in the presence of a metal salt in the spinning bath.

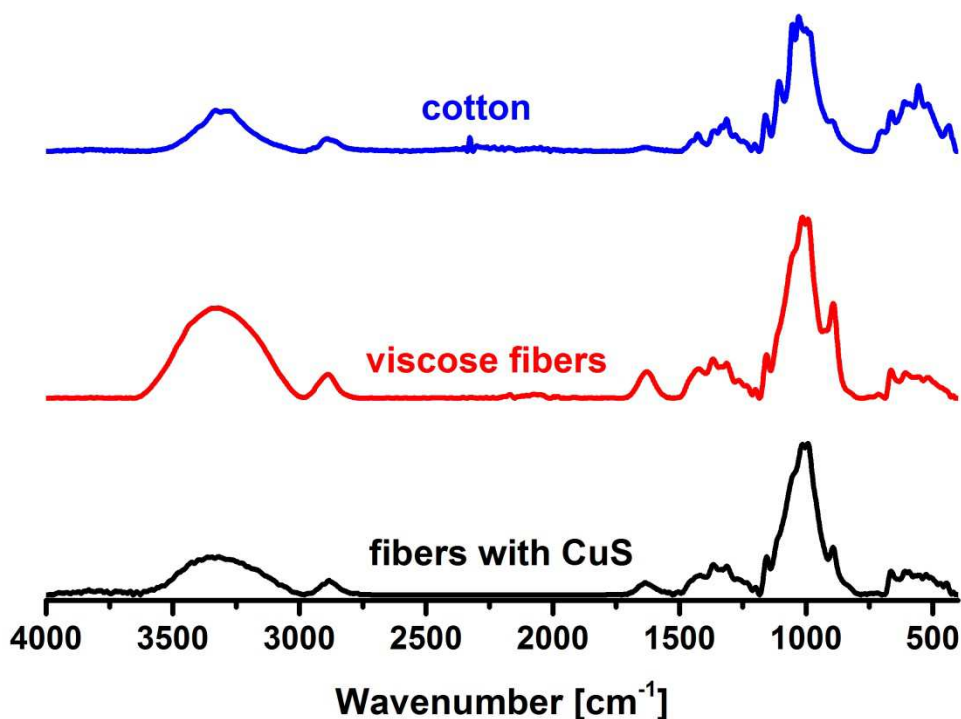


Figure 49 ATR IR Spectra of cotton, regenerated cellulose and CuS containing viscose fibers

Figure 49 presents ATR IR spectra of cotton used as starting material, regenerated viscose fibers obtained through the standard process and copper sulfide coated viscose fibers obtained in the presence of copper(II)chloride in the spinning bath.

The difference between the cotton fleece spectrum and the spectrum of the regenerated fibers is already discussed before. For the spectra of normal viscose fibers and the CuS coated fibers it can be noticed that the only difference which appears, is the intensity of the broad band in the region of $3600 - 3000 \text{ cm}^{-1}$. But due to the fact that all the appearing signals are comparable and no further signals occur in the spectrum of CuS containing fibers

it can be assumed that the presence of metal salts in the spinning bath does not affect the viscose regeneration back to cellulose II.

4.6 Correlation between viscose age and metal uptake

The investigation of the correlation between the metal salt concentrations in the spinning bath and the amount of metals fixed on the different fibers has provided some interesting results. Therefore, also the influence of the viscose age on the metal uptake is investigated in a side experiment.

A viscose solution aged for one- or three- days of the same viscose batch are used for the regeneration of viscose fibers in the presence of 1wt% CuCl₂ in the spinning bath. The following fiber treatment and the analysis via ICPMS to determine the metal uptake is equal for both samples. The resulting metal amounts fixed onto the fiber surface are listed in Table 13.

Table 13 Copper uptake in viscose solutions aged for one and three days

Sample	Cu [g/kg]	
	Average	Deviation
<i>1wt% CuCl₂ viscose aged one day</i>	183	9
<i>1wt% CuCl₂ viscose aged three days</i>	233	7
<i>1wt% CuCl₂ viscose aged three days²</i>	255	12

As it is shown in the table above, there is a significant correlation between the viscose age and the metal uptake. In the viscose aged one day, the metal uptake was lower as in the three day aged one. To underline these results, also the ICPMS result of another sample, generated from a viscose solution aged for three day is shown. Although this sample originates from another viscose batch the copper uptake is comparable. An explanation for this could be that during the viscose aging process some CS₂ groups are separated from the cellulose xanthates again and the free CS₂ groups can react easier with the present copper cations in the spinning bath.

The data resulted through this experiment points out an interesting trend which has to be further investigated to verify the obtained results.

² The viscose used for this fiber synthesis is from another viscose batch as used for the regeneration of the other two samples

4.7 Investigation of the particle size in correlation to process parameters

Additional to the investigations of the influence of different parameters on the metal uptake, it is also tried to explore the influence and the correlation between the crystal size and varying process parameters. Therefore three process parameters, the acid concentration in the spinning bath (15%, 25%, 40%), the regeneration time in the spinning bath (5 min, 10 min, 20 min) and the viscose age (1 day, 2 day, 3 day) are varied and the resulting CuS particles on the viscose fibers are investigated through SEM imaging.

Acid concentration

In the case of fibers spun in 15% and 25% sulfuric acid solutions, the fibers are comparable to the fibers obtained in previous experiments. The fibers spun in a copper containing 40% sulfuric acid solution, are almost completely dissolved after 5 minutes of regeneration due to the high acid content in the bath.

For the samples prepared in 15% or 25% sulfuric acid solutions, any correlation between the particle size and the acid concentration could not be determined.

Regeneration time:

The elongation of the regeneration time from 5 to 20 minutes showed no visible effect on the resulting fibers, there is also no influence on the particle size detectable in the SEM images.

Viscose age:

As it is already determined that there is a correlation between metal uptake and viscose age, it is also interesting if there is an influence on the particle size caused by the viscose age. But as in the two experiments before, there is no difference in the resulting particles visible through SEM imaging.

In the following figure only two arrangements, once between the viscose age and once between the acid concentrations, are illustrated. An influence of changing parameters onto the crystal size could not be detected.

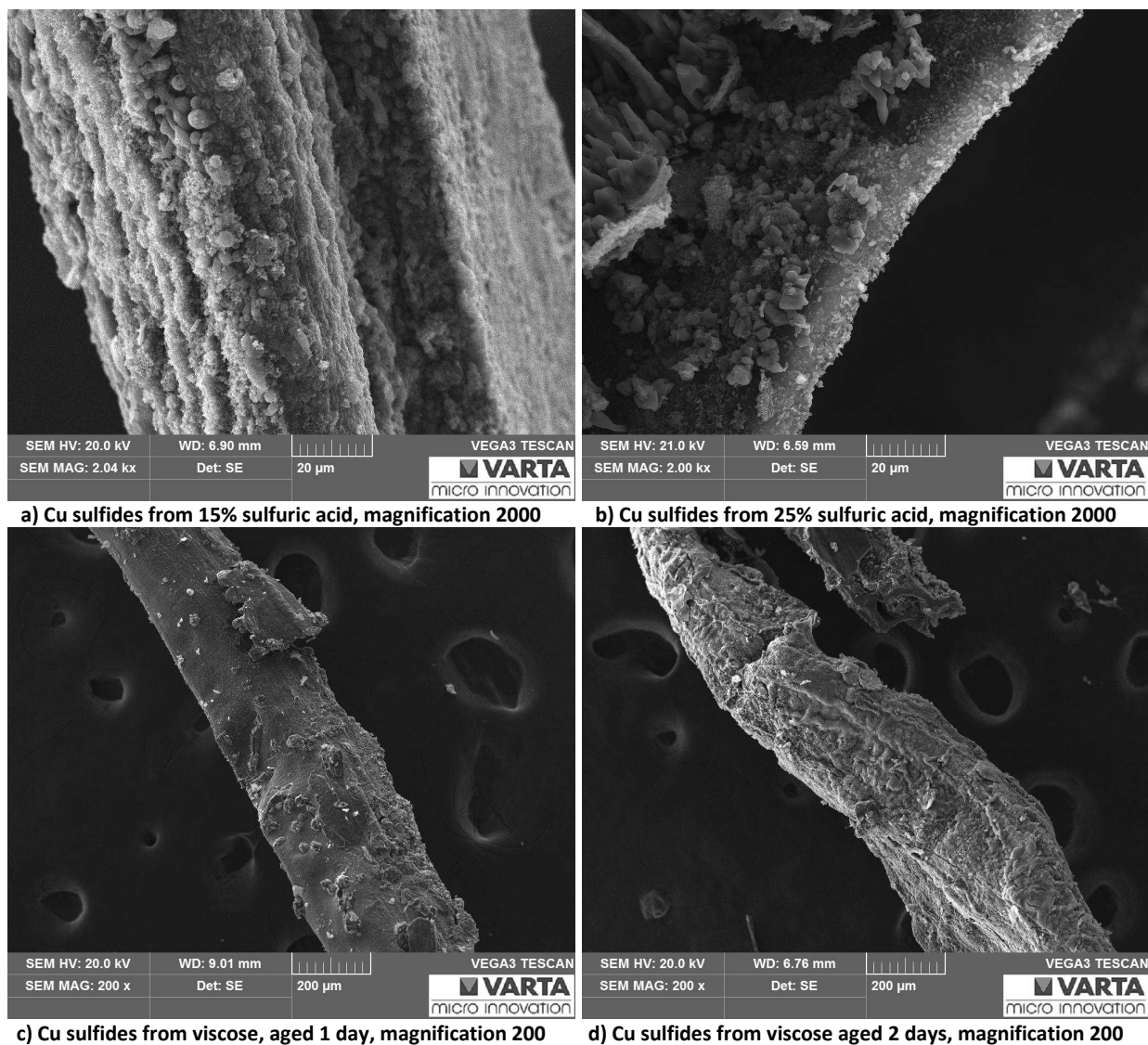


Figure 50 Examples for SEM images obtained by investigating the influence of varying process parameters on the size of the resulting copper sulfide crystals.

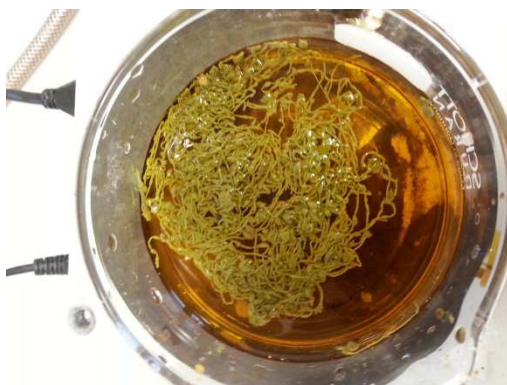
In fact, a correlation between varying process parameters and the size or structure of the resulting copper sulfide crystals fixed on the fiber surface is not detectable. Maybe there is really no correlation, or maybe the resolution of the SEM is not sufficient to detect any correlations. But more probably the particle size distribution of the developing metal sulfides is too wide-spread to detect a significant change in the size of the rising particles. So to get more information about this topic, another investigation technique or a modified sample preparation, where the size distribution of the crystals is adjustable, has to be used.

4.8 Incorporation of tungsten oxide and tungsten sulfide into the viscose

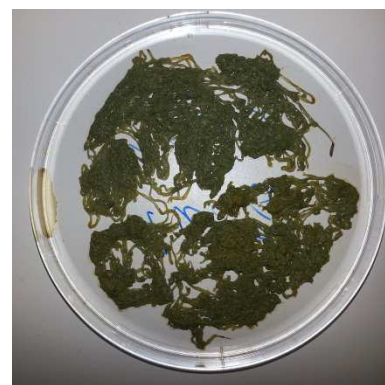
Tungsten(IV)sulfide is an inorganic material able to form nanotubes. WS_2 nanotubes have already been investigated as strengthening materials for the improvement of mechanical properties in polymer composites. The use of WS_2 led to a significant increase in the Young's module, compression yield strength and flexural yield strength. (86) (87) These interesting results are the reason, why the spinnability of tungsten containing viscose is investigated too.

4.8.1 Results for the incorporation of WO_3 into the viscose

The product obtained from the tungsten(VI)oxide containing viscose solution can be described as green fibers (Figure 51), what is a noticeable difference to the normal viscose process. The washing solution is colored orange after the washing step. An XRD analysis of the fibers is executed, to get some information if and which structure the tungsten remains in the fibers.



a) Washing of tungsten containing fibers



b) Resulting fibers after washing

Figure 51 Fibers obtained after mixing tungsten(VI)oxide into viscose and regenerating the viscose in sulfuric acid

In Figure 52 the XRD diffractograms of the tungsten containing fibers clearly confirm the presence of monoclinic WO_3 . So the resulting information is that the tungsten(VI)oxide does not dissolve into the viscose solution and therefore no reaction to the desired tungsten sulfide during the regeneration process is possible.

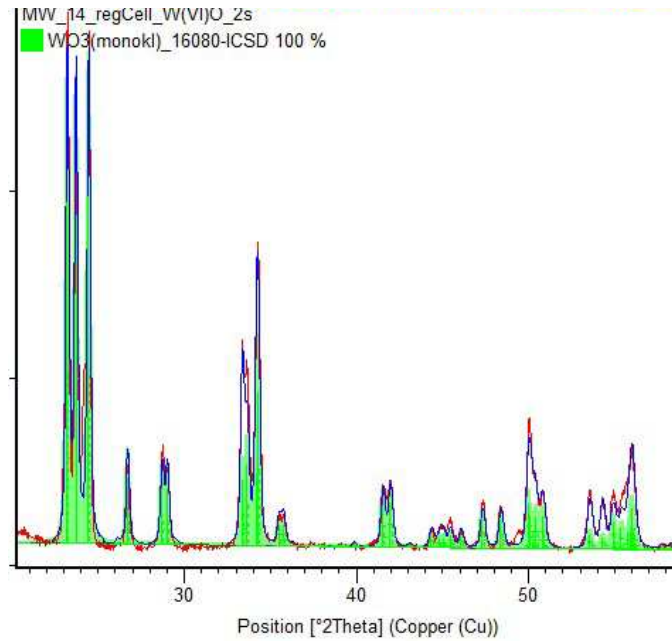
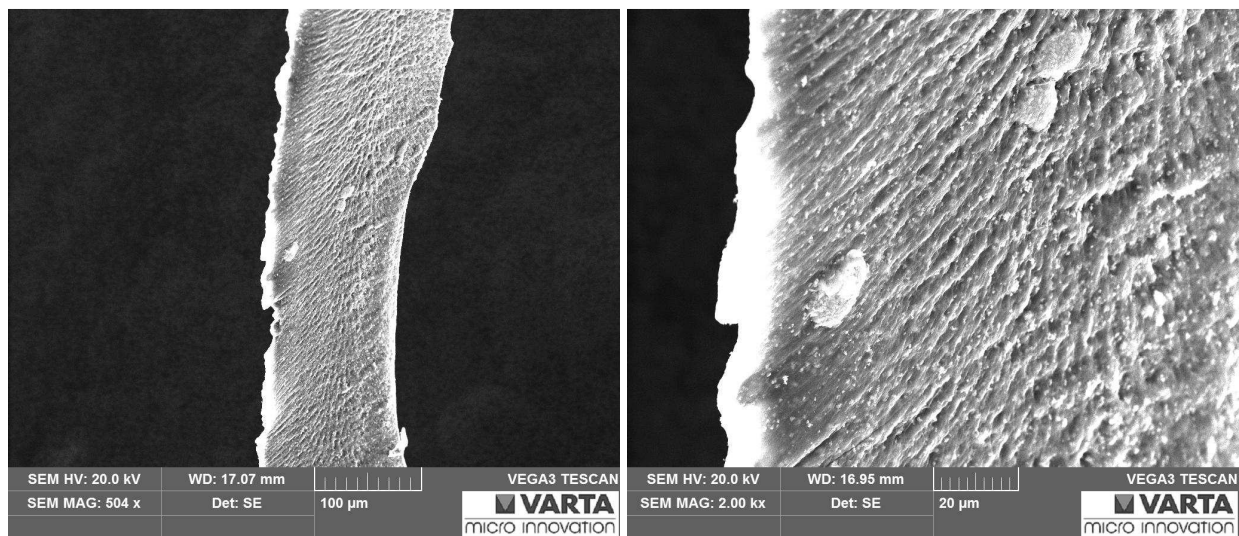


Figure 52 Spectra of tungsten containing fibers compared to monocline tungsten(VI)oxide

After the information is obtained that the tungsten(VI)oxide does not react with the sulfur groups during stirring or regeneration, the fibers are investigated through a scanning electron microscope to see if the inclusion of WO_3 shows an effect onto the fiber structure.



a) Tungsten(VI)oxide containing fiber, magnification 500

b) Tungsten(VI)oxide containing fiber, magnification 2000

Figure 53 SEM images of tungsten(VI)oxide containing fibers in different magnifications

In the SEM images the fibers show a relatively rough surface with regularly distributed small particles on it. The small particles probably consist of tungsten oxide particles, the rough surface may be formed via the inclusion of tungsten oxide particles in the fiber matrix.

4.8.2 Results for the incorporation of WS₂ into the viscose solution

Equal to tungsten(VI)oxide also tungsten disulfide was mixed into the viscose solution, the resulting fibers look like the tungsten(VI)oxide containing fibers. To investigate the structure of the tungsten remaining into the fibers ones more XRD characterization is used. The resulting diffractogram is illustrated in Figure 54. In the diffractogram also the reflections of a WS₂ reference are shown and it is visible that the two spectra match to 100%. Hence it is obvious that also tungsten disulfide stays unchanged in the viscose solution.

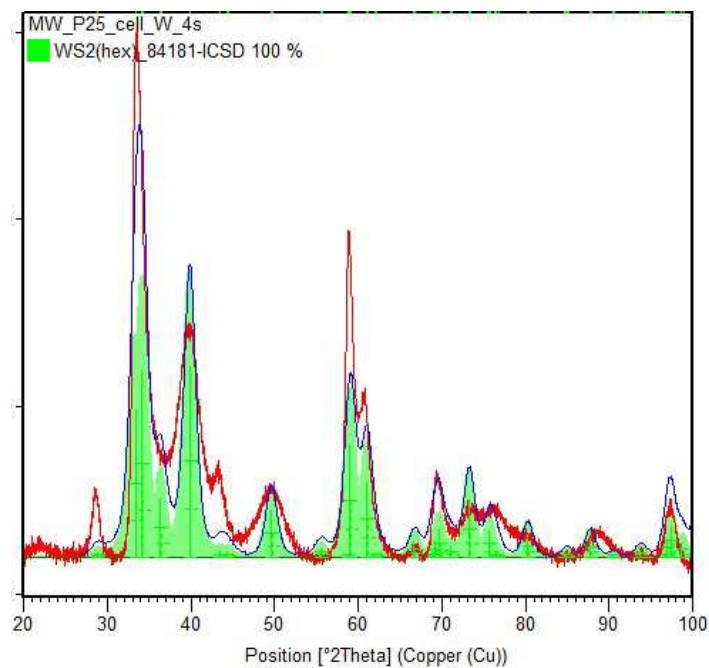


Figure 54 Diffractogram of WS₂ containing viscose fibers compared with a WS₂ reference

The SEM images only differ through a smooth fiber surface to the images obtained from the WO₃ including fibers, but also in this fibers, small particles with a regular distribution are detectable on the fiber surface.

To sum up this chapter, the incorporation of tungsten particles in the viscose is possible but the tungsten particles are not only insoluble in water, they stay unchanged in the viscose solution too. A formation of nanotubes is at least with the analysis tried not detectable.

4.9 Cellulose films and the uptake of metal sulfides onto the film matrix

The production of cellulose thin films is also part of these investigations, because cellulose thin films also known as cellophane, are another important product obtained from cellulose xanthate. The principle of the industrial cellulose film production differs to fiber synthesis only by the use of a slot nozzle instead of a spinneret. (77) (88)

Due to the fact that it is not easy to develop a lab scale extrusion method for cellulose xanthate in a rather short time, an alternative approach was chosen.

The production of cellulose films as described in 3.7 works without any problems up to the point where the films are dried. During the drying step the films start to shrink and deform in a way that the films can hardly be used for any application or characterization tests.

4.9.1 Storage experiments with cellulose films

Due to the shrinking of the cellulose films, it is attempted to store the films in de-ionized water and glycerol solutions with varying concentrations (2%, 5%, and 10%). The idea behind the use of glycerol is its common use as softener for polymers and membranes and therefore it should also work with cellulose films. (89)

In a first experiment the films are transferred into the glycerin containing storage medium either directly after regeneration, or after drying on air, or after drying in an oven and stored for one week.

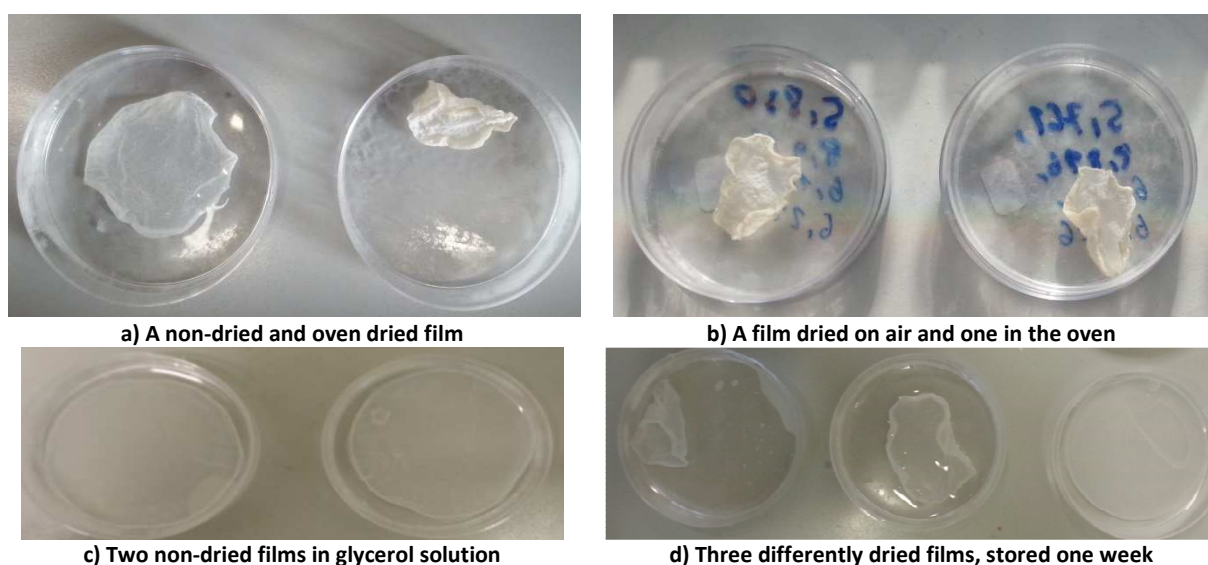


Figure 55 Shows cellulose films in different steps of the storage experiment in glycerol solutions

After one week of storage the following conclusion can be drawn. The films transferred into the glycerol solution directly after regeneration look like they did at the beginning. The films dried on air, which shrank less than the films dried in the oven (Figure 55b) unfold nearly complete after one week, and also the smoothness of the films is comparable to the non-dried films. The films dried in the oven at 50°C showed the highest shrinking, which is still visible after one week in the glycerol solution. To gain some information about the effect and possible uptake of glycerol into the cellulose matrix the films are washed thoroughly, dried again at 50°C for 24 hours and weight on the next day.

Table 14 Overview of weight increase for the films stored in glycerol

	<i>Before storage</i>	<i>After storage</i>
<i>Without drying 2wt% glycerol</i>		0.067
<i>Without drying 5wt% glycerol</i>		0.095
<i>Without drying 10wt% glycerol</i>		0.138
<i>3h oven 50°C 2wt% glycerol</i>	0.043	0.056
<i>3h oven 50°C 5wt% glycerol</i>	0.043	0.106
<i>3h oven 50°C 10wt% glycerol</i>	0.041	0.124
<i>4h dried at RT 2wt% glycerol</i>	0.043	0.059
<i>4h dried at RT 5wt% glycerol</i>	0.043	0.078
<i>4h dried at RT 10wt% glycerol</i>	0.046	0.150
<i>Non dried, water</i>	0.044	0.046
<i>4h dried at RT, water</i>	0.045	0.046

In Table 14 the single weights are listed. It is determined that there is no difference in weight between the two drying methods and therefore drying on air seems to be the better method because the shrinking of the films is lower.

Although the storage in the glycerol solutions works quite well and the films unfold at least partly the weight increases significantly, even in the films stored at low concentrations and hence it is shown that glycerol penetrates the cellulose matrix and stays in the films even after washing them again.

In a second try, non-dried and cellulose films dried at room temperature are stored in water for one week. After storing the films for one week in water they are dried again and their weight is controlled. The films stored in water showed no significant increase in weight, but

only the non-dried films stay flat. The dried films stayed shrank in the water, the weights of the single films before and after storage are also shown in Table 14.

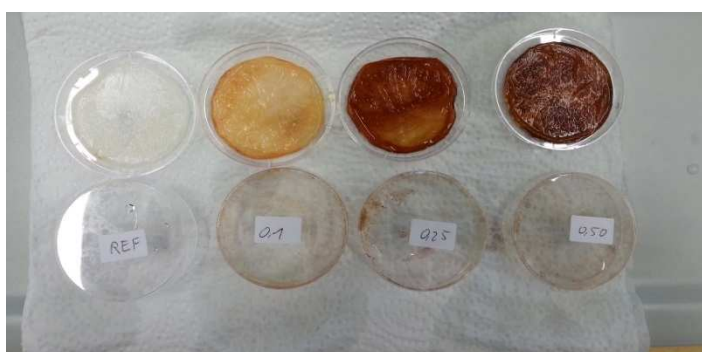
In another experiment flat films are produced under pressure caused by a piece of metal laid onto a perforated plastic layer. The films dried under the charged plastic layer also shrank a little bit, but they at least, stayed rather flat and therefore could be used in application tests.

4.9.2 Metal uptake in cellulose films during the regeneration step

In analogy to the fiber synthesis it is also tried to immobilize metal sulfides onto the cellulose films using the same basic principle. The desired metal cation is dissolved in the spinning bath and should react with the sulfur of the xanthate groups. The regeneration of cellulose films in metal salt containing spinning baths is executed with all the salts used for the fiber synthesis. Films are regenerated in a copper, silver, tin, cobalt or nickel containing bath and they show the same changes in structure as observed during the fiber synthesis. All the regenerated films differ in color compared to normal cellulose films and the metal sulfides do not disappear even during extensive washing with de-ionized water. For the films regenerated in the presence of zinc or iron cations no visible differences to normal cellulose films are observed. These experiments indicate that the in situ adhesion of metal sulfides during the regeneration of cellulose xanthate films works in a similar manner than for fibers.



a) Cellulose films during regeneration



b) Cellulose films regenerated in different concentrations of SnCl_2

Figure 56 Regeneration of cellulose xanthate films into metal cations containing spinning baths during and after regeneration

In Figure 56 it is shown that not only the uptake of metal sulfides on dried viscose films is done with success, it is also illustrated that the cation concentration present in the spinning bath has an influence on the amount of metal fixed on the cellulose surface.

The films are investigated through ATR IR spectroscopy, to gain some analytical data which correlates with the noticed observations.

The ATR-IR spectra are comparable to the spectra resulting from the metal sulfide containing viscose fibers and hence not presented again. In the spectra neither new bands are visible nor any bands disappear. Hence it can be said that the presence and uptake of metal sulfides in the regeneration step has no influence on the obtained films, which consist of cellulose II.

4.10 Metal sulfide containing films in antibacterial studies

In a final test, a possible application for the regenerated viscose products is investigated. In these studies, the antibacterial properties of copper sulfide coated cellulose films against staphylococcus aureus should be analyzed and compared to cellulose films according to EN ISO 20743. As it is presented in the table below, the bacterial counts at the beginning of the experiment are in a comparable range of $1 \cdot 10^3 \cdot L^{-1}$ up to $6 \cdot 10^{33} \cdot L^{-1}$ in both tested materials. After the bacterial solution was absorbed into the films and incubation for one day, the two samples clearly differ. In the case of the normal cellulose films, the total bacterial count decreases, but there is a significant amount of bacteria detected after incubation. The high variation in the single reference samples could be caused by several reasons. It is possible that the used recovery process is not the perfect one for these investigations and hence simply not all of the bacteria are recovered. Another possibility could be that there are still some impurities present in the films, which may be potentially harmful to the bacteria. It may be possible that a large amount of the staphylococcus bacteria is already killed due to the repeated drying of the cellulose films in the incubator after damping the bacterial solution onto the films.

But in contrast to the normal cellulose films, it is obvious that no bacteria survived on the copper sulfide coated films and hence the antibacterial properties of in situ copper sulfide coated cellulose films is documented. Although the antibacterial tests have to be optimized and repeated with other bacteria strains to get the ultimate proof for the antibacterial effect of copper coated cellulose films, the obtained results are promising.

Table 15 List of resulting bacterial counts before and after 24 hours of incubating the metal sulfide coated cellulose films and the normal cellulose films

	<i>After 0 hours in film contact</i>		<i>After 24 hours in film contact</i>	
	Platted amount [μl]	Total bacterial [L^{-1}]	Platted amount [μl]	Total bacterial [L^{-1}]
<i>Ref 1</i>	500	$4.5 \cdot 10^3$	100	-
<i>Ref 2</i>	500	$5.1 \cdot 10^3$	100	$3.0 \cdot 10^2$
<i>Ref 3</i>	500	$5.8 \cdot 10^3$	100	$8.0 \cdot 10^2$
<i>CuS 1</i>	500	$0.9 \cdot 10^3$	100	-
<i>CuS 2</i>	500	$4.7 \cdot 10^3$	100	-
<i>CuS 3</i>	500	$4.4 \cdot 10^3$	100	-

4.11 Conclusion

In a final statement all investigations performed and all the results obtained, should be taken into consideration once more. The viscose process starts with the reaction from cellulose I to alkali cellulose. The alkali cellulose synthesis as performed in the lab and also the storage of the alkali cellulose over a restricted time frame works without any complications. In the following process step, the alkali cellulose is reacted with CS_2 to yield cellulose xanthate. The xanthation reaction itself could also be performed without any complications. The storage of the resulting viscose solutions and particularly the determination and the adjustment of the viscose age could be further optimized to get more consistency into the following viscose regeneration step. The regeneration of the viscose fibers into diluted sulfuric acid leads to the desired viscose fibers consisting of cellulose II. The quality of the fibers could definitely be improved by the modification of various process parameters, but this was not the primary target of this master thesis. The primary target was the in situ synthesis of metal sulfides and their immobilization onto the cellulose matrix of fibers and films. In extensive investigations it is demonstrated that this target has been achieved in the case of copper, tin, silver, nickel and cobalt sulfides. In contrast, the immobilization of zinc or iron sulfides on the cellulose matrix could not be successfully realized. It is also proven that the metal sulfides are not incorporated into the cellulose matrix, instead they are well immobilized in the interface region due to the engaging phase boundaries.

In a final test, a first possible application for the obtained products is investigated. This experiment shows in a promising way that the copper sulfide coated cellulose films possess potentially an antibacterial effect.

The results of this thesis provide a good starting basis for further investigations and product development in this research area.

5 Appendix

5.1 List of figures

Figure 1 Worldwide fiber production from 1900 up to 2008 (2)	2
Figure 2 Flow scheme for the viscose process with all the process streams involved (1)	3
Figure 3 Overview of different intermolecular and intramolecular bindings in cellulose I and cellulose II (10)	4
Figure 4 Illustration of the alkali cellulose synthesis, with corresponding reaction conditions and exorbitant NaOH charge	6
Figure 5 Illustration of the xanthation reaction with exorbitant substitution shown in the figure	7
Figure 6: Acid catalyzed dehydration of cellulose (29)	13
Figure 7 Nano crystalline copper sulfides as photo catalysts in the degradation of organic pollutants (53)	17
Figure 8 Production scheme for high performance hydrogen producing hybrid materials (72)	20
Figure 9 Alkali cellulose syntheses in laboratory scale a) stirring of cotton in NaOH solution b) 24h dried alkali cellulose	22
Figure 10 Different process steps in the xanthation of alkali cellulose to cellulose xanthate in the laboratory scale	24
Figure 11 Needles tested for fiber spinning	26
Figure 12 Developing of a automatized lab scale viscose fiber production unit with all the single parts needed	27
Figure 13 Process steps in the synthesis of metal sulfide coated viscose fibers	29
Figure 14 Illustrations of the production steps in cellulose film synthesis	33
Figure 15 AT-IR spectra of cotton fleece (starting material) and alkali cellulose	38
Figure 16 ATR-IR spectra of freshly prepared alkali cellulose and a sample stored at 4°C over a period of 30 days	39
Figure 17 30 day long stored alkali cellulose at different temperature or varying light exposure	40
Figure 18 IR spectra of the cotton fleece, the alkali cellulose and the resulting cellulose xanthate	42
Figure 19 Cellulose xanthate after a storage period of 1 respectively 5 days under atmospheric influence	43
Figure 20 Influence of a 14 day lasting storage period onto a cellulose xanthate solution	43
Figure 21 Fiber in 25% sulfuric acid	46
Figure 22 Fiber after regeneration in 15% H ₂ SO ₄	46
Figure 23 Images of a viscose fiber, obtained from standard spinning process in varying magnifications	47
Figure 24 ATR-IR spectra of a cotton fiber and a viscose fiber	47
Figure 25 The fiber plant in operation and the resulting fibers after the regeneration in 15% sulfuric acid	49
Figure 26 Scheme of sodium exchange due to the presence of metal chloride salts in the spinning bath	50
Figure 27 Standard and in CuCl ₂ regenerated fibers	51
Figure 28 CuS containing fiber magnification 400	51
Figure 29 Comparison between non-treated and CuS modified viscose fibers obtained from the lab scale fiber plant	52
Figure 30 XRD analysis of normal and CuS containing viscose fibers	53
Figure 31 measured XRD spectrum of viscose fibers with CuS compared to a spectrum of hexagonal CuS	54
Figure 32 Viscose fibers spun into a SnCl ₂ containing spinning bath directly after the spinning process and after drying	55
Figure 33 SnS particles on viscose fibers regenerated in a spinning bath with SnCl ₂ inside, detected through SEM	56
Figure 34 Spectra of tin particle containing fibers compared with other tin crystal	56
Figure 35 Washing solutions after five minutes of fiber washing	57
Figure 36 Viscose fibers regenerated in a nickel containing spinning bath and the particles detected on the fiber surface	58
Figure 37 XRD spectra of standard viscose fibers, untampered and carbonized Ni particle carrying fibers	59

Figure 38 Accordance from XRD spectra of nickel oxide and viscose fibers with Ni particles _____	59
Figure 39 Illustration of the obtained fibers after spinning in a cobalt containing bath and a SEM image of the fibers _____	60
Figure 40 Illustration of the fibers obtained after the spinning process and after 5 minutes of washing in deionized water _____	61
Figure 41 SEM images of the fibers obtained through viscose spinning in an iron containing spinning bath _____	62
Figure 42 XRD spectra for fibers regenerated in presence of iron and zinc salts in the spinning bath _____	62
Figure 43 Fibers obtained after injection of viscose in a zinc(II)sulfide containing spinning bath _____	63
Figure 44 A light microscopy and an SEM image of the viscose fibers obtained by spinning in presence of zinc(II)chloride _____	64
Figure 45 Illustration of the fibers and the spinning bath after fiber synthesis and of the dried silver containing particles _____	64
Figure 46 SEM images of the fibers obtained through viscose spinning in a silver(I)nitrate containing spinning bath _____	65
Figure 47 Spectra of silver particle containing fibers compared to silver disulfide _____	66
Figure 48 Cross section of cellulose fibers regenerated in a silver cation containing spinning bath in varying magnification _____	68
Figure 49 ATR IR Spectra of cotton, regenerated cellulose and CuS containing viscose fibers _____	70
Figure 50 Examples for SEM images obtained by investigating the influence of varying process parameters on the size of the resulting copper sulfide crystals. _____	73
Figure 51 Fibers obtained after mixing tungsten(VI)oxide into viscose and regenerating the viscose in sulfuric acid _____	74
Figure 52 Spectra of tungsten containing fibers compared to monocline tungsten(VI)oxide _____	75
Figure 53 SEM images of tungsten(VI)oxide containing fibers in different magnifications _____	75
Figure 54 Diffractogram of WS ₂ containing viscose fibers compared with a WS ₂ reference _____	76
Figure 55 Shows cellulose films in different steps of the storage experiment in glycerol solutions _____	77
Figure 56 Regeneration of cellulose xanthate films into metal cations containing spinning baths during and after regeneration _____	79

5.2 List of tables

<i>Table 1 Overview of different fiber types used in textile and technical application (1)</i>	1
<i>Table 2 Overview of possible applications for different inorganic nano structures on cellulosic fibers (42)</i>	16
<i>Table 3 Sum up of the used chemicals</i>	36
<i>Table 4 List of alkali cellulose reactions</i>	37
<i>Table 5 Summary of the experiments to the alkali cellulose stability</i>	41
<i>Table 6 Overview of xanthation reactions</i>	41
<i>Table 7 Single calibration measurements with m-cresol for the determination of k</i>	44
<i>Table 8 Aging process of viscose solution stored under oxygen atmosphere documented through the kinematic viscosity</i>	44
<i>Table 9 Aging process of viscose solution stored under nitrogen atmosphere documented through the kinematic viscosity</i>	44
<i>Table 10 Effects of the sulfuric acid concentration on the viscose spinning process</i>	45
<i>Table 11 List of elemental contents in fiber matrix and crystallites detected through SEM-EDX</i>	53
<i>Table 12 Overview of the metal uptake by varying salt concentrations in the spinning bath</i>	67
<i>Table 13 Copper uptake in viscose solutions aged for one and three days</i>	71
<i>Table 14 Overview of weight increase for the films stored in glycerol</i>	78
<i>Table 15 List of resulting bacterial counts before and after 24 hours of incubating the metal sulfide coated cellulose films and the normal cellulose films</i>	81

5.3 List of references

1. www.lenzing.com. [Online] Lenzing AG, 16. 05 2016. [Zitat vom: 16. 05 2016.] <http://www.lenzing.com/fasern/faserarten.html>.
2. **WWF**. *Hintergrundinformation Bekleidung und Umwelt*. Berlin : WWF, 2010.
3. **Klare, H.** *Acta Pol.* 1985, Bd. 36, S. 347-352.
4. **Hon, D.** *Cellulose*. 1994, Bd. 1, S. 1-25.
5. **Schönbein, C. F.** *Sitzungsber. Konigl. Bay. Akad. d. Wiss.* 1863, Bd. II, 166.
6. **Schweizer, E. J.** *prakt. Chemie*. 1857, Bd. 73, S. 109 ff.
7. **Svan, I. W.** *Brit. Pat.* 5978. 1883.
8. **Cross, C. F., Bevane, J., Beadle., C.** *Brit. Pat.* 8700. 1892.
9. **Salih, S. M.** *Fourier Transform: Materials Analysis*. Rijeka : InTech, 2012. S. 44-68. ISBN 978-953-51-0594-7.
10. **Berthelot., J., Credou, T.** *J. Mater. Chem.* 2014, Bd. 2, S. 4767-4788.
11. **Burton, J. O., Rasch, R. H.** *J. Res. Natl. Inst. Stan.* Bd. 6, S. 603-619.
12. **Sixta, H.** *Lenz. Ber.* 1986, Bd. 61, S. 5-11.
13. **Schleicher, H., Phillipp, B., Kunze, J., Fink, H.** *Lenz. Ber.* 1985, Bd. 59, S. 45-51.
14. **Götze, K.** *Chemiefasern nach dem Viskoseverfahren (Reyon und Zellwolle)*. Berlin : Springer Verlag, 1951. ISBN: 978-3-642-49507-6.
15. **Klemm, D., Phillipp, B., Heinze, T., Heinze, U., Wagenknecht, W.** *Comprehensive Cellulose Chemistry, Functionalization of Cellulose (Volume 2)*. Weinheim an der Bergstraße : Wiley-VCH, 1998. ISBN-10: 3527294899.
16. **Bandel, W.** *Makro. Chem.* 1953, Bd. 11, S. 87-96.
17. **Fink, H., Ganster, J., Lehmann, A.** *Cellulose*. 2014, Bd. 21, S. 31-51.
18. **Lohs, K., Stephan, U.** *Fachlexikon Toxikologie, 4. Auflage*. Berlin : Springer-Verlag, 2008. ISBN: 978-3540-27337-0.
19. **Marini, I., Svoboda, H., Korger, D.** *Lenz. Ber.* 198, Bd. 57, S. 25-30.
20. **Marini, J., Ruf, H., Wimmer, A.** *Chemiefasern/Text.-Ind.* 1987, Bd. 37, S. 89 ff.
21. **Aitken, R.** *J. Soc. Dyers. Colour.* 1983, 99, S. 150 ff.
22. **Roggenstein, W.** *Lenz. Ber.* 2011, 89, S. 72-77.

23. Akil, A. M., Edeerozey, M., Hazizan, M. *Mater. Lett.* 2007, Bd. 61, S. 2023 ff.
24. Joseph K, Mattoso L. H. C, Toledo R. D., Thomas S., de Carvalho L. H., Pothen L., Kala S., James B. *Nat. Poly. Agrof. Comp.* 2000, S. 159 ff.
25. Hill C.A.S., Abdul Khalil H.P.S., Hale M. D. *Ind. Crops. Prod.* 1998, Bd. 8, S. 53–63.
26. Matsuda, H. *Chemical Modification of Lignocellulosic Materials*. New York : Marcel Dekker, 1996. S. 159. ISBN: 978-0824750572.
27. Ushakov, S. H. *Fiz.-Mat. Nauk.* 1943, Bd. 1.
28. Horrocks, A. R. *Rev. Prog. Color.* 1986, 16, S. 62-101.
29. Hüpfl F., Gotschy J. *Lenz. Ber.* 1972, Bd. 33, S. 28-32.
30. Kretze T., Jeler S., Strnad S. *Mater. Res. Innov.* 2002, Bd. 5, S. 277-283.
31. Roessler S., Zimmermann R., Scharnweber D., Werner C., Worch H. *Colloids Surf.* 2002, Bd. 40, S. 387-395.
32. Fu G., Vary P., Lin C. T. *J. Phys. Chem.* 2005, Bd. 109, S. 8889-8898.
33. Rai M., Yadav A., Gade A. *Biotechnol. Adv.* 2009, Bd. 27, S. 76-83.
34. Jeong S.H., Yeo S. Y., Yi S. C. *J. Mater. Sci.* 2005, Bd. 40, S. 5407–5411.
35. Jeong S.H., Wang Y. H., Yi S. C. *J. Mater. Sci.* 2005, Bd. 40, S. 5413-5418.
36. Breitwiesera D., Moghaddama M. M., Spirk S., Baghbanzadeha M., Pivecd T., Fasl H., Ribitsch V., Kappe C. O. *Carbohydr. Polym.* 2013, Bd. 1, S. 677–686.
37. Pan Z.W., Dai Z.R., Wang Z.L. *Science.* 2001, Bd. 291, S. 1947–1949.
38. Xiong M., Gu G. ,You B., Wu L. *J. Appl. Polym. Sci.* 2003, Bd. 90, S. 1923-1931.
39. Becheri A., Dürr M., Nostro P. L., Baglioni P. *J. Nanopart. Res.* 2007, Bd. 10, S. 679-689.
40. Wel Q., Yu L., Wu N., Hong S. *J. Ind. Text.* 2008, Bd. 37, S. 275-283.
41. Zhang Y., Peng H., Huang W., Zhou Y., Yan D. *J. Colloid Interface Sci.* 2008, 325, S. 371-376.
42. Dastjerd R., Montazer M. *Colloids Surf.* 2010, Bd. 79, S. 5-18.
43. Persano L., Camposeo A., Di Benedetto F., Stabile R., Laera A. M. , Piscopiello E., Tapfer L., Pisignano D. *Adv. Mater.* 2012, Bd. 24, S. 5320–5326.
44. Pardo R., Zayat M., Levy D. *Chem. Soc. Rev.* 2011, Bd. 40, S. 672–687.
45. P., Nguyen T. *Surf. Coat. Technol.* 2011, Bd. 206, S. 742-752.
46. Qiao T., Xu Q. *Energy Environ. Sci.* 2011, Bd. 4, S. 2700–2720.

47. Meng Z.D., Ghosh T., Zhu L., Choi J. G., Park C. Y., Oh W. C. *J. Mater. Chem.* 2012, Bd. 22, S. 16127-16135.
48. Nagasuna K., Akita T. , Fujishima M. , Tada H. *Langmuir.* 2011, Bd. 27, S. 7294-7300.
49. Sadovnikov S.I., Gusev A.I., Rempel A.A. *Phys. Chem. Chem. Phys.* 2015, Bd. 17, S. 12466-12471.
50. Yamamoto T., Tanaka K., Kubota E., Osakada K. *Chem. Mater.* 1993, Bd. 5, S. 1352-1357.
51. Sowel G. M., Mattox R. R. *J. Vac. Sci. technol.* 1974, Bd. 11, S. 793 .
52. Inoue M., Cruz-Vazquez C., Inoue M. B., Nebesny K. W., Fernando Q. *Synth. Met.* 1993, Bde. 55-57, S. 3748.
53. Xu W., Zhu S., Liang Y., Li Y., Cui Z., Yang Z. *Scient. Rep.* 2015, Bd. 5, S. 18125 ff.
54. Ogah O.E., Reddy K.R. , Zoppi G., Forbesl. , Miles R. W. *Thin Solid Films.* 2011, Bd. 519, S. 7425 ff.
55. Gao C., . She H.L, Sun L., Shen Z. *Mater. Lett.* 2011, Bd. 65, S. 1413 ff.
56. Mathews N.R., Anaya H.B.M., Cortes-Jacome M.A., Angeles-Chavez ., Toledo-Antonio J.A. *J. Electrochem. Soc.* Bd. 157, S. 337 ff.
57. www.tribotecc.at. [Online] tribotecc. [Zitat vom: 11. 05 2016.] www.tribotecc.at.
58. Gao M. R., Xu Y. F., Jiang J., Yu S. H. *Chem. Soc. Rev.* 2013, 42, S. 2986–3017.
59. Zhou Y., Yan D., Xu H., Feng J, Jiang X. Yue J., Yang J., Qian Y. *Nano Energy.* 2015, 12, S. 528–537.
60. Mahmood N., Zhang C., Hou Y. *Small.* 2013, 9, S. 1321–1328.
61. Kong C., Min S., Lu G. *ACS Catal.* 2014, Bd. 4, S. 2763–2769.
62. Falkowski J. M., Concannon N. M., Yan B., Surendranath Y. *J. Am. Chem. Soc.* 2015, Bd. 137, S. 7978-7981.
63. Rui X., Tan H., Yan Q.,. *Nanoscale.* 2014, Bd. 6, S. 9889–9924.
64. Fang X., Wu L., Hu L. *Adv. Mater.* 2011, 23, S. 585-598.
65. Gautam U.K., Fang X., Bando Y., Zhan J.H., Golberg D. *ACS Nano.* 2008, Bd. 2, S. 1015 - 1021.
66. Bang J.H., Hemich R.J., Suslick K.S. *Adv. Mater.* 2008, 20, S. 2599-2603.
67. Fang X., Zhai T., Gautam U. K., Li L., Wu L., Bando Y., Golberg D. *Prog. Mater. Sci.* 2011, 56, S. 175-287.
68. Ong H.C., Chang R.P.H. *Appl. Phys. Lett.* 2001, Bd. 79, S. 3612-3614.
69. Jiang J.Z., Larsen R.K., Lin R., Morup S., Chorkendorff I., NielsenK., Hansen K., West K. *J. Solid State Chem.* 1998, 138, S. 114-125.
70. Ozverdi A., Erdem M. *J. Environ. Sci. Technol.* 2007, Bd. 41, S. 7699 - 7705.

71. **Lin Z.S., Xian W.H., Cheng .** *J. Chin. Phys.* 2014, Bd. 23, S. 148 ff.
72. **Shuang Y., Bowen W., Xiaodi G., Shuangxia Y., Lianying W. , Jing H.** *Cat. Comm.* 2016, 76, S. 37-41.
73. **Hu J.S., . Ren L.L, Guo Y.G. , Liang H.P., Cao A.M. , Wan L.J., Bai C.L.** *Angew. Chem. Int. Ed.* 2004, 44, S. 1269–1273.
74. **Jang J.S., Yu C.J., Choi S.H. , Ji S.M., Kim E.S., Lee J.S.** *J. Catal.* 2008, Bd. 254, S. 144-155.
75. **Yang J., Wang D., Han H., Li C.** *Acc. Chem. Res.* 2013, Bd. 46, S. 1900–1909.
76. **Guo W.X., Zhang F., Lin C.J., Wang Z.L.** *Adv. Mater.* 2012, 24, S. 4761-4764.
77. **Javme G., BalslerK.** *Das Papier.* 1964, Bd. 18, S. 746.
78. **G., Socrates.** *infrared characteristic group frequncies.* Chichester : Wiley, 1980. S. 66 ff. ISBN: 0471942308.
79. **Lauer K., Skark L.** *J. Polym. Sci. A Polym.* 1956, 20, S. 394 - 404.
80. **Zemplén, Géza.** *Biochemisches Handlexikon: XIII. Band.* berlin : Springer, 1931. S. 153 pp. ISBN: 9783642908293.
81. **Ogura K., Sobue H.** *J. Polym. Sci.* 1968, 6, S. 63 - 67.
82. **Wertz J, Mercier J., Bédué O.** *Cellulose Science and Technology.* Lausanne : CRC Press, 2010. S. 196 pp. ISBN: 9781439807996.
83. **www.carlroth.com.** [Online] 25. 06 2015. [Zitat vom: 27. 04 2016.]
https://www.carlroth.com/downloads/sdb/de/9/SDB_9269_DE_DE.pdf.
84. **Lim W. P., Wong C. T., Ang S. L., Low H. Y., Chin W. S.** *Chem. Mater.* 2006, Bd. 18, S. 6170-6177.
85. **Grau J., Akinc M.** *J. Am. Ceram. Soc.* 1996, Bd. 74, S. 1073-1082.
86. **Zhu, Y.** *J. Am. Chem. Soc.* 2005, Bd. 127, S. 16263.
87. **E. Lassner, W. D.Schubert.** *Tungsten: Properties, Chemistry, Technology of the Element, Alloys, and Chemical Compounds.* Berlin : Springer, 1999. S. 374 ff. ISBN 978-0-306-45053-2.
88. **Abts, Georg.** *Kunststoff-Wissen für Einsteiger.* 2. Auflage. München : Carl Hanser Verlag, 2014. S. 140 ff. ISBN: 978-3-446-43925-2.
89. **www.seilnacht.com.** [Online] seilnacht. [Zitat vom: 09. 5 2016.]
http://www.seilnacht.com/Chemie/ch_glyce.htm.